PET imaging to measure therapy-related occupancy and disease-induced changes of expression of adenosine A1 receptors in the rodent brain

Paul, Souman

PET Imaging to Measure Therapy-Related Occupancy and Disease-Induced Changes of Expression of Adenosine A_1 Receptors in the Rodent Brain

Soumen Paul

Printing of this thesis was supported by: University of Groningen, University Medical Center Groningen and Groningen University Institute for Drug Exploration

Paranymphs:

Willem-Jan Kuik, MSc
Ee Soo Lee, M.Med.Sc

Cover design: Willem-Jan Kuik, Soumen Paul

Printed by: WÖHRMANN PRINT SERVICE

ISBN: 978-90-367-6843-6 (printed version)
ISBN: 978-90-367-6842-9 (electronic copy)

university of groningen

PET Imaging to Measure Therapy-Related Occupancy and Disease-Induced Changes of Expression of Adenosine A_1 Receptors in the Rodent Brain

PhD thesis

to obtain the degree of PhD at the
University of Groningen
on the authority of the
Rector Magnificus Prof. E. Sterken
and in accordance with
the decision by the College of Deans.

This thesis will be defended in public on

Monday 24 March 2014 at 14:30 hours

by

Soumen Paul

born on 1 January 1984
in Burdwan,India

Supervisors:
Prof. R.A.J.O. Dierckx
Prof. P.H.Elsinga

Co-supervisors:
Dr. A.van.Waarde

Assessment committee:
Prof. PGM Luiten
Prof. HPH Kremer
Prof. C Halldin

This thesis is dedicated to my Parents

Content

Chapter I

General Introduction

Soumen Paul[1], Kiichi Ishiwata[2], Philip H. Elsinga[1, 3] Rudi A.J.O. Dierckx[1, 3] and Aren van Waarde[1]

[1] *Nuclear Medicine and Molecular Imaging, University Medical Center Groningen, University of Groningen, Groningen, The Netherlands*

[2] *Positron Medical Center, Tokyo Metropolitan Institute of Gerontology, Tokyo, Japan*

[3] *Department of Nuclear Medicine, University Hospital Ghent, Ghent, Belgium*

Curr.Med.Chem. 2011; 18(31):4820-4835

Abstract

Adenosine is a neuromodulator with several functions in the central nervous system (CNS), such as inhibition of neuronal activity in many signaling pathways. Most of the sedating, anxiolytic, seizure-inhibiting and protective actions of adenosine are mediated by adenosine A1 receptors (A1R) on the surface of neurons and glia. Positron Emission Tomography (PET) is a powerful in vivo imaging tool which can be applied to investigate the physiologic and pathologic roles of A1R in the human brain, and to elucidate the mechanism of action of therapeutic drugs targeting adenosine receptors, nucleoside transporters and adenosine-degrading enzymes. In this Introduction, we discuss (i) functions of adenosine and its receptors in cerebral metabolism; (ii) radioligands for A1R imaging: xanthine antagonists, non-xanthine antagonists, and agonists; (iii) roles of A1R in health and disease, viz. sleep-wake regulation, modulation of memory retention and retrieval, mediating the effects of alcohol consumption, protecting neurons during ischemia and reperfusion, suppression of seizures, modulating neuroinflammation and limiting brain damage in neurodegenerative disorders. The application of PET imaging could lead to novel insights in these areas. Finally (iv), we discuss the application of PET in pharmacodynamic studies and we examine therapeutic applications of adenosine kinase inhibitors, e.g. in the treatment of pain, inflammation, and epilepsy. Finally we discuss the aims and outline of the thesis.

1.1. Sources, Regulation and Fate of Extracellular Adenosine

The purine nucleoside adenosine is not a classical signaling substance, as adenosine is neither stored nor released from vesicles. The nucleoside plays a neuromodulatory role by affecting the excitability of neurons that release neurotransmitters such as glutamate, gamma-amino butyric acid (GABA), acetylcholine and dopamine [1-12]. Adenosine is involved in homeostatic reduction of cellular excitability during stress and trauma *via* its interaction with receptors on the cell surface. Moreover, adenosine is involved in the regulation of synaptic plasticity. Balanced activation of inhibitory and facilitatory adenosine receptors modulates long term potentiation (e.g., in the hippocampus) [13-15]. Metabolic pathways involved in the formation and removal of adenosine are presented in **Fig**. (**1**). Extracellular adenosine may originate from intracellular adenosine - which can pass the plasma membrane *via* an equilibrative nucleoside transporter (ENT), or by hydrolysis of locally released adenine nucleotides such as adenosine triphosphate (ATP), adenosine diphosphate (ADP), adenosine

monophosphate (AMP) and to a lesser extent cyclic adenosine monophosphate (cAMP). Production of extracellular adenosine is the result of the breakdown of such nucleotides by ecto-nucleotidases [16-18]. The rate-limiting step is the conversion of AMP to adenosine which is catalyzed by ecto-5'-nucleotidase (CD73). The biochemical and pharmacological properties of this enzyme have been extensively characterized [16, 19]. 5'- Nucleotidase is inhibited by ATP and ADP [18]. The quantititative importance of this mechanism has been confirmed by a kinetic characterization of the breakdown of extracellular ATP at the cholinergic striatal synapse [20]. Extracellular adenosine is subject to metabolic degradation by adenosine deaminase (ADA) which results in the formation of inosine [21]. Another route of adenosine inactivation is the reversible reaction catalyzed by S-adenosyl homocysteine (SAH) hydrolase [22]. Formation of SAH from adenosine and homocysteine is restricted since homocysteine levels are rate-limiting.In the brain, the SAH pathway is a quantitatively negligible pathway of adenosine catabolism [23]. The major route of adenosine removal under normal conditions is phosphorylation to AMP by adenosine kinase (AK).

1.2. Classification of Adenosine Receptors

The adenosine receptor (AR) family consists of the A_1, A_{2A}, A_{2B} and A_3 subtypes (A_1R. A_{2A}R, A_{2B}R and A_3R, respectively).A_1R and A_3R inhibit whereas A_{2A}R and A_{2B}R stimulate production of the second messenger, cAMP. A_1R and A_{2A}R are activated by nanomolar concentrations of adenosine whereas A_{2B}R and A_3R become activated only when adenosine levels rise into the micromolar range during inflammation, hypoxia or ischemia [24-26]. The four AR subtypes from rat, mouse, human and other species have been pharmacologically recognized, cloned, purified and expressed [27-29].

1.3. Regional Distribution and Signaling of A_1R

The A_1R is the most strongly preserved AR subtype among different animal species [28]. A_1Rs exhibit the highest affinities for adenosine and synthetic agonists of all AR subtypes [30]. They are distributed throughout the body and are also highly expressed in the brain, especially in hippocampus, frontal cortex, thalamic nuclei, basal ganglia and dorsal horn of the spinal cord. Peripheral organs with high A_1R expression include eye, adrenal gland, heart and aorta.The regional distributions of A_1R in human and rodent brains are similar but not completely identical. In human cerebellum, A_1R densities are low in contrast to rat cerebellum, where moderate A_1R expression is noted [31-36]. Different neurons express different levels of A_1R. In rat brain, the highest A_1R immunoreactivity is observed in pyramidal neurons of layer 5 of the cerebral cortex, and in pyramidal cells in fields CA2 and CA3 of the hippocampus. In layer 5, immunoreactivity is detected in cell bodies, dendrites and initial segments of axons [37].

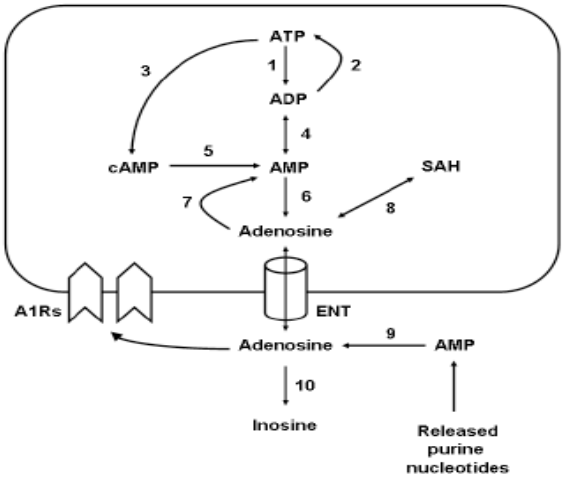

Fig. (1). Metabolic scheme showing the pathways of adenosine formation and removal. Enzymes involved are: 1. ATPases, 2. oxidative phosporylation (and creatine kinase), 3. adenylyl cyclase, 4. adenylate kinase, 5. phosphodiesterase, 6. 5'-nucleotidase, 7. adenosine kinase, 8. SAH hydrolase, 9. ecto-5'- nucleotidase (CD73), 10. adenosine deaminase.

Activation of A_1Rs inhibits adenylyl cyclase, closes voltage dependent Ca^{2+} channels, and activates K^+ channels. Signalling of this AR subtype occurs through $G_{i/o}$ pathways in various cells (including neurons). As a result, the neuronal activity is suppressed [38, 39]. In presynaptic regions, adenosine inhibits neurotransmitter and neuropeptide release, including the release of glutamate, substance P and calcitonin gene related peptide [40]. In postsynaptic areas, adenosine abolishes sensory transmission and causes membrane hyperpolarisation [41,42].

2. Radioligands for A_1R Imaging

PET is a medical imaging technique providing information on tissue biochemistry rather than anatomy. PET imaging has several unique properties: high sensitivity, low radiation dose, possibility to correct data for attenuation and scatter (thus quantitative), radioactive labeling of natural substances or drugs with high specific radioactivity so that these can be used as tracers to monitor the pharmacokinetics of the non-radioactive compounds. PET may therefore be applied to measure regional AR densities in the living human brain and the dose-dependent occupancy of cerebral AR by therapeutic drugs. A comprehensive overview

of PET tracers for the different AR subtypes has been presented in some recent reviews [43, 44]. Several ligands for PET imaging of A_1R have been prepared .These include xanthine A_1R antagonists, non-xanthine A_1R antagonists and A_1R agonists. All compounds bind with nanomolar affinity to A_1R. The best-characterized tracers are [^{11}C] MPDX and [^{18}F] CPFPX. Both can be applied for PET studies of cerebral A_1R in humans. The long physical half life of ^{18}F (109.8 min) as compared to ^{11}C (20.4 min) allows longer scanning times with [^{18}F] CPFPX than with [^{11}C] MPDX. Because of this difference in half life, [^{18}F] CPFPX can be distributed to remote imaging sites without cyclotron facilities, in contrast to [^{11}C] MPDX. However, the radiation dose that subjects will receive after injection of [^{18}F] CPFPX (300 MBq) is greater than that of [^{11}C] MPDX (300 MBq): 5.3 mSv vs. 1.05 mSv, respectively ([45] and Ishiwata, unpublished data). Thus, multiple-injection protocols are possible with [^{11}C] MPDX but not with [^{18}F] CPFPX. Since each tracer has specific advantages and disadvantages, tracer selection will be based on historic interest and the facilities at one's disposal rather than on clear superiority of a certain compound. Efforts to develop A_1R ligands for PET with improved properties might focus on antagonists with reduced lipophilicity and improved water solubility, e.g. compounds with non-xanthine structures. However, the first reported example of such tracers, [^{11}C] FR194921, did not produce better results in experimental animals than [^{11}C] MPDX or [^{18}F] CPFPX [46].

Ligand	A_1R affinity	Studies performed	Findings	References
Xanthines				
[^{11}C]KF15372 (8-Dicyclopropylmethyl-3-propylxanthine)	3.0 nM (K_i)	Biodistribution study in mice	About 57% specific binding (to A_1R not A_2R)	[254-256]
		Ex vivo autoradiography (mice/rats)	Tracer distribution in brain reflects regional A_1R density	
			Decreased binding in superior colliculus after unilateral eye removal	
		PET study in anesthetized monkeys	Tracer distribution in brain reflects regional A_1R density	
			About 50% reduction in uptake after treatment with "cold" KF15372	
[^{11}C]EPDX (2-Ethyl-8-dicyclopropyl-methyl-3-propylxanthine)	1.7 nM (K_i)	Biodistribution study in mice	About 50% specific binding (to A_1R not A_2R)	[257]
[^{11}C]MPDX (8-Dicyclopropylmethyl-1-methyl-3-propylxanthine)	4.2 nM (K_i)	Biodistribution study in mice	Initial brain uptake higher than EPDX and KF15372 but faster washout.	[257] [258]
		Metabolite analysis in mice	Dosimetry data indicate acceptable radiation dose in human studies.	[257,259,260]
		Ex vivo autoradiography (rats)	Metabolites appear in plasma but brain activity is mainly parent at 30 min.	[261]
		Radiochemical synthesis improved.	Decreased binding in superior colliculus after unilateral eye removal.	[262] [263]
		PET study in anesthetized cats	About 55% specific binding (to A_1R not A_2R).	
			In animal model of dystonia, tracer binding in hippocampus is decreased.	[155,156]

		PET study in anesthetized monkey	Distribution volume of tracer in brain reflects regional A_1R density.	[258] [264,265]
		Human PET study	Bound tracer can be displaced by an excess of cold A_1R antagonist.	[266]

		(healthy volunteers)	In a cat model of stroke, losses of A_1R can be detected in ischemic areas. The magnitude of these losses indicates severity of the insult and predicts subsequent complications (including mortality). Good brain uptake, distribution reflects regional A_1R density. Tracer distribution in brain reflects regional A_1R density. Pattern differs from that of a flow tracer or a glucose analog. Distribution volume (Logan plot) or binding potential (compartment model analysis) can be used for quantification purposes.	
[^{18}F]CPFPX (8-Cyclopentyl-3-[3-fluoropropyl]-1-propyl-xanthine)	0.6-1.4 nM (K_d mouse, pig, human) 4.4 nM (K_d rat)	Biodistribution study in mice Metabolite analysis in mice Ex vivo autoradiography (rats) Animal PET study in rats Human PET study (healthy volunteers) Metabolite study (liver microsomes)	Distribution in brain reflects regional A_1R density. Metabolites appear in plasma but brain activity is mainly parent at 60 min. About 70% of brain uptake is specific (to A_1R) and reversible. Tracer distribution in brain reflects regional A_1R density (>90% specific). Brain well-visualized, bound tracer can be displaced by A_1R antagonist. Tracer distribution in brain reflects regional A_1R density. Tracer kinetics in human brain are appropriate for quantititative imaging. Distribution volume (Logan plot) or binding potential (compartment model analysis) can be used for quantification purposes. Simplified study protocols are possible (venous rather than arterial blood sampling, bolus-infusion or single bolus administration of the tracer). Short scanning protocols (60 min) are possible in humans. Bound tracer can be displaced by cold CPFPX in all brain	[267] [268] [269] [270] [271,272] [273] [224] [274] [275,276]

			regions. Non-invasive procedure (reference tissue model) is suitable for quantification of A_1R in human brain. Tracer is metabolized by cytochrome CYP1A2. Its metabolism can be inhibited by therapeutic drugs like fluvoxamine.	
[^{131}I]CPIPX [1] (8-Cyclopentyl-3-[*(E)*-3-iodoprop-2-en-1-yl]-1-propylxanthine)	0.8-7.9 nM (K_d rat, pig cortex)	Ex vivo autoradiography (rats)	Tracer binding is largely nonspecific. Thus, this ligand is not suitable for imaging purposes. The iodine radiolabeling results also in loss of selectivity for the A_1R.	[277]
Non-xanthines				
[^{11}C]FR194921 (2-(1-methyl-4-piperidinyl)-6-(2-phenylpyrazolo[1,5-a]-pyridin-3-yl)-3(2H)-pyridazinone)	2.9 nM (K_i)	Ex vivo autoradiography (rats) PET study in conscious monkeys	Tracer distribution in brain reflects regional A_1R density. About 50% specific binding (to A_1R not A_2R). Brain well-visualized, tracer accumulates in cortex, striatum, thalamus.	[46] [46]
Agonists				
5-O-(methyl[^{75}Se]seleno)-*N6*-cyclopentyladenosine	0.9 nM (K_i) (pig cortex)	Radiochemical synthesis described	No in vivo data reported	[278]
5'-*N*-(2-[^{18}F]fluoroethyl)-carboxamidoadenosine	Nanomolar range	Radiochemical synthesis described	No in vivo data reported May bind not only to A_1R but also to other AR subtypes	[279]

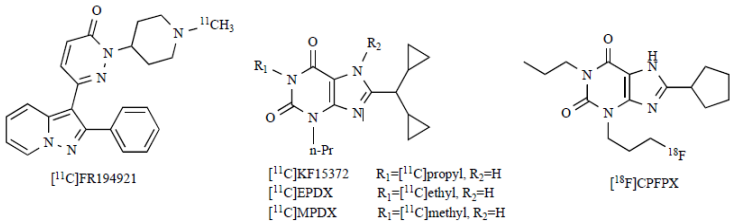

Fig. (2). Antagonist radioligands for PET imaging of A_1R.

3. Physiological role of A_1R and changes of A_1R expression in disorders of the CNS

3.1 Sleep-Wake Regulation

Adenosine plays an important role in the induction of sleep after prolonged wakefulness [47]. Prolonged wakefulness with its associated prolonged neuronal activity increases extracellular adenosine levels in the forebrain of conscious cats, whereas these levels diminish during sleep [48]. A [^{18}F]CPFPX-PET study in humans has indicated that in addition to changes of extracellular adenosine, A_1R are upregulated in cortical and subcortical regions of the brain after prolonged wakefulness (max. 15.3%), which suggests that changes of A_1R expression are contributing to homeostatic sleep regulation [49]. Short periods of total sleep deprivation (3 or 6 h) result in increases of A_1R mRNA but no detectable increases of A_1R expression in rat brain [50]. However, longer periods of total sleep deprivation in rodents (12 or 24 h) are accompanied by a significant upregulation of A_1R (up to 14%) in various brain areas [51,52]. [^{3}H]Phenylisopropyladenosine (PIA, Figure 3) saturation binding assays have indicated that A_1R densities in cortical and subcortical regions of rat brain are increased not only after total sleep deprivation, but also after 48 and 96 h of partial, rapid eye movement (REM) sleep deprivation, whereas affinity (K_d) values for agonist binding are not significantly altered [53]. After restriction of sleep and also after performance of a difficult learning task, cerebral synchronized slow wave activity (SWA) is enhanced during the next sleeping period, and this activity is related to the subsequent improvement of cognitive performance [54,55]. Activation of A_1R is necessary for the increase of SWA. If this increase is impaired (e.g. because of knockout of the A_1R gene) animals fail to maintain normal cognitive function. Thus, adenosine appears to be an important homeostatic sleep factor, and A_1Rs are involved in the regulation of sleep.

After administration of a selective A_1R agonist, *N6*-Cyclopentyladenosine (CPA, Figure 3), either by the systemic or the cerebroventricular route, SWA increased in rats during non-REM sleep [56]. Such stimulation of A_1R mimics the effect of total sleep deprivation in rodents. A similar effect on sleep is observed when extracellular adenosine levels in the mammalian brain are raised by administering inhibitors of nucleoside transport [57]. When levels of extracellular adenosine in the basal forebrain are raised by microdialysis, vigilance of rats is significantly impaired [58]. This effect on vigilance is completely blocked after co-administration of a selective A_1R antagonist, 8-cyclopentyltheophylline (CPT, Figure 3), with adenosine [58]. On the other hand, infusion of CPT into the basal forebrain diminishes the sleeping ability (both slow-wave and REM sleep) of cats [57]. Infusion of A_1R antisense in the cholinergic basal forebrain of rats inhibits the translation of A_1R mRNA, resulting in decreased non-REM sleep and increased wakefulness [59]. Such pharmacological experiments have provided additional support for the important role of A_1R in sleep regulation. Agonists for this receptor usually promote [60-62] while antagonists diminish [60,63] sleep.

In rat brain, prolonged wakefulness with accompanying increases of extracellular adenosine and stimulation of A_1R increases the activity of the transcription factor NF-kappaB [64,65]. This transcription factor regulates expression of several modulatory substances, such as interleukin-1-ß and tumor necrosis factor α, which shows a diurnal rhythm. Some effects of adenosine on sleep homeostasis, particularly the phenomenon of "sleep debt" may be triggered via this mechanism.

Orexinergic neurons in the lateral hypothalamus also express A_1R [66]. Adenosine and A_1R agonists inhibit activity of the hypocretin/orexin neurons in this area via A_1R which promotes sleep [67,68]. On the other hand, blockade of A_1R in such neurons causes a pronounced increase in wakefulness [68,69]. Adenosine reduces the frequency of action potentials in hypocretin/orexin neurons by depressing excitatory synaptic transmission to these cells. An additional mechanism involved in the sleep-promoting effects of adenosine may be suppression of the activity of histaminergic neurons in the tuberomammillary nucleus via A_1R [70]. Thus, in addition to its effects in basal forebrain, adenosine promotes sleep by reducing the activity of orexinergic and histaminergic neurons in the hypothalamus [67].

An additional brain region involved in sleep regulation is the pontine reticular formation. Microinjection of the A_1R agonist *N6*-cyclopentyladenosine (CPA) or inhibition of the formation of cAMP in this area increases REM sleep [71]. Another study has shown that administration of an A_1R agonist (*N6*-p-sulfophenyladenosine) decreases the (arousal-promoting) release of the neurotransmitter acetylcholine and increases the recovery time from halothane anesthesia [7].

Neurons in the previously mentioned brain areas are wake-active. Thus, suppression of their activity via stimulation of A_1R promotes sleep. In contrast to the regions mentioned above, the lateral preoptic area of rat hypothalamus is an area with an abundance of sleep-active neurons. A_1R agonists and the adenosine transport inhibitor

4-nitrobenzyl-thioinosine have opposite effects in this area as in other regions of the brain, i.e. they increase wakefulness rather than sleep [72]. Thus, the adenosine-mediated effects on the sleep-wake cycle are both neuron- and region-dependent.

PET may be applied to study the involvement of A_1R in the regulation of human sleep. Increased expression of A_1R in the human cortex after prolonged wakefulness has already been demonstrated [49]. Future PET studies could examine the effect of partial (REM) sleep deprivation in humans, and cerebral A_1R expression in sleeping disorders like narcolepsy.

3.2 Learning and memory

Acute stimulation of A_1R by agonists at micromolar doses has been reported to severely impair both the acquisition and retention of memory in various animal and in vitro models, such as long-term potentiation in rat hippocampal slices [73], passive avoidance retention in mice [74,75], working memory in a three-panel test [76], and acquisition of conditional fear conditioning [77] or short-term social memory in rats [78]. These cognitive deficits are attenuated, or abolished, when brain slices or experimental animals are pretreated with selective A_1R antagonists such as DPCPX. Thus, activation of A_1R in many regions of the CNS (hippocampus, ventral striatum, posterior cingulate cortex) may negatively modulate information processing in the brain and may impair memory retention [73-76]. Depending on the test setup (dose, region of administration, time of the day), acute administration of a selective A_1R antagonist has either no effect or it can facilitate memory performance of rodents [75,78,79].

In contrast to acute administration, chronic administration of an A_1R agonist (daily i.p. injections of CPA during a 9-day period) results in facilitation of spatial learning and memory of mice tested in a Morris water maze. These improvements are probably related to downregulation of A_1R [80].

However, studies of the behavioral phenotype of mice lacking A_1R have indicated that A_1R are not essential for rodent learning. Such mice show normal motor coordination but reduced muscle strength. Overall spontaneous motor activity is similar to that of wild-type controls, but activity peaks during the light/dark cycle are flattened, which is consistent with A_1R regulating the sleep-wake rhythm. $A_1R^{-/-}$ mice show enhanced aggression and decreased exploratory behavior indicating increased anxiety. However, their working memory in five different water maze tasks is not significantly impaired. The knockouts have a shorter lifespan than controls (LT_{50} reduced from 26 to 20 months), which suggests that A_1R play an important protective role in mammalian tissues during aging [81,82]. In a follow-up study which included a six-arm radial tunnel maze test, $A_1R^{-/-}$ mice were found to display normal spatial learning but to habituate more slowly to the test environment [83]. Thus, stimulation of A_1R may be required for habituation, i.e. suppression of the processing of irrelevant information.

3.3 Effects of ethanol

Various effects of alcohol consumption appear to be mediated by adenosine and A_1R. Ethanol metabolism in the liver causes formation of acetate, which circulates in the body at millimolar concentrations and is finally incorporated into acetyl-coenzyme A with concomitant production of AMP and adenosine [84]. Acute administration of ethanol results also in inhibition of the facilitated diffusion of nucleosides [84,85]. The inhibitory effect is specific for one particular subtype of ENT (ENT1) [86,87] and can be observed both in cultured cells [84,85,88] and in cerebellar synaptosomes [89,90]. Thus, ethanol augments the rate of adenosine formation and reduces adenosine uptake. Both mechanisms may increase the extracellular levels of adenosine.

Initial attempts at measuring changes of adenosine levels within the brain after administration of ethanol or acetate were unsuccessful, probably because it is difficult to homogenize tissue, or to collect adenosine, while avoiding adenosine degradation [91,92]. Later analytical and microdialysis studies indicated that the levels of acetate and extracellular adenosine in cortical areas of rat brain are significantly increased (up to 4-fold) after administration of physiologically relevant doses of ethanol [93,94].

A functional relationship between ethanol and adenosine was suggested by the fact that dipyridamole, an inhibitor of ENT1, promotes ethanol-induced motor impairment (EIMI) [95]. Increases of EIMI were also noted after administration of the ENT inhibitor dilazep or the AR agonist *R*-PIA, whereas the AR antagonist theophylline suppressed EIMI [96] Several subsequent studies demonstrated that A_1R agonists accentuate and A_1R antagonists attenuate EIMI, when infused into the motor cortex [97] or striatum [98,99]. AR antagonists like theophylline or caffeine (Figure 3), and lipophilic AR agonists like cyclohexyladenosine (CHA) modulate EIMI also after systemic administration. Experiments in which subtype-selective AR antagonists were administered either alone or in combination with agonists have indicated that the A_1R subtype is involved in modulation of EIMI, although a contribution of A_2R cannot be ruled out [97,99,100]. Co-administration of cAMP analogs, pertussis toxin or the *(R)*- and *(S)*-enantiomers of AR agonists with ethanol suggested involvement of G-protein-coupled A_1R and adenylate cyclase [101,102]. The importance of A_1R was proven by the fact that A_1R antisense, applied orally, systemically or directly into the striatum or cerebellum reduced the regional A_1R density and antagonized EIMI, whereas a mismatch control sequence had no effect [103,104]. A_1R in the motor cortex, striatum and cerebellum, but not in hippocampus [98] appear to affect EIMI via adenosine-induced decreases in glutamate release [105,106] and/or changes of chloride conductance via chloride channels coupled to the GABA-benzodiazepine receptor complex [102,107].

Besides playing a role in EIMI, adenosine is involved in other physiological responses related to the consumption of ethanol. The ENT1 inhibitor dipyridamole

prolongs, and the AR antagonist theophylline reduces the duration of ethanol-induced sleep [95]. Ethanol and acetate also potentiate the anesthetic effect of sevoflurane and isoflurane through metabolically generated adenosine and stimulation of A_1R [108-111]. In humans, the AR antagonist caffeine reverses most of the sedating effects of ethanol (sleepiness, lack of alertness, impaired memory) but not ethanol-induced dizziness [112]. A recent study in rodents showed that ethanol promotes non-REM sleep but does not affect REM sleep. The somnogenic effect of ethanol is related to adenosine inhibition of wake-promoting neurons in the basal forebrain via A_1R. Bilateral microinjections of the selective A_1R antagonist DPCPX in this area reduce the effect of ethanol on non-REM sleep [113]. A study in which ethanol was administered to mice, either alone or in combination with selective AR agonists and antagonists, and animals were tested for anxiety in the elevated plus-maze, has indicated that activation of A_1R also mediates the anxiolytic effect of ethanol [114].

Adenosine and A_1R are not only involved in the motor impairing, sleep-promoting and sedating effects of ethanol, but also in counteracting the negative symptoms of ethanol withdrawal. Withdrawal signs in rats such as tremors and audiogenically induced seizures are suppressed by an A_1R agonist (CCPA), and this beneficial effect is blocked after co-administration of an A_1R antagonist (DPCPX) [115]. Other negative symptoms of ethanol withdrawal, such as hyperexcitability [116] and increased anxiety [117,118] are also ameliorated upon stimulation of A_1R. AR antagonists (DPCPX, caffeine) are neurotoxic when administered during ethanol withdrawal, particularly in female mice, and these neurotoxic effects are reversed by an A_1R agonist (CCPA). Sex differences observed for neurotoxicity of A1R antagonists during ethanol withdrawal are probably related to N-methyl-D-aspartic acid (NMDA)-receptor-mediated downstream signaling which is more pronounced in females than in males [119,120].

Observed changes of A_1R densities in rodent brain during ethanol exposure appear to be dependent on the experimental paradigm, the radioligand which is used for binding assays and the brain area that is studied. Using the agonist [^{3}H]*R*-PIA, increases of B_{max} without any change of K_d were noted in the cerebral cortex of rats, 15 min after administration of ethanol (1.5 g/kg, [96]). In a later study, the same authors noted that the observed increase (+ 40.7%) is transient, receptor densities returning to the control value within 60 minutes [121]. Chronic administration of ethanol is also accompanied by an increased binding (+23%) of the agonist 2-chloro-*N6*-cyclopentyladenosine ([^{3}H] CCPA, Figure 3) in rat cerebral cortex. This increase persists longer than the one observed after acute administration. Elevated receptor densities are observed 3, 12 and 24 h after the last consumption of ethanol, but the ethanol effect disappears after 3 to 6 days [122]. Increased binding of the A_1R agonist [^{3}H]CHA was also noted in the cerebral cortex of mice following chronic administration of ethanol [123]. The increase is most pronounced after multiple episodes of ethanol withdrawal, and may be a compensatory inhibitory response to withdrawal seizures [124]. In contrast to the changes observed with A_1R agonists, cortical binding of the A_1R antagonist [^{3}H]DPCPX is not affected by ethanol treatment [116,122]. Whereas most studies reported a transient increase of A_1R agonist binding upon acute or

chronic administration of ethanol, one old [95] and one recent [125] study reported decreases of A_1R expression in some brain areas of rats. Decreased A_1R expression in the wake-promoting basal forebrain may be related to insomnia associated with ethanol withdrawal [125].

Only a single PET study has examined changes of A_1R expression after acute exposure of animals to ethanol [126]. In that study, Wistar rats were treated with a combination of ethanol and the AK inhibitor ABT-702, and scanned with the A_1R ligand [^{11}C] MPDX. A striking (40-45%) increase of tracer distribution volume and binding potential was noted in target areas such as hippocampus, striatum and cerebral cortex, 20-90 min after treatment. Additional PET studies could be performed to study the effect of ethanol only, either in rodents or in the human brain.

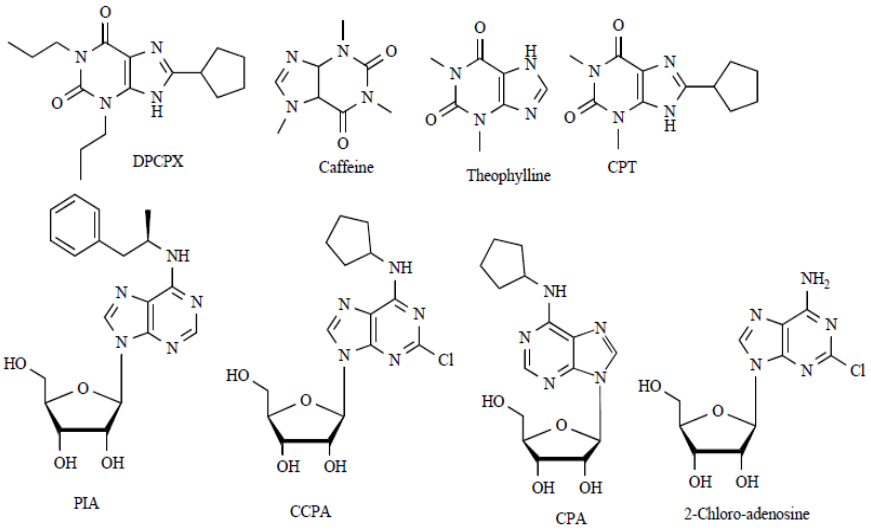

Fig. (3). AR ligands which are often used in binding studies. Top row: antagonists, bottom row: agonists.

3.4 Cerebral ischemia

Levels of extracellular adenosine in the brain are dramatically increased during ischemia. In patients with transient ischemic attack (TIA) or stroke, a rapid rise of the plasma concentration of adenosine occurs in peripheral venous blood, presumably because of spillover from the brain, and this increase persists for days (TIA) or weeks (stroke) [127]. Extracellular adenosine in the brain inhibits synaptic neurotransmission including the release of excitatory amino acids [128,129], leading to a better matching of energy demand and energy supply in ischemic areas and a reduction of delayed excitotoxicity [130]. Through A_1R, adenosine promotes both the spontaneous electrical shutdown of the ischemic brain [131] and post-ischemic electrocortical burst suppression [132,133]. When levels of extracellular adenosine in mouse brain are reduced by transgenic overexpression of AK, postischemic cell death is increased [134].

The importance of A_1R stimulation was also evident in studies regarding ischemic preconditioning. When neurons or living animals are exposed to a short period of sublethal ischemia, they are better protected to a subsequent serious ischemic insult. This beneficial effect of preconditioning disappears in the presence of an A_1R antagonist like DPCPX, suggesting that A_1R stimulation is involved [135-139]. The mechanisms underlying induction of rapid tolerance by a sublethal ischemic insult are not fully understood. Increases in protein kinase C activity, mitogen-activated protein (MAP) kinase activity, Akt activity, nitric oxide production and mitochondrial K_{ATP} channels may all be involved [135-139]. Activation of presynaptic K^+ channels via stimulation of A_1R may decrease evoked neurotransmitter release by hyperpolarization of the presynaptic membrane and thus improve resistance of the brain to ischemia.

In various animal and in vitro models, acute administration of A_1R agonists [140-143], inhibitors of adenosine uptake (propentofylline but not dipyridamole) [144], or inhibitors of AK [134] has been shown to result in protection against ischemic brain damage and reperfusion injury. Long-term treatment of gerbils with caffeine causes an upregulation of cerebral A_1R (10-17%) and greater resistance of neurons to ischemia induced by bilateral carotid artery occlusion [145]. Increasing the binding of adenosine to A_1R by administration of an allosteric enhancer also results in decreased brain damage after a hypoxic insult [146]. In contrast, acute administration of an A_1R antagonist such as DPCPX aggravates the consequences of cerebral ischemia [141,142,147].

Therapeutic application of A_1R agonists in stroke patients may be complicated by the fact that such compounds can have diametrically opposite effects after chronic and acute administration. Acute treatment with an A_1R agonist may reduce postischemic neuronal losses whereas chronic treatment with the same compound increases brain damage [142,148]. Other agonists are neuroprotective even during chronic treatment [149]. The underlying mechanisms are far from clear since the consequences of chronic administration of A_1R ligands can not always be related to up- or downregulation of A_1R [142].

Many studies have examined changes of A_1R expression in the brain of experimental animals after cerebral ischemia. In most studies, rapid decreases of A_1R mRNA and protein were observed during reperfusion [150-152] but in one study, decreases were noted at the mRNA but not the protein level [153]. These (slightly) discrepant findings may be due to the fact that different models of ischemia were employed and animals were examined at different intervals after the ischemic insult. Some changes appear only at intervals greater than 24 hours. Changes of A_1R expression during ischemia have been little examined, as opposed to changes during reperfusion. In a single study, increases of A_1R expression (at the mRNA and protein level) were noted during bilateral carotid artery ligation with a return to normal values immediately after reperfusion [154]. An interesting study from Japan examined changes of cerebral A_1R in cat brain following an ischemic insult, using PET and the radioligand ^{11}C-MPDX. Decreases of A_1R were noted, and the magnitude of these losses increased with increasing severity of the insult. The extent of ^{11}C-MPDX binding directly after reperfusion appeared to be a sensitive predictor of survival and disease symptoms during the follow-up period which lasted up to 2 months [155,156].

3.5 Epilepsy

Adenosine inhibits the release of excitatory neurotransmitters and suppresses cellular activity and energy demand. Based on this evidence, it has been proposed that adenosine is a powerful endogenous anticonvulsant substance [157]. In amygdala-kindled rats, intracerebrally administered A_1R agonists, such as 2-chloroadenosine (Figure 3) and PIA, could indeed suppress seizures [158-162]. These substances were also effective in other animal models of eplilepsy, such as entorhinal cortex kindling [163], piriform cortex kindling [164], hippocampal kindling [162,165], caudate nucleus kindling [162], intrahippocampal injection of kainic acid [166], intraperitoneal injection of pilocarpine [167] and hypoxia-induced convulsions [168]. The location of intracerebral administration is probably important for the therapeutic outcome [169]. In many studies, co-administration of A_1R antagonists was shown to result in a reduction of the anticonvulsant effect, which indicates that the A_1R subtype is involved in the beneficial action of the agonists.

Inhibitors of the enzyme AK can be systemically administered and can increase extracellular adenosine levels in metabolically active brain regions. Such compounds show similar anticonvulsant actions as A_1R agonists but lack the undesired peripheral side effects of these drugs [170]. AK is regionally overexpressed in epilepsy and this overexpression appears to contribute to the development and progression of seizure activity [134,171,172]. Local administration of adenosine by implanting encapsulated myoblasts could be a promising strategy for long term treatment of focal epilepsy [173]

Further evidence for the involvement of the A_1R in seizure suppression was obtained in animal models where A_1R antagonists were administered. In a cat model of

epilepsy (general seizures induced by intracortical injection of penicillin), the A_1R antagonist CPT significantly prolonged the cycle period of seizures by increasing the duration of ictal discharge, in contrast to 7-aminobutyric acid or opioid peptides [174]. Adenosine may accumulate during the ictal phase and be cleared during the interictal phase in status epilepticus. In a rat model of epilepsy (electrically induced seizures), secondary seizures were prolonged after administration of an A_1R antagonist, and partial seizures were converted into generalized motor seizures [175]. In another rat model of epilepsy (i.p. administration of pilocarpine), the A_1R antagonists DPCPX and 3,7-dimethyl-1-propargylxanthine (DPMX) showed proconvulsant effects, by significantly reducing the latency to develop status epilepticus [167]. Theophylline also lowered the seizure threshold and prolonged hyperthermia-induced seizures in juvenile rats [176]. Using a selective A_1R antagonist (CPT), evidence was obtained that the inhibitory effect of low frequency stimulation of the perforant path on kindling acquisition in rats is mediated by stimulation of A_1R [177].

Changes of cerebral A_1R densities have been assessed both in animal models of epilepsy and in human brain post mortem. In a rat model of acute general seizure (i.p. injection of a convulsive dose of bicuculline), a widespread increase of A_1R (^{3}H-CHA binding) was noted, which was particularly evident in hippocampus, amygdala, substantia nigra and septum [178]. In a mouse model of general seizure (pentylentetrazol-induced convulsion) [179], A_1R were upregulated in most brain areas but downregulated in the basal ganglia [180]. In tissue samples acquired from patients with temporal lobe epilepsy, a 48% increase of A_1R density was observed in neocortex as compared to control samples from non-epileptic subjects [181].

However, in another study on human temporal lobe epilepsy, A_1R binding in temporal cortex was found to be reduced compared to normal postmortem controls [182]. A 15% decline of A_1R density was also noted in the basal ganglia and thalamic nuclei of genetic absence epilepsy rats from Strasbourg compared to wild-type littermates [183]. Even greater losses of A_1R were noted in the hippocampus and cerebral cortex of kainate-treated, hippocampus-kindled and amygdala-kindled rats, animal models of chronic epilepsy [184-187].

These conflicting results (either an upregulation or downregulation of A_1R) may be related to differences in the experimental setup in animal models and differences in patient selection in human studies. An acute seizure, or a limited number of seizures may be accompanied by upregulation of A_1R, or increased coupling of A_1R to G-proteins [188,189], as a protective mechanism enhancing the anticonvulsant effect of endogenous adenosine. However, chronic seizures may cause a significant death of neurons with accompanying losses of A_1R. The effects of partial and general seizures may also be different and the age (or developmental stage) of the subjects may affect the response of A_1R to kindling [178,190].

3.6 Traumatic brain injury

Studies in A_1R knockout mice have confirmed that this subtype plays an important role in suppressing neuronal hyperactivity. When normal and A_1R knockout mice were subjected to controlled cortical impact – an animal model of traumatic brain injury (TBI) - seizure scores were much higher in the knockouts and only the knockout animals developed lethal status epilepticus [191]. Similarly, unilateral hippocampal kainate injection caused non-convulsive status epilepticus in wild-type mice but severe convulsions and subsequent death of the animals in A_1R knockouts [192]. The authors concluded that activation of A_1R by adenosine is crucial in keeping an epileptic focus localized. Status epilepticus results in widespread adenosine release throughout the brain and suppression of the excitability of neurons remote from the epileptic focus via stimulation of A_1R. In A_1R knockout mice, this protective mechanism is lacking, so that severe convulsions and lethal status epilepticus can develop [192]. In another animal study on mild TBI, A_1R knockout mice were shown to display a 20-50% enhanced microglial response compared to their wild-type littermates. Moreover, stimulation of A_1R in BV-2 (immortalized mouse microglia) cells inhibited microglial proliferation [193]. Thus, A_1Rs appear to play an anti-inflammatory role in TBI-induced neuroinflammation.

To the best of our knowledge, no PET studies on changes of A_1R expression in epileptic patients or in animal models of epilepsy and TBI have been performed. Thus, there is considerable opportunity for imaging studies in this area.

3.7 Neuroinflammation

Besides its well-known function as an inhibitor of neuronal overactivity and its involvement in the regulation of sleep, adenosine has been proposed to act as an endogenous anti-inflammatory agent [194]. In the CNS, A_1Rs are expressed not only on neurons but also on glia [195]. A_1R stimulation in microglia, the endogenous immune cells of the brain, may have both pro- and anti-inflammatory effects, depending on the presence or absence of other factors in the environment, such as phorbol 12-myristate 13-acetate [196]. An early study reported that simultaneous activation of both A_1R and $A_{2A}R$ stimulates microglial proliferation, whereas selective A_1R or $A_{2A}R$ agonists when applied alone have no effect [195]. However, later studies have indicated that in most situations, A_1R agonists suppress neuroinflammation.

In cultured astrocytes, CCPA enhanced the release of nerve growth factor [197], a compound which is essential for neuronal protection and a suppressor of neuroinflammation within the specific environment of the brain [198]. In plasmacytoid dendritic cells, adenosine has been suggested to play a dual role: first, chemotaxis to the site of inflammation is stimulated via A_1R, then, the extent of the inflammatory response is

limited by inhibition of the production of several cytokines such as interleukin-6, interleukin-12 and interferon-α [199].

The importance of A_1R in controlling neuroinflammation was highlighted by studies of experimental allergic encephalomyelitis (EAE). Mice lacking A_1R developed a much more severe, progressive-relapsing form of EAE than their wild-type littermates. Reduced densities of A_1R in microglia of wild-type mice were observed during the neuro-inflammatory phase of EAE. Upregulation of A_1R by treatment of normal mice with caffeine reduces EAE severity, and this beneficial effect of caffeine can be enhanced by concomitant administration of an A_1R agonist [200]. In a rat model of neuroinflammation (EAE induced by guinea pig spinal cord homogenates), chronic caffeine treatment results in up-regulation of A_1R and attenuation of EAE pathology [201]. Experimentally induced neuroinflammation by chronic infusion of lipopolysaccharide (LPS) into the fourth ventricle of young rats, and natural microglia activation in aged rats are also attenuated after treatment of animals with caffeine [202]. In contrast to EAE (an animal model of chronic neuro-inflammation which is associated with a downregulation of A_1R), acute inflammation of mouse brain after administration of LPS leads to increased A_1R expression in cortical areas and this response is dependent on the transcription factor NF-kappaB [203].An interesting study examined the role of A_1R in brain tumors. Gliomas do not consist only of tumor cells but to a large extent (up to 30%) also of microglia and macrophages. Microglial cells accumulate particularly at the tumor rim. In the tumor environment, microglia acquires a different phenotype which is associated with expression of matrix metalloprotease II (MMP2). After acquisition of this novel phenotype, the microglial cells do not suppress but can actually promote tumor growth and invasion since these processes are MMP2-dependent. Experimental glioblastomas grew more vigorously and were associated with larger numbers of microglial cells in A_1R knockout mice than in wild-type mice. In wild-type animals, A_1R were up-regulated in microglia in contact with tumor cells but not in the rest of the brain. When glioma and microglia cells were cultured together in vitro, A_1R agonists suppressed the growth of tumor cells, but in the absence of microglia, the same compounds stimulated tumor growth. Thus, adenosine attenuates glioblastoma growth, acting through microglial A_1R [204].

Changes in cerebral A_1R density caused by glioma invasion have been examined with the tracer [^{18}F] CPFPX and PET, both in an animal model (F98 glioma-bearing rats) and in a patient with recurrent glioblastoma multiforme. In the animal model, A_1R were also quantified by in vitro and in vivo autoradiography and immunohistochemical analysis. A_1R were shown to be upregulated (by 36 to 46%) in a zone directly surrounding the tumor, and to be localized in activated astrocytes [205]. It would be interesting to study changes of A_1R expression with microPET in animal models of neuroinflammation (e.g., the EAE model, the LPS model, or virally induced encephalitis). Such studies have not yet been reported.

3.8 Human diseases of the CNS

3.8.1 Alzheimer's disease (AD)

Since A_1R signaling can be neuroprotective, many investigators examined changes of regional A_1R density in human brain in neurodegenerative disorders. Initial autoradiographic studies were focused on AD and the hippocampus, a brain region involved in memory. A significant loss of A_1R was observed in the CA1 (-47%) and dentate gyrus molecular layers (-46%) of the hippocampus but not in the CA3 [206]. Another study reported 40-60% decreases in all areas of the hippocampus, the most striking losses occurring in the molecular layer of the dentate gyrus [207]. Still another investigation reported substantial decreases in the dentate gyrus but A_1R densities close to normal in CA1 and CA3 [208]. The former two investigations used the A_1R agonist [^{3}H] CHA whereas the last study employed the antagonist ligand [^{3}H] CPDPX.

Binding of an A_1R agonist ([^{3}H] *R*-PIA) and antagonist ([^{3}H] CPDPX) in the AD hippocampus were later directly compared. Both ligands detected prominent losses of A_1R in the dentate gyrus. Decreased agonist binding was observed in CA1 and outer layers of the parahippocampal gyrus, whereas losses of antagonist binding were noted in the subiculum and CA3. These decreases reflected reductions of receptor number (B_{max}) rather than reductions of the affinity (K_D) of A_1R for the radioligands [209].In the striatum of AD patients, 30-36% losses of A_1R were noted both in the caudate nucleus and putamen, and these losses appeared to parallel the decrease of choline acetyl transferase [210].

An immunohistochemical study from Spain showed that A_1R are redistributed in the hippocampus and cerebral cortex of AD patients in comparison to age-matched controls. A_1R accumulate in degenerating neurons and are co-localized with ß-amyloid in senile plaques and with tau in neurons with tau deposition. Studies in the human neuroblastoma cell line SH-SY5Y indicated that A_1R stimulation increases the production of soluble forms of amyloid precursor protein, and the phosphorylation and translocation of tau to the cytoskeleton. By inhibiting the deposition of amyloid and enhancing the translocation of tau, A_1R stimulation may slow down the process of neurodegeneration [211].

An upregulation of A_1R was detected in the frontal cortex of AD patients (both at early and advanced stages of the disease), using quantitative autoradiography and the radioligand [^{3}H]DPCPX [212]. However, a PET study in AD patients and elderly normal subjects indicated significant decreases of the binding potential of [^{11}C]MPDX in the temporal and medial temporal cortices and thalamus of the patients with no significant change in other areas of the brain [213] (Figure 4). Discrepant findings in human studies may be related to the facts that different patient groups were selected (early vs. late onset AD), different brain regions were examined, and different techniques were used for quantification (immunohistochemistry, ligand binding). Moreover, a transient upregulation of A_1R may be followed by an eventual receptor loss.

3.8.2 Pick's and Creutzfeld-Jakob disease

In the frontal cortex of individuals with Pick's [214] and Creutzfeldt-Jakob [215] disease, similar increases of A_1R density were noted as in patients with AD, using quantitative autoradiography and [^{3}H]DPCPX. No PET studies with [^{11}C] MPDX or [^{18}F] CPFPX in such patients have been reported.

3.8.3 Multiple sclerosis (MS)

Several studies have reported changes of AR signaling in patients with MS. Plasma levels of TNF-α in such patients are significantly higher and levels of adenosine are significantly lower than in control subjects. Stimulation of peripheral blood mononuclear cells (PBMC) with a selective A_1R agonist (*R*-PIA) inhibits the mitogen-stimulated production of TNF-α in healthy subjects but not in MS patients, whereas the opposite is observed for the mitogen-stimulated production of interleukin-6 [216]. A_1R densities in PBMC and in brain tissue from MS-patients are significantly decreased (by 53% and 49%, respectively) compared to age-matched controls [217]. Thus, both A_1R densities and the coupling of A_1R to cytokine signaling systems appear to be altered in MS. However, no PET studies with A_1R ligands have been performed in this patient group.

3.8.4 Parkinson's disease

In the 1-methyl-4-phenyl-1,2,3,6-tetrahydropyridine mouse model of Parkinson's disease, the drug paeoniflorin proved capable of reducing neurodegeneration and inhibiting neuroinflammation by activation of A_1R [218]. Thus, modulation of neuroinflammation via A_1R may be a novel approach towards treatment of neurodegenerative disease.
Deep brain stimulation (DBS) is frequently applied for the treatment of movement disorders and may also benefit individuals with psychiatric disease. Recently, it was shown that the mechanism underlying the beneficial effect of DBS is a local release of ATP which is extracellularly metabolized to adenosine and suppresses tremor via A_1R. The effect of DBS can be mimicked by intrathalamic infusion of A_1R agonists. On the other hand, AR antagonists like caffeine can trigger or exacerbate essential tremor [219].

3.8.5 Schizophrenia

A partial loss of A_1R during birth and a corresponding reduction of the control of dopamine activity in later life has been proposed to play a role in the inhibitory deficit in schizophrenia [220,221]. Association between a single nucleotide polymorphism of the A_1R gene (rs3766553) and schizophrenia was indeed noted in a Japanese population [222]. PET studies of cerebral A_1R in patients with schizophrenia have not yet been performed.

4. Pharmacodynamic studies

4.1 A_1R (ant) agonists

PET has important applications in the study of pharmacodynamics, i.e. assessment of the effects of drugs in the healthy and diseased body, including their mechanisms of action and the relationship between drug concentration and effect. During the development of CNS drugs, PET is often used to measure the dose-dependent occupancy of target receptors in the human brain by a non-radioactive test compound. PET is also capable of measuring the metabolic response of tissues to treatment quantitatively, repeatedly and noninvasively, both in experimental animals and humans.

Only a few PET studies regarding A_1R occupancy by cold antagonists have been reported in the literature. An interesting paper from Germany showed that the binding of ^{18}F-CPFPX in rat brain is reduced after treatment of animals with caffeine, shortly before injection of the tracer. At a dose of 4 mg/kg, corresponding to consumption of three to four cups of coffee by a human being, tracer binding was strongly (ca. 50%) suppressed, suggesting ~70% receptor occupancy [223]. Another study showed that ^{18}F-CPFPX bound to A_1R in human brain can be dose-dependently displaced by injecting non-radioactive CPFPX [224]. A microPET study from our own group has indicated that A_1R in rat brain are almost completely occupied after administration of DPCPX (3 mg/kg, i.p.), 20 min before injection of ^{11}C-MPDX [126].

Thus, the dose-dependent occupancy of A_1R in the brain by test drugs may be assessed by PET. Dose-dependent effects of A_1R agonists (or AK inhibitors, see 4.2) on organ metabolism could be assessed as well, using the radiolabeled glucose analog [^{18}F]FDG, but such studies have not yet been reported.

4.2 AK inhibitors

AK regulates intra- and extracellular adenosine concentrations by phosphorylation of adenosine to AMP. Although ADA also removes adenosine by converting it to inosine, the reaction catalyzed by AK is the most important pathway of adenosine removal under physiological conditions [225]. Since the major adenosine-specific nucleoside carrier acts as a non-concentrative, bi-directional, facilitated diffusion transporter, adenosine transport is driven by the concentration gradient across the cell membrane. Inhibition of AK raises intracellular adenosine, diminishes the concentration gradient and decreases the cellular uptake of adenosine, resulting in increased extracellular adenosine concentrations, particular under pathophysiological conditions and in tissues or brain regions where the formation of adenosine is increased by net catabolism of ATP [226-228]. An in vivo study in rats has shown that AK inhibitors (AKIs) augment the increases of extracellular adenosine during excitotoxic insults in the striatum but do not affect striatal adenosine levels in vehicle-treated controls [228]. Thus, AKIs represent a strategy for potentiating the protective actions of endogenous adenosine during tissue trauma [229]. This therapeutic approach may be advantageous in cases where not a single subtype (e.g., A_1R) but rather a multiplicity of AR subtypes should be stimulated for the beneficial effect [230].

Three applications of AKIs have been proposed. First, intrathecally administered AR agonists [231-233] and AKIs [232-234] have antinociceptive effects in experimental animals. These effects are counteracted by selective A_1R antagonists but not by $A_{2A}R$ antagonists suggesting involvement of A_1R stimulation [228,232,235,236]. Novel AKIs such as ABT-702 and A-286501 can also be given subcutaneously or orally and are then effective in animal models of acute, inflammatory and neuropathic pain [235,237-239]. Substantial interest in the use of AKIs was raised by the fact that these compounds can be equally effective as morphine for the suppression of pain but show less potential to develop tolerance [238,240,241]. The use of AKIs rather than AR agonists allows an adequate separation between antinociceptive and motor-impairing effects [242]. Second, AR agonists and AKIs have shown anti-inflammatory efficacy in various animal models of acute and chronic inflammation [238,239,243-248]. A third potential application of AKIs is in the treatment of epilepsy. These compounds suppress seizures in rodent models, such as the bicuculline-induced seizure [249] and the maximal electroshock [170,250,251] model, presumably via an interaction of adenosine with cerebral A_1R. For that reason and because upregulation of the enzyme AK is involved in epileptogenesis [171], AKIs are considered promising anticonvulsants [170,252,253].

If a ligand could be developed of which the binding is sensitive to competition by endogenous adenosine, PET imaging could be applied to assess changes of extracellular adenosine induced by AKIs.

5. Conclusion

The purine nucleoside adenosine and its A_1R are implied in many physiological functions, such as regulation of the sleep-wake cycle, aggression, and anxiety, habituation of animals to a novel environment, protection of cells against the negative consequences of hypoxia and ischemia. Adenosinergic signaling is also implied in ethanol-induced motor impairment, and withdrawal symptoms after ethanol abuse. Stimulation of A_1R has anticonvulsant and anti-inflammatory actions. Changes of A_1R expression have been noted in animal models of epilepsy, the micro-environment of brain tumors, and various diseases of the human CNS such as AD, Pick's disease, Creutzfeld-Jakob disease, MS and schizophrenia. Since appropriate ligands for PET imaging of A_1R are now available, PET can be applied to elucidate the role of A_1R in the normal and diseased human brain and to study the pharmacodynamics of A_1R agonists and AKI.

6. Aims and outline of the thesis

The aim of this thesis is to apply PET imaging to measure therapy-related occupancy and disease-induced changes of expression of adenosine A_1 receptors in the (rodent) brain. We used the radiolabeled xanthine [^{11}C]-MPDX as tracer for evaluation of drug occupancy. Changes of A_1R expression were examined in a rodent encephalitis model.

Chapter 1: The initial chapter is a general introduction and literature review concerning PET imaging of adenosine A_1 receptors and the function of these binding sites in health and disease.

Chapter 2: The following chapter was a pilot study validating the use of [^{11}C]-MPDX for quantitative microPET studies of cerebral A_1R in rodents. A regional distribution of radioactivity was observed which corresponded closely to regional densities of adenosine A_1 receptors known from autoradiography. Tracer binding was blocked by the selective A_1R antagonist DPCPX. However, raising extracellular adenosine by pretreating rats with ethanol and the adenosine kinase inhibitor ABT-702 did not result in measurable competition between adenosine and [^{11}C]-MPDX.

Chapter 3:. A_1R agonists or adenosine kinase inhibitors may be beneficial in the treatment of neurodegenerative diseases, epilepsy, inflammation and various forms of pain. By using PET it is possible to measure the fraction of receptor populations which is occupied by cold (non-radioactive) drugs in the living brain. Thus, occupancy of a target receptor can be related to the intensity of the therapeutic effect or to unwanted side effects. In chapter 4 we evaluated if [^{11}C]-MPDX and PET can be used to assess A_1R occupancy in the rodent brain by a non-radioactive agonist (N^6-cyclopentyladenosine) and antagonist (caffeine).

Chapter 4: Adenosine A_1 receptors are implied in modulation of neuroinflammation. Upregulation of A_1Rs may also have neuroprotective properties. In chapter 4 we applied PET and [^{11}C] MPDX to quantify changes of A_1R expression in rat brain as a consequence of herpes simplex virus-induced encephalitis. We also performed a qualitative immunohistochemistry study of A_1R in the same animal model.

Chapter 5: With increasing prevalence of brain disorders there is an increasing demand for CNS drugs, but many potential candidates fail to cross the blood-brain barrier (BBB). Thus, there is a need to modulate BBB permeability and facilitate the entry of therapeutic drugs. Stimulation of adenosine A_1 and A_{2A} receptors may be possible strategy to reach this aim. We attempted to develop a PET assay which can assess changes in blood-brain-barrier permeability and can be used to examine the effects of permeability-modulating drugs. Two hydrophilic tracers (a CXCR4 antagonist and dopamine agonist) were used in this attempt.

Chapter 6 summarizes the findings of the studies reported in chapters 2 to 5. The final chapter, ***chapter 7,*** is a description of future perspectives and a conclusion.

7. References

[1] Marchi, M.; Raiteri, L.; Risso, F.; Vallarino, A.; Bonfanti, A.; Monopoli, A.; Ongini, E.; Raiteri, M. Effects of adenosine A1 and A2A receptor activation on the evoked release of glutamate from rat cerebrocortical synaptosomes. *Br. J. Pharmacol.*, **2002,** 136, 434-440

[2] Quarta, D.; Ferre, S.; Solinas, M.; You, Z.B.; Hockemeyer, J.; Popoli, P.; Goldberg, S.R. Opposite modulatory roles for adenosine A1 and A2A receptors on glutamate and dopamine release in the shell of the nucleus accumbens. Effects of chronic caffeine exposure. *J. Neurochem.*, **2004,** 88, 1151-1158

[3] Ciruela, F.; Casado, V.; Rodrigues, R.J.; Lujan, R.; Burgueno, J.; Canals, M.; Borycz, J.; Rebola, N.; Goldberg, S.R.; Mallol, J.; Cortes, A.; Canela, E.I.; Lopez-Gimenez, J.F.; Milligan, G.; Lluis, C.; Cunha, R.A.; Ferre, S.; Franco, R. Presynaptic control of striatal glutamatergic neurotransmission by adenosine A1-A2A receptor heteromers. *J. Neurosci.*, **2006,** 26, 2080-2087

[4] Floran, B.; Barajas, C.; Floran, L.; Erlij, D.; Aceves, J. Adenosine A1 receptors control dopamine D1-dependent [(3)H]GABA release in slices of substantia nigra pars reticulata and motor behavior in the rat. *Neuroscience*, **2002,** 115, 743-751

[5] Jeong, H.J.; Jang, I.S.; Nabekura, J.; Akaike, N. Adenosine A1 receptor-mediated presynaptic inhibition of GABAergic transmission in immature rat hippocampal CA1 neurons. *J. Neurophysiol.*, **2003,** 89, 1214-1222

[6] Yum, D.S.; Cho, J.H.; Choi, I.S.; Nakamura, M.; Lee, J.J.; Lee, M.G.; Choi, B.J.; Choi, J.K.; Jang, I.S. Adenosine A(1) receptors inhibit GABAergic transmission in rat tuberomammillary nucleus neurons. *J. Neurochem.*, **2008,** 106, 361-371

[7] Tanase, D.; Baghdoyan, H.A.; Lydic, R. Dialysis delivery of an adenosine A1 receptor agonist to the pontine reticular formation decreases acetylcholine release and increases anesthesia recovery time. *Anesthesiology*, **2003,** 98, 912-920

[8] Arrigoni, E.; Chamberlin, N.L.; Saper, C.B.; McCarley, R.W. Adenosine inhibits basal forebrain cholinergic and noncholinergic neurons in vitro. *Neuroscience*, **2006,** 140, 403-413

[9] Van Dort, C.J.; Baghdoyan, H.A.; Lydic, R. Adenosine A(1) and A(2A) receptors in mouse prefrontal cortex modulate acetylcholine release and behavioral arousal. *J. Neurosci.*, **2009,** 29, 871-881

[10] Ballarin, M.; Reiriz, J.; Ambrosio, S.; Mahy, N. Effect of locally infused 2-chloroadenosine, an A1 receptor agonist, on spontaneous and evoked dopamine release in rat neostriatum. *Neurosci. Lett.*, **1995,** 185, 29-32

[11] Jin, S.; Fredholm, B.B. Adenosine A1 receptors mediate hypoxia-induced inhibition of electrically evoked transmitter release from rat striatal slices. *Eur. J. Pharmacol.*, **1997,** 329, 107-113

[12] Borycz, J.; Pereira, M.F.; Melani, A.; Rodrigues, R.J.; Kofalvi, A.; Panlilio, L.; Pedata, F.; Goldberg, S.R.; Cunha, R.A.; Ferre, S. Differential glutamate-dependent and glutamate-independent adenosine A1 receptor-mediated modulation of dopamine release in different striatal compartments. *J. Neurochem.*, **2007,** 101, 355-363

[13] Costenla, A.R.; de Mendonca, A.; Ribeiro, J.A. Adenosine modulates synaptic plasticity in hippocampal slices from aged rats. *Brain Res.*, **1999,** 851, 228-234

[14] de Mendonca, A.; Ribeiro, J.A. Endogenous adenosine modulates long-term potentiation in the hippocampus. *Neuroscience*, **1994,** 62, 385-390

[15] Rex, C.S.; Kramar, E.A.; Colgin, L.L.; Lin, B.; Gall, C.M.; Lynch, G. Long-term potentiation is impaired in middle-aged rats: regional specificity and reversal by adenosine receptor antagonists. *J. Neurosci.*, **2005,** 25, 5956-5966

[16] Zimmermann, H. Biochemistry, localization and functional roles of ecto-nucleotidases in the nervous system. *Prog. Neurobiol.*, **1996,** 49, 589-618

[17] Zimmermann, H. Extracellular metabolism of ATP and other nucleotides. *Naunyn Schmiedebergs Arch. Pharmacol.*, **2000,** 362, 299-309

[18] Dunwiddie, T.V.; Diao, L.; Proctor, W.R. Adenine nucleotides undergo rapid, quantitative conversion to adenosine in the extracellular space in rat hippocampus. *J. Neurosci.*, **1997,** 17, 7673-7682

[19] Latini, S.; Pedata, F. Adenosine in the central nervous system: release mechanisms and extracellular concentrations. *J. Neurochem.*, **2001,** 79, 463-484

[20] James, S.; Richardson, P.J. Production of adenosine from extracellular ATP at the striatal cholinergic synapse. *J. Neurochem.*, **1993,** 60, 219-227

[21] Nagy, J.I.; Geiger, J.D.; Daddona, P.E. Adenosine uptake sites in rat brain: identification using [3H]nitrobenzylthioinosine and co-localization with adenosine deaminase. *Neurosci. Lett.*, **1985,** 55, 47-53

[22] Patel, B.T.; Tudball, N. Localization of S-adenosylhomocysteine hydrolase and adenosine deaminase immunoreactivities in rat brain. *Brain Res.*, **1986,** 370, 250-264

[23] Reddington, M.; Pusch, R. Adenosine metabolism in a rat hippocampal slice preparation: incorporation into S-adenosylhomocysteine. *J. Neurochem.*, **1983,** 40, 285-290

[24] Collis, M.G.; Hourani, S.M. Adenosine receptor subtypes. *Trends Pharmacol. Sci.*, **1993,** 14, 360-366

[25] Fredholm, B.B.; Abbracchio, M.P.; Burnstock, G.; Daly, J.W.; Harden, T.K.; Jacobson, K.A.; Leff, P.; Williams, M. Nomenclature and classification of purinoceptors. *Pharmacol. Rev.*, **1994,** 46, 143-156

[26] Haas, H.L.; Selbach, O. Functions of neuronal adenosine receptors. *Naunyn Schmiedebergs Arch. Pharmacol.*, **2000,** 362, 375-381

[27] Fredholm, B.B.; Ijzerman, A.P.; Jacobson, K.A.; Klotz, K.N.; Linden, J. International Union of Pharmacology. XXV. Nomenclature and classification of adenosine receptors. *Pharmacol. Rev.*, **2001,** 53, 527-552

[28] Fredholm, B.B.; Arslan, G.; Halldner, L.; Kull, B.; Schulte, G.; Wasserman, W. Structure and function of adenosine receptors and their genes. *Naunyn Schmiedebergs Arch. Pharmacol.*, **2000,** 362, 364-374

[29] Mahan, L.C.; McVittie, L.D.; Smyk-Randall, E.M.; Nakata, H.; Monsma, F.J., Jr.; Gerfen, C.R.; Sibley, D.R. Cloning and expression of an A1 adenosine receptor from rat brain. *Mol. Pharmacol.*, **1991,** 40, 1-7

[30] Daly, J.W.; Padgett, W.L. Agonist activity of 2- and 5'-substituted adenosine analogs and their N6-cycloalkyl derivatives at A1- and A2-adenosine receptors coupled to adenylate cyclase. *Biochem. Pharmacol.*, **1992,** 43, 1089-1093

[31] Dixon, A.K.; Gubitz, A.K.; Sirinathsinghji, D.J.; Richardson, P.J.; Freeman, T.C. Tissue distribution of adenosine receptor mRNAs in the rat. *Br. J. Pharmacol.*, **1996,** 118, 1461-1468

[32] Fastbom, J.; Pazos, A.; Probst, A.; Palacios, J.M. Adenosine A1 receptors in the human brain: a quantitative autoradiographic study. *Neuroscience*, **1987,** 22, 827-839

[33] Fastbom, J.; Pazos, A.; Palacios, J.M. The distribution of adenosine A1 receptors and 5'-nucleotidase in the brain of some commonly used experimental animals. *Neuroscience*, **1987,** 22, 813-826

[34] Rivkees, S.A.; Price, S.L.; Zhou, F.C. Immunohistochemical detection of A1 adenosine receptors in rat brain with emphasis on localization in the hippocampal formation, cerebral cortex, cerebellum, and basal ganglia. *Brain Res.*, **1995,** 677, 193-203

[35] Schindler, M.; Harris, C.A.; Hayes, B.; Papotti, M.; Humphrey, P.P. Immunohistochemical localization of adenosine A1 receptors in human brain regions. *Neurosci. Lett.*, **2001,** 297, 211-215

[36] Svenningsson, P.; Hall, H.; Sedvall, G.; Fredholm, B.B. Distribution of adenosine receptors in the postmortem human brain: an extended autoradiographic study. *Synapse*, **1997,** 27, 322-335

[37] Ochiishi, T.; Chen, L.; Yukawa, A.; Saitoh, Y.; Sekino, Y.; Arai, T.; Nakata, H.; Miyamoto, H. Cellular localization of adenosine A1 receptors in rat forebrain: immunohistochemical analysis using adenosine A1 receptor-specific monoclonal antibody. *J. Comp Neurol.*, **1999,** 411, 301-316

[38] van Calker, D.; Muller, M.; Hamprecht, B. Adenosine regulates via two different types of receptors, the accumulation of cyclic AMP in cultured brain cells. *J. Neurochem.*, **1979,** 33, 999-1005

[39] Linden, J. Molecular approach to adenosine receptors: receptor-mediated mechanisms of tissue protection. *Annu. Rev. Pharmacol. Toxicol.*, **2001,** 41, 775-787

[40] Santicioli, P.; Del Bianco, E.; Tramontana, M.; Maggi, C.A. Adenosine inhibits action potential-dependent release of calcitonin gene-related peptide- and substance P-like immunoreactivities from primary afferents in rat spinal cord. *Neurosci. Lett.*, **1992,** 144, 211-214

[41] Salter, M.W.; De Koninck, Y.; Henry, J.L. Physiological roles for adenosine and ATP in synaptic transmission in the spinal dorsal horn. *Prog. Neurobiol.*, **1993,** 41, 125-156

[42] Li, J.; Perl, E.R. Adenosine inhibition of synaptic transmission in the substantia gelatinosa. *J. Neurophysiol.*, **1994,** 72, 1611-1621

[43] Ishiwata, K.; Kimura, Y.; de Vries, E.F.; Elsinga, P.H. PET tracers for mapping adenosine receptors as probes for diagnosis of CNS disorders. *CNS Agents Med. Chem.*, **2007,** 7, 57-77

[44] Bauer, A.; Ishiwata, K. Adenosine receptor ligands and PET imaging of the CNS. *Handb. Exp. Pharmacol.*, **2009,** 617-642

[45] Herzog, H.; Elmenhorst, D.; Winz, O.; Bauer, A. Biodistribution and radiation dosimetry of the A1 adenosine receptor ligand 18F-CPFPX determined from human whole-body PET. *Eur. J. Nucl. Med. Mol. Imaging*, **2008,** 35, 1499-1506

[46] Matsuya, T.; Takamatsu, H.; Murakami, Y.; Noda, A.; Ichise, R.; Awaga, Y.; Nishimura, S. Synthesis and evaluation of [11C]FR194921 as a nonxanthine-type PET tracer for adenosine A1 receptors in the brain. *Nucl. Med. Biol.*, **2005,** 32, 837-844

[47] Basheer, R.; Strecker, R.E.; Thakkar, M.M.; McCarley, R.W. Adenosine and sleep-wake regulation. *Prog. Neurobiol.*, **2004,** 73, 379-396

[48] Porkka-Heiskanen, T.; Strecker, R.E.; Thakkar, M.; Bjorkum, A.A.; Greene, R.W.; McCarley, R.W. Adenosine: a mediator of the sleep-inducing effects of prolonged wakefulness. *Science*, **1997,** 276, 1265-1268

[49] Elmenhorst, D.; Meyer, P.T.; Winz, O.H.; Matusch, A.; Ermert, J.; Coenen, H.H.; Basheer, R.; Haas, H.L.; Zilles, K.; Bauer, A. Sleep deprivation increases A1 adenosine receptor binding in the human brain: a positron emission tomography study. *J. Neurosci.*, **2007,** 27, 2410-2415

[50] Basheer, R.; Halldner, L.; Alanko, L.; McCarley, R.W.; Fredholm, B.B.; Porkka-Heiskanen, T. Opposite changes in adenosine A1 and A2A receptor mRNA in the rat following sleep deprivation. *Neuroreport*, **2001,** 12, 1577-1580

[51] Basheer, R.; Bauer, A.; Elmenhorst, D.; Ramesh, V.; McCarley, R.W. Sleep deprivation upregulates A1 adenosine receptors in the rat basal forebrain. *Neuroreport*, **2007,** 18, 1895-1899

[52] Elmenhorst, D.; Basheer, R.; McCarley, R.W.; Bauer, A. Sleep deprivation increases A(1) adenosine receptor density in the rat brain. *Brain Res.*, **2009,** 1258, 53-58

[53] Yanik, G.; Radulovacki, M. REM sleep deprivation up-regulates adenosine A1 receptors. *Brain Res.*, **1987,** 402, 362-364

[54] Bjorness, T.E.; Kelly, C.L.; Gao, T.; Poffenberger, V.; Greene, R.W. Control and function of the homeostatic sleep response by adenosine A1 receptors. *J. Neurosci.*, **2009,** 29, 1267-1276

[55] Huber, R.; Ghilardi, M.F.; Massimini, M.; Tononi, G. Local sleep and learning. *Nature*, **2004,** 430, 78-81

[56] Benington, J.H.; Kodali, S.K.; Heller, H.C. Stimulation of A1 adenosine receptors mimics the electroencephalographic effects of sleep deprivation. *Brain Res.*, **1995,** 692, 79-85

[57] Strecker, R.E.; Morairty, S.; Thakkar, M.M.; Porkka-Heiskanen, T.; Basheer, R.; Dauphin, L.J.; Rainnie, D.G.; Portas, C.M.; Greene, R.W.; McCarley, R.W. Adenosinergic modulation of basal forebrain and preoptic/anterior hypothalamic neuronal activity in the control of behavioral state. *Behav. Brain Res.*, **2000,** 115, 183-204

[58] Christie, M.A.; Bolortuya, Y.; Chen, L.C.; McKenna, J.T.; McCarley, R.W.; Strecker, R.E. Microdialysis elevation of adenosine in the basal forebrain produces vigilance impairments in the rat psychomotor vigilance task. *Sleep*, **2008,** 31, 1393-1398

[59] Thakkar, M.M.; Winston, S.; McCarley, R.W. A1 receptor and adenosinergic homeostatic regulation of sleep-wakefulness: effects of antisense to the A1 receptor in the cholinergic basal forebrain. *J. Neurosci.*, **2003,** 23, 4278-4287

[60] Dunwiddie, T.V.; Masino, S.A. The role and regulation of adenosine in the central nervous system. *Annu. Rev. Neurosci.*, **2001,** 24, 31-55

[61] Portas, C.M.; Thakkar, M.; Rainnie, D.G.; Greene, R.W.; McCarley, R.W. Role of adenosine in behavioral state modulation: a microdialysis study in the freely moving cat. *Neuroscience*, **1997,** 79, 225-235

[62] Ticho, S.R.; Radulovacki, M. Role of adenosine in sleep and temperature regulation in the preoptic area of rats. *Pharmacol. Biochem. Behav.*, **1991,** 40, 33-40

[63] Lin, A.S.; Uhde, T.W.; Slate, S.O.; McCann, U.D. Effects of intravenous caffeine administered to healthy males during sleep. *Depress. Anxiety.*, **1997,** 5, 21-28

[64] Basheer, R.; Rainnie, D.G.; Porkka-Heiskanen, T.; Ramesh, V.; McCarley, R.W. Adenosine, prolonged wakefulness, and A1-activated NF-kappaB DNA binding in the basal forebrain of the rat. *Neuroscience*, **2001,** 104, 731-739

[65] Ramesh, V.; Thatte, H.S.; McCarley, R.W.; Basheer, R. Adenosine and sleep deprivation promote NF-kappaB nuclear translocation in cholinergic basal forebrain. *J. Neurochem.*, **2007,** 100, 1351-1363

[66] Thakkar, M.M.; Winston, S.; McCarley, R.W. Orexin neurons of the hypothalamus express adenosine A1 receptors. *Brain Res.*, **2002,** 944, 190-194

[67] Liu, Z.W.; Gao, X.B. Adenosine inhibits activity of hypocretin/orexin neurons by the A1 receptor in the lateral hypothalamus: a possible sleep-promoting effect. *J. Neurophysiol.*, **2007,** 97, 837-848

[68] Alam, M.N.; Kumar, S.; Rai, S.; Methippara, M.; Szymusiak, R.; McGinty, D. Role of adenosine A(1) receptor in the perifornical-lateral hypothalamic area in sleep-wake regulation in rats. *Brain Res.*, **2009,** 1304, 96-104

[69] Thakkar, M.M.; Engemann, S.C.; Walsh, K.M.; Sahota, P.K. Adenosine and the homeostatic control of sleep: effects of A1 receptor blockade in the perifornical lateral hypothalamus on sleep-wakefulness. *Neuroscience*, **2008,** 153, 875-880

[70] Oishi, Y.; Huang, Z.L.; Fredholm, B.B.; Urade, Y.; Hayaishi, O. Adenosine in the tuberomammillary nucleus inhibits the histaminergic system via A1 receptors and promotes non-rapid eye movement sleep. *Proc. Natl. Acad. Sci. U. S. A*, **2008,** 105, 19992-19997

[71] Marks, G.A.; Birabil, C.G.; Speciale, S.G. Adenosine A1 receptors mediate inhibition of cAMP formation in vitro in the pontine, REM sleep induction zone. *Brain Res.*, **2005,** 1061, 124-127

[72] Methippara, M.M.; Kumar, S.; Alam, M.N.; Szymusiak, R.; McGinty, D. Effects on sleep of microdialysis of adenosine A1 and A2a receptor analogs into the lateral preoptic area of rats. *Am. J. Physiol Regul. Integr. Comp Physiol*, **2005,** 289, R1715-R1723

[73] Arai, A.; Kessler, M.; Lynch, G. The effects of adenosine on the development of long-term potentiation. *Neurosci. Lett.*, **1990,** 119, 41-44

[74] Normile, H.J.; Gaston, S.; Johnson, G.; Barraco, R.A. Activation of adenosine A1 receptors in the nucleus accumbens impairs inhibitory avoidance memory. *Behav. Neural Biol.*, **1994,** 62, 163-166

[75] Normile, H.J.; Barraco, R.A. N6-cyclopentyladenosine impairs passive avoidance retention by selective action at A1 receptors. *Brain Res. Bull.*, **1991,** 27, 101-104

[76] Ohno, M.; Watanabe, S. Working memory failure by stimulation of hippocampal adenosine A1 receptors in rats. *Neuroreport*, **1996,** 7, 3013-3016

[77] Corodimas, K.P.; Tomita, H. Adenosine A1 receptor activation selectively impairs the acquisition of contextual fear conditioning in rats. *Behav. Neurosci.*, **2001,** 115, 1283-1290

[78] Prediger, R.D.; Takahashi, R.N. Modulation of short-term social memory in rats by adenosine A1 and A(2A) receptors. *Neurosci. Lett.*, **2005,** 376, 160-165

[79] Pereira, G.S.; Mello e Souza; Vinade, E.R.; Choi, H.; Rodrigues, C.; Battastini, A.M.; Izquierdo, I.; Sarkis, J.J.; Bonan, C.D. Blockade of adenosine A1 receptors in the posterior cingulate cortex facilitates memory in rats. *Eur. J. Pharmacol.*, **2002,** 437, 151-154

[80] Von Lubitz, D.K.; Paul, I.A.; Bartus, R.T.; Jacobson, K.A. Effects of chronic administration of adenosine A1 receptor agonist and antagonist on spatial learning and memory. *Eur. J. Pharmacol.*, **1993,** 249, 271-280

[81] Gimenez-Llort, L.; Fernandez-Teruel, A.; Escorihuela, R.M.; Fredholm, B.B.; Tobena, A.; Pekny, M.; Johansson, B. Mice lacking the adenosine A1 receptor are anxious and aggressive, but are normal learners with reduced muscle strength and survival rate. *Eur. J. Neurosci.*, **2002,** 16, 547-550

[82] Lang, U.E.; Lang, F.; Richter, K.; Vallon, V.; Lipp, H.P.; Schnermann, J.; Wolfer, D.P. Emotional instability but intact spatial cognition in adenosine receptor 1 knock out mice. *Behav. Brain Res.*, **2003,** 145, 179-188

[83] Gimenez-Llort, L.; Masino, S.A.; Diao, L.; Fernandez-Teruel, A.; Tobena, A.; Halldner, L.; Fredholm, B.B. Mice lacking the adenosine A1 receptor have normal spatial learning and plasticity in the CA1 region of the hippocampus, but they habituate more slowly. *Synapse*, **2005,** 57, 8-16

[84] Nagy, L.E. Ethanol metabolism and inhibition of nucleoside uptake lead to increased extracellular adenosine in hepatocytes. *Am. J. Physiol*, **1992,** 262, C1175-C1180

[85] Nagy, L.E.; Diamond, I.; Casso, D.J.; Franklin, C.; Gordon, A.S. Ethanol increases extracellular adenosine by inhibiting adenosine uptake via the nucleoside transporter. *J. Biol. Chem.*, **1990,** 265, 1946-1951

[86] Krauss, S.W.; Ghirnikar, R.B.; Diamond, I.; Gordon, A.S. Inhibition of adenosine uptake by ethanol is specific for one class of nucleoside transporters. *Mol. Pharmacol.*, **1993,** 44, 1021-1026

[87] Choi, D.S.; Cascini, M.G.; Mailliard, W.; Young, H.; Paredes, P.; McMahon, T.; Diamond, I.; Bonci, A.; Messing, R.O. The type 1 equilibrative nucleoside transporter regulates ethanol intoxication and preference. *Nat. Neurosci.*, **2004,** 7, 855-861

[88] Allen-Gipson, D.S.; Jarrell, J.C.; Bailey, K.L.; Robinson, J.E.; Kharbanda, K.K.; Sisson, J.H.; Wyatt, T.A. Ethanol blocks adenosine uptake via inhibiting the nucleoside transport system in bronchial epithelial cells. *Alcohol Clin. Exp. Res.*, **2009,** 33, 791-798

[89] Clark, M.; Dar, M.S. Effect of acute ethanol on uptake of [3H]adenosine by rat cerebellar synaptosomes. *Alcohol Clin. Exp. Res.*, **1989,** 13, 371-377

[90] Clark, M.; Dar, M.S. Effect of acute ethanol on release of endogenous adenosine from rat cerebellar synaptosomes. *J. Neurochem.*, **1989,** 52, 1859-1865

[91] Clark, M.; Dar, M.S. The effects of various methods of sacrifice and of ethanol on adenosine levels in selected areas of rat brain. *J. Neurosci. Methods*, **1988,** 25, 243-249

[92] Phillis, J.W.; O'Regan, M.H.; Perkins, L.M. Actions of ethanol and acetate on rat cortical neurons: ethanol/adenosine interactions. *Alcohol*, **1992,** 9, 541-546

[93] Kiselevski, Y.; Oganesian, N.; Zimatkin, S.; Szutowicz, A.; Angielski, S.; Niezabitowski, P.; Uracz, W.; Gryglewski, R.J. Acetate metabolism in brain mechanisms of adaptation to ethanol. *Med. Sci. Monit.*, **2003,** 9, BR178-BR182

[94] Sharma, R.; Engemann, S.C.; Sahota, P.; Thakkar, M.M. Effects of ethanol on extracellular levels of adenosine in the basal forebrain: an in vivo microdialysis study in freely behaving rats. *Alcohol Clin. Exp. Res.*, **2010,** 34, 813-818

[95] Dar, M.S.; Mustafa, S.J.; Wooles, W.R. Possible role of adenosine in the CNS effects of ethanol. *Life Sci.*, **1983,** 33, 1363-1374

[96] Clark, M.; Dar, M.S. Mediation of acute ethanol-induced motor disturbances by cerebellar adenosine in rats. *Pharmacol. Biochem. Behav.*, **1988,** 30, 155-161

[97] Barwick, V.S.; Dar, M.S. Adenosinergic modulation of ethanol-induced motor incoordination in the rat motor cortex. *Prog. Neuropsychopharmacol. Biol. Psychiatry*, **1998,** 22, 587-607

[98] Meng, Z.H.; Dar, M.S. Possible role of striatal adenosine in the modulation of acute ethanol-induced motor incoordination in rats. *Alcohol Clin. Exp. Res.*, **1995,** 19, 892-901

[99] Dar, M.S. Modulation of ethanol-induced motor incoordination by mouse striatal A(1) adenosinergic receptor. *Brain Res. Bull.*, **2001,** 55, 513-520

[100] Connole, L.; Harkin, A.; Maginn, M. Adenosine A1 receptor blockade mimics caffeine's attenuation of ethanol-induced motor incoordination. *Basic Clin. Pharmacol. Toxicol.*, **2004,** 95, 299-304

[101] Dar, M.S. Mouse cerebellar adenosinergic modulation of ethanol-induced motor incoordination: possible involvement of cAMP. *Brain Res.*, **1997,** 749, 263-274

[102] Dar, M.S. Brain adenosinergic modulation of acute ethanol-induced motor impairment. *Alcohol Alcohol Suppl*, **1993,** 2, 425-429

[103] Dar, M.S.; Mustafa, S.J. Acute ethanol/cannabinoid-induced ataxia and its antagonism by oral/systemic/intracerebellar A1 adenosine receptor antisense in mice. *Brain Res.*, **2002,** 957, 53-60

[104] Phan, T.A.; Gray, A.M.; Nyce, J.W. Intrastriatal adenosine A1 receptor antisense oligodeoxynucleotide blocks ethanol-induced motor incoordination. *Eur. J. Pharmacol.*, **1997,** 323, R5-R7

[105] Reynolds, J.D.; Brien, J.F. The role of adenosine A1 receptor activation in ethanol-induced inhibition of stimulated glutamate release in the hippocampus of the fetal and adult guinea pig. *Alcohol*, **1995,** 12, 151-157

[106] Clark, M.; Dar, M.S. Release of endogenous glutamate from rat cerebellar synaptosomes: interactions with adenosine and ethanol. *Life Sci.*, **1989,** 44, 1625-1635

[107] Meng, Z.H.; Anwer, J.; Dar, M.S. The striatal adenosinergic modulation of ethanol-induced motor incoordination in rats: possible role of chloride flux. *Brain Res.*, **1997,** 776, 235-245

[108] Carmichael, F.J.; Israel, Y.; Crawford, M.; Minhas, K.; Saldivia, V.; Sandrin, S.; Campisi, P.; Orrego, H. Central nervous system effects of acetate: contribution to the central effects of ethanol. *J. Pharmacol. Exp. Ther.*, **1991,** 259, 403-408

[109] Carmichael, F.J.; Orrego, H.; Israel, Y. Acetate-induced adenosine mediated effects of ethanol. *Alcohol Alcohol Suppl*, **1993,** 2, 411-418

[110] Israel, Y.; Orrego, H.; Carmichael, F.J. Acetate-mediated effects of ethanol. *Alcohol Clin. Exp. Res.*, **1994,** 18, 144-148

[111] Campisi, P.; Carmichael, F.J.; Crawford, M.; Orrego, H.; Khanna, J.M. Role of adenosine in the ethanol-induced potentiation of the effects of general anesthetics in rats. *Eur. J. Pharmacol.*, **1997,** 325, 165-172

[112] Drake, C.L.; Roehrs, T.; Turner, L.; Scofield, H.M.; Roth, T. Caffeine reversal of ethanol effects on the multiple sleep latency test, memory, and psychomotor performance. *Neuropsychopharmacology*, **2003,** 28, 371-378

[113] Thakkar, M.M.; Engemann, S.C.; Sharma, R.; Sahota, P. Role of wake-promoting basal forebrain and adenosinergic mechanisms in sleep-promoting effects of ethanol. *Alcohol Clin. Exp. Res.*, **2010,** 34, 997-1005

[114] Prediger, R.D.; Batista, L.C.; Takahashi, R.N. Adenosine A1 receptors modulate the anxiolytic-like effect of ethanol in the elevated plus-maze in mice. *Eur. J. Pharmacol.*, **2004,** 499, 147-154

[115] Concas, A.; Cuccheddu, T.; Floris, S.; Mascia, M.P.; Biggio, G. 2-Chloro-N6-cyclopentyladenosine (CCPA), an adenosine A1 receptor agonist, suppresses ethanol withdrawal syndrome in rats. *Alcohol Alcohol*, **1994,** 29, 261-264

[116] Kaplan, G.B.; Bharmal, N.H.; Leite-Morris, K.A.; Adams, W.R. Role of adenosine A1 and A2A receptors in the alcohol withdrawal syndrome. *Alcohol*, **1999,** 19, 157-162

[117] Gatch, M.B.; Wallis, C.J.; Lal, H. The effects of adenosine ligands R-PIA and CPT on ethanol withdrawal. *Alcohol*, **1999,** 19, 9-14

[118] Prediger, R.D.; da Silva, G.E.; Batista, L.C.; Bittencourt, A.L.; Takahashi, R.N. Activation of adenosine A1 receptors reduces anxiety-like behavior during acute ethanol withdrawal (hangover) in mice. *Neuropsychopharmacology*, **2006,** 31, 2210-2220

[119] Butler, T.R.; Smith, K.J.; Self, R.L.; Braden, B.B.; Prendergast, M.A. Sex differences in the neurotoxic effects of adenosine A1 receptor antagonism during ethanol withdrawal: reversal with an A1 receptor agonist or an NMDA receptor antagonist. *Alcohol Clin. Exp. Res.*, **2008,** 32, 1260-1270

[120] Butler, T.R.; Smith, K.J.; Berry, J.N.; Sharrett-Field, L.J.; Prendergast, M.A. Sex differences in caffeine neurotoxicity following chronic ethanol exposure and withdrawal. *Alcohol Alcohol*, **2009,** 44, 567-574

[121] Clark, M.; Dar, M.S. In vitro autoradiographic evidence for adenosine modulation of ethanol-induced motor disturbances in rats. *Alcohol Alcohol Suppl*, **1991,** 1, 203-206

[122] Concas, A.; Mascia, M.P.; Cuccheddu, T.; Floris, S.; Mostallino, M.C.; Perra, C.; Satta, S.; Biggio, G. Chronic ethanol intoxication enhances [3H]CCPA binding and does not reduce A1 adenosine receptor function in rat cerebellum. *Pharmacol. Biochem. Behav.*, **1996,** 53, 249-255

[123] Daly, J.W.; Shi, D.; Wong, V.; Nikodijevic, O. Chronic effects of ethanol on central adenosine function of mice. *Brain Res.*, **1994,** 650, 153-156

[124] Jarvis, M.F.; Becker, H.C. Single and repeated episodes of ethanol withdrawal increase adenosine A1, but not A2A, receptor density in mouse brain. *Brain Res.*, **1998,** 786, 80-88

[125] Sharma, R.; Engemann, S.; Sahota, P.; Thakkar, M.M. Role of adenosine and wake-promoting basal forebrain in insomnia and associated sleep disruptions caused by ethanol dependence. *J. Neurochem.*, **2010,** 115, 782-794

[126] Paul, S.; Khanapur, S.; Rybczynska, A.A.; Kwizera, C.; Sijbesma, J.W.; Ishiwata, K.; Willemsen, A.T.; Elsinga, P.H.; Dierckx, R.A.; van Waarde A. Small-Animal PET Study of Adenosine A1 Receptors in Rat Brain: Blocking Receptors and Raising Extracellular Adenosine. *J Nucl. Med.*, **2011,** 52, 1293-1300

[127] Laghi Pasini, F.; Guideri, F.; Picano, E.; Parenti, G.; Petersen, C.; Varga, A.; Di Perri, T. Increase in plasma adenosine during brain ischemia in man: a study during transient ischemic attacks, and stroke. *Brain Res. Bull.*, **2000,** 51, 327-330

[128] O'Regan, M.H.; Simpson, R.E.; Perkins, L.M.; Phillis, J.W. Adenosine receptor agonists inhibit the release of gamma-aminobutyric acid (GABA) from the ischemic rat cerebral cortex. *Brain Res.*, **1992,** 582, 22-26

[129] Simpson, R.E.; O'Regan, M.H.; Perkins, L.M.; Phillis, J.W. Excitatory transmitter amino acid release from the ischemic rat cerebral cortex: effects of adenosine receptor agonists and antagonists. *J. Neurochem.*, **1992,** 58, 1683-1690

[130] Marangos, P.J. Adenosinergic approaches to stroke therapeutics. *Med. Hypotheses*, **1990,** 32, 45-49

[131] Ilie, A.; Ciocan, D.; Zagrean, A.M.; Nita, D.A.; Zagrean, L.; Moldovan, M. Endogenous activation of adenosine A(1) receptors accelerates ischemic suppression of spontaneous electrocortical activity. *J. Neurophysiol.*, **2006,** 96, 2809-2814

[132] Ilie, A.; Ciocan, D.; Constantinescu, A.O.; Zagrean, A.M.; Nita, D.A.; Zagrean, L.; Moldovan, M. Endogenous activation of adenosine A1 receptors promotes post-ischemic electrocortical burst suppression. *Neuroscience*, **2009,** 159, 1070-1078

[133] Pearson, T.; Damian, K.; Lynas, R.E.; Frenguelli, B.G. Sustained elevation of extracellular adenosine and activation of A1 receptors underlie the post-ischaemic inhibition of neuronal function in rat hippocampus in vitro. *J. Neurochem.*, **2006,** 97, 1357-1368

[134] Pignataro, G.; Simon, R.P.; Boison, D. Transgenic overexpression of adenosine kinase aggravates cell death in ischemia. *J. Cereb. Blood Flow Metab*, **2007,** 27, 1-5

[135] Heurteaux, C.; Lauritzen, I.; Widmann, C.; Lazdunski, M. Essential role of adenosine, adenosine A1 receptors, and ATP-sensitive K+ channels in cerebral ischemic preconditioning. *Proc. Natl. Acad. Sci. U. S. A*, **1995,** 92, 4666-4670

[136] Nakamura, M.; Nakakimura, K.; Matsumoto, M.; Sakabe, T. Rapid tolerance to focal cerebral ischemia in rats is attenuated by adenosine A1 receptor antagonist. *J. Cereb. Blood Flow Metab*, **2002,** 22, 161-170

[137] Akaiwa, K.; Akashi, H.; Harada, H.; Sakashita, H.; Hiromatsu, S.; Kano, T.; Aoyagi, S. Moderate cerebral venous congestion induces rapid cerebral protection via adenosine A1 receptor activation. *Brain Res.*, **2006,** 1122, 47-55

[138] Liu, Y.; Xiong, L.; Chen, S.; Wang, Q. Isoflurane tolerance against focal cerebral ischemia is attenuated by adenosine A1 receptor antagonists. *Can. J. Anaesth.*, **2006,** 53, 194-201

[139] Mizumura, T.; Auchampach, J.A.; Linden, J.; Bruns, R.F.; Gross, G.J. PD 81,723, an allosteric enhancer of the A1 adenosine receptor, lowers the threshold for ischemic preconditioning in dogs. *Circ. Res.*, **1996,** 79, 415-423

[140] Heron, A.; Lekieffre, D.; Le Peillet, E.; Lasbennes, F.; Seylaz, J.; Plotkine, M.; Boulu, R.G. Effects of an A1 adenosine receptor agonist on the neurochemical, behavioral and histological consequences of ischemia. *Brain Res.*, **1994,** 641, 217-224

[141] Tominaga, K.; Shibata, S.; Watanabe, S. A neuroprotective effect of adenosine A1-receptor agonists on ischemia-induced decrease in 2-deoxyglucose uptake in rat hippocampal slices. *Neurosci. Lett.*, **1992,** 145, 67-70

[142] Von Lubitz, D.K.; Lin, R.C.; Melman, N.; Ji, X.D.; Carter, M.F.; Jacobson, K.A. Chronic administration of selective adenosine A1 receptor agonist or antagonist in cerebral ischemia. *Eur. J. Pharmacol.*, **1994,** 256, 161-167

[143] Von Lubitz, D.K.; Beenhakker, M.; Lin, R.C.; Carter, M.F.; Paul, I.A.; Bischofberger, N.; Jacobson, K.A. Reduction of postischemic brain damage and memory deficits following treatment with the selective adenosine A1 receptor agonist. *Eur. J. Pharmacol.*, **1996,** 302, 43-48

[144] Sweeney, M.I. Neuroprotective effects of adenosine in cerebral ischemia: window of opportunity. *Neurosci. Biobehav. Rev.*, **1997,** 21, 207-217

[145] Rudolphi, K.A.; Keil, M.; Fastbom, J.; Fredholm, B.B. Ischaemic damage in gerbil hippocampus is reduced following upregulation of adenosine (A1) receptors by caffeine treatment. *Neurosci. Lett.*, **1989,** 103, 275-280

[146] Halle, J.N.; Kasper, C.E.; Gidday, J.M.; Koos, B.J. Enhancing adenosine A1 receptor binding reduces hypoxic-ischemic brain injury in newborn rats. *Brain Res.*, **1997,** 759, 309-312

[147] Phillis, J.W. The effects of selective A1 and A2a adenosine receptor antagonists on cerebral ischemic injury in the gerbil. *Brain Res.*, **1995,** 705, 79-84

[148] Jacobson, K.A.; Von Lubitz, D.K.; Daly, J.W.; Fredholm, B.B. Adenosine receptor ligands: differences with acute versus chronic treatment. *Trends Pharmacol. Sci.*, **1996,** 17, 108-113

[149] Von Lubitz, D.K.; Lin, R.C.; Bischofberger, N.; Beenhakker, M.; Boyd, M.; Lipartowska, R.; Jacobson, K.A. Protection against ischemic damage by adenosine amine congener, a potent and selective adenosine A1 receptor agonist. *Eur. J. Pharmacol.*, **1999,** 369, 313-317

[150] Aden, U.; Lindstrom, K.; Bona, E.; Hagberg, H.; Fredholm, B.B. Changes in adenosine receptors in the neonatal rat brain following hypoxic ischemia. *Brain Res. Mol. Brain Res.*, **1994,** 23, 354-358

[151] Araki, T.; Kato, H.; Kogure, K.; Saito, T. Postischemic alteration of muscarinic acetylcholine, adenosine A1 and calcium antagonist binding sites in selectively vulnerable areas: an autoradiographic study of gerbil brain. *J. Neurol. Sci.*, **1991,** 106, 206-212

[152] Nagasawa, H.; Araki, T.; Kogure, K. Alteration of adenosine A1 receptor binding in the post-ischaemic rat brain. *Neuroreport*, **1994,** 5, 1453-1456

[153] Shen, H.; Zhang, L.; Yuen, D.; Logan, R.; Jung, B.P.; Zhang, G.; Eubanks, J.H. Expression and function of A1 adenosine receptors in the rat hippocampus following transient forebrain ischemia. *Neuroscience*, **2002,** 114, 547-556

[154] Lai, D.M.; Tu, Y.K.; Liu, I.M.; Cheng, J.T. Increase of adenosine A1 receptor gene expression in cerebral ischemia of Wistar rats. *Neurosci. Lett.*, **2005,** 387, 59-61

[155] Nariai, T.; Shimada, Y.; Ishiwata, K.; Nagaoka, T.; Shimada, J.; Kuroiwa, T.; Ono, K.I.; Hirakawa, K.; Senda, M.; Ohno, K. PET neuroreceptor imaging as predictor of severe cerebral ischemic insult. *Acta Neurochir. Suppl*, **2003,** 86, 45-48

[156] Nariai, T.; Shimada, Y.; Ishiwata, K.; Nagaoka, T.; Shimada, J.; Kuroiwa, T.; Ono, K.; Ohno, K.; Hirakawa, K.; Senda, M. PET imaging of adenosine A(1) receptors with (11)C-MPDX as an indicator of severe cerebral ischemic insult. *J. Nucl. Med.*, **2003,** 44, 1839-1844

[157] Dunwiddie, T.V. Adenosine and suppression of seizures. *Adv. Neurol.*, **1999,** 79, 1001-1010

[158] Abdul-Ghani, A.S.; Attwell, P.J.; Bradford, H.F. The protective effect of 2-chloroadenosine against the development of amygdala kindling and on amygdala-kindled seizures. *Eur. J. Pharmacol.*, **1997,** 326, 7-14

[159] Barraco, R.A.; Swanson, T.H.; Phillis, J.W.; Berman, R.F. Anticonvulsant effects of adenosine analogues on amygdaloid-kindled seizures in rats. *Neurosci. Lett.*, **1984,** 46, 317-322

[160] Bortolotto, Z.A.; Mello, L.E.; Turski, L.; Cavalheiro, E.A. Effects of 2-chloroadenosine on amygdaloid and hippocampal kindled seizures. *Arch. Int. Pharmacodyn. Ther.*, **1985,** 277, 313-320

[161] Rezvani, M.E.; Mirnajafi-Zadeh, J.; Fathollahi, Y.; Palizvan, M.R. Anticonvulsant effect of A1 but not A2A adenosine receptors of piriform cortex in amygdala-kindled rats. *Can. J. Physiol Pharmacol.*, **2007,** 85, 606-612

[162] Rosen, J.B.; Berman, R.F. Differential effects of adenosine analogs on amygdala, hippocampus, and caudate nucleus kindled seizures. *Epilepsia*, **1987,** 28, 658-666

[163] Heidarianpour, A.; Sadeghian, E.; Mirnajafi-Zadeh, J.; Fathollahi, Y.; Mohammad-Zadeh, M. Anticonvulsant effects of N6-cyclohexyladenosine microinjected into the CA1 region of the hippocampus on entorhinal cortex-kindled seizures in rats. *Epileptic. Disord.*, **2006,** 8, 259-266

[164] Hosseinmardi, N.; Mirnajafi-Zadeh, J.; Fathollahi, Y.; Shahabi, P. The role of adenosine A1 and A2A receptors of entorhinal cortex on piriform cortex kindled seizures in rats. *Pharmacol. Res.*, **2007,** 56, 110-117

[165] Namvar, S.; Mirnajafi-Zadeh, J.; Fathollahi, Y.; Zeraati, M. The role of piriform cortex adenosine A1 receptors on hippocampal kindling. *Can. J. Neurol. Sci.*, **2008,** 35, 226-231

[166] Gouder, N.; Fritschy, J.M.; Boison, D. Seizure suppression by adenosine A1 receptor activation in a mouse model of pharmacoresistant epilepsy. *Epilepsia*, **2003,** 44, 877-885

[167] Vianna, E.P.; Ferreira, A.T.; Dona, F.; Cavalheiro, E.A.; Silva Fernandes, M.J. Modulation of seizures and synaptic plasticity by adenosinergic receptors in an experimental model of temporal lobe epilepsy induced by pilocarpine in rats. *Epilepsia*, **2005,** 46 Suppl 5, 166-173

[168] Zgodzinski, W.; Rubaj, A.; Kleinrok, Z.; Sieklucka-Dziuba, M. Effect of adenosine A1 and A2 receptor stimulation on hypoxia-induced convulsions in adult mice. *Pol. J. Pharmacol.*, **2001,** 53, 83-92

[169] Shahabi, P.; Mirnajafi-Zadeh, J.; Fathollahi, Y.; Hoseinmardi, N.; Rezvani, M.E.; Eslami-far, A. Amygdala adenosine A1 receptors have no anticonvulsant effect on piriform cortex-kindled seizures in rat. *Can. J. Physiol Pharmacol.*, **2006,** 84, 913-921

[170] Wiesner, J.B.; Ugarkar, B.G.; Castellino, A.J.; Barankiewicz, J.; Dumas, D.P.; Gruber, H.E.; Foster, A.C.; Erion, M.D. Adenosine kinase inhibitors as a novel approach to anticonvulsant therapy. *J. Pharmacol. Exp. Ther.*, **1999,** 289, 1669-1677

[171] Gouder, N.; Scheurer, L.; Fritschy, J.M.; Boison, D. Overexpression of adenosine kinase in epileptic hippocampus contributes to epileptogenesis. *J. Neurosci.*, **2004,** 24, 692-701

[172] Li, T.; Quan Lan, J.; Fredholm, B.B.; Simon, R.P.; Boison, D. Adenosine dysfunction in astrogliosis: cause for seizure generation? *Neuron Glia Biol.*, **2007,** 3, 353-366

[173] Guttinger, M.; Padrun, V.; Pralong, W.F.; Boison, D. Seizure suppression and lack of adenosine A1 receptor desensitization after focal long-term delivery of adenosine by encapsulated myoblasts. *Exp. Neurol.*, **2005,** 193, 53-64

[174] Eldridge, F.L.; Paydarfar, D.; Scott, S.C.; Dowell, R.T. Role of endogenous adenosine in recurrent generalized seizures. *Exp. Neurol.*, **1989,** 103, 179-185

[175] Dragunow, M.; Robertson, H.A. 8-Cyclopentyl 1,3-dimethylxanthine prolongs epileptic seizures in rats. *Brain Res.*, **1987,** 417, 377-379

[176] Fukuda, M.; Suzuki, Y.; Hino, H.; Kuzume, K.; Morimoto, T.; Ishii, E. Adenosine A1 receptor blockage mediates theophylline-associated seizures. *Epilepsia*, **2010,** 51, 483-487

[177] Mohammad-Zadeh, M.; Mirnajafi-Zadeh, J.; Fathollahi, Y.; Javan, M.; Jahanshahi, A.; Noorbakhsh, S.M.; Motamedi, F. The role of adenosine A(1) receptors in mediating the inhibitory effects of low frequency stimulation of perforant path on kindling acquisition in rats. *Neuroscience*, **2009,** 158, 1632-1643

[178] Daval, J.; Werck, M. Autoradiographic changes in brain adenosine A1 receptors and their coupling to G proteins following seizures in the developing rat. *Brain Res. Dev. Brain Res.*, **1991,** 59, 237-247

[179] Tchekalarova, J.; Sotiriou, E.; Georgiev, V.; Kostopoulos, G.; Angelatou, F. Up-regulation of adenosine A1 receptor binding in pentylenetetrazol kindling in mice: effects of angiotensin IV. *Brain Res.*, **2005,** 1032, 94-103

[180] Pagonopoulou, O.; Angelatou, F.; Kostopoulos, G. Effect of pentylentetrazol-induced seizures on A1 adenosine receptor regional density in the mouse brain: a quantitative autoradiographic study. *Neuroscience*, **1993,** 56, 711-716

[181] Angelatou, F.; Pagonopoulou, O.; Maraziotis, T.; Olivier, A.; Villemeure, J.G.; Avoli, M.; Kostopoulos, G. Upregulation of A1 adenosine receptors in human temporal lobe epilepsy: a quantitative autoradiographic study. *Neurosci. Lett.*, **1993,** 163, 11-14

[182] Glass, M.; Faull, R.L.; Bullock, J.Y.; Jansen, K.; Mee, E.W.; Walker, E.B.; Synek, B.J.; Dragunow, M. Loss of A1 adenosine receptors in human temporal lobe epilepsy. *Brain Res.*, **1996,** 710, 56-68

[183] Ekonomou, A.; Angelatou, F.; Vergnes, M.; Kostopoulos, G. Lower density of A1 adenosine receptors in nucleus reticularis thalami in rats with genetic absence epilepsy. *Neuroreport*, **1998,** 9, 2135-2140

[184] Ochiishi, T.; Takita, M.; Ikemoto, M.; Nakata, H.; Suzuki, S.S. Immunohistochemical analysis on the role of adenosine A1 receptors in epilepsy. *Neuroreport*, **1999,** 10, 3535-3541

[185] Ekonomou, A.; Sperk, G.; Kostopoulos, G.; Angelatou, F. Reduction of A1 adenosine receptors in rat hippocampus after kainic acid-induced limbic seizures. *Neurosci. Lett.*, **2000,** 284, 49-52

[186] Rebola, N.; Coelho, J.E.; Costenla, A.R.; Lopes, L.V.; Parada, A.; Oliveira, C.R.; Soares-da-Silva, P.; de Mendonca, A.; Cunha, R.A. Decrease of adenosine A1 receptor density and of adenosine neuromodulation in the hippocampus of kindled rats. *Eur. J. Neurosci.*, **2003,** 18, 820-828

[187] Rebola, N.; Porciuncula, L.O.; Lopes, L.V.; Oliveira, C.R.; Soares-da-Silva, P.; Cunha, R.A. Long-term effect of convulsive behavior on the density of adenosine A1 and A 2A receptors in the rat cerebral cortex. *Epilepsia*, **2005,** 46 Suppl 5, 159-165

[188] Aden, U.; O'Connor, W.T.; Berman, R.F. Changes in purine levels and adenosine receptors in kindled seizures in the rat. *Neuroreport*, **2004,** 15, 1585-1589

[189] Simonato, M.; Varani, K.; Muzzolini, A.; Bianchi, C.; Beani, L.; Borea, P.A. Adenosine A1 receptors in the rat brain in the kindling model of epilepsy. *Eur. J. Pharmacol.*, **1994,** 265, 121-124

[190] Doriat, J.F.; Koziel, V.; Humbert, A.C.; Daval, J.L. Medium- and long-term alterations of brain A1 and A2A adenosine receptor characteristics following repeated seizures in developing rats. *Epilepsy Res.*, **1999,** 35, 219-228

[191] Kochanek, P.M.; Vagni, V.A.; Janesko, K.L.; Washington, C.B.; Crumrine, P.K.; Garman, R.H.; Jenkins, L.W.; Clark, R.S.; Homanics, G.E.; Dixon, C.E.; Schnermann, J.; Jackson, E.K. Adenosine A1 receptor knockout mice develop lethal status epilepticus after experimental traumatic brain injury. *J. Cereb. Blood Flow Metab*, **2006,** 26, 565-575

[192] Fedele, D.E.; Li, T.; Lan, J.Q.; Fredholm, B.B.; Boison, D. Adenosine A1 receptors are crucial in keeping an epileptic focus localized. *Exp. Neurol.*, **2006,** 200, 184-190

[193] Haselkorn, M.L.; Shellington, D.K.; Jackson, E.K.; Vagni, V.A.; Janesko-Feldman, K.; Dubey, R.K.; Gillespie, D.G.; Cheng, D.; Bell, M.J.; Jenkins, L.W.; Homanics, G.E.; Schnermann, J.; Kochanek, P.M. Adenosine A1 receptor activation as a brake on the microglial response after experimental traumatic brain injury in mice. *J. Neurotrauma*, **2010,** 27, 901-910

[194] Cronstein, B.N. Adenosine, an endogenous anti-inflammatory agent. *J. Appl. Physiol*, **1994,** 76, 5-13

[195] Gebicke-Haerter, P.J.; Christoffel, F.; Timmer, J.; Northoff, H.; Berger, M.; van Calker, D. Both adenosine A1- and A2-receptors are required to stimulate microglial proliferation. *Neurochem. Int.*, **1996,** 29, 37-42

[196] Hasko, G.; Pacher, P.; Vizi, E.S.; Illes, P. Adenosine receptor signaling in the brain immune system. *Trends Pharmacol. Sci.*, **2005,** 26, 511-516

[197] Ciccarelli, R.; Di Iorio, P.; Bruno, V.; Battaglia, G.; D'Alimonte, I.; D'Onofrio, M.; Nicoletti, F.; Caciagli, F. Activation of A(1) adenosine or mGlu3 metabotropic glutamate receptors enhances the release of nerve growth factor and S-100beta protein from cultured astrocytes. *Glia*, **1999,** 27, 275-281

[198] Villoslada, P.; Genain, C.P. Role of nerve growth factor and other trophic factors in brain inflammation. *Prog. Brain Res.*, **2004,** 146, 403-414

[199] Schnurr, M.; Toy, T.; Shin, A.; Hartmann, G.; Rothenfusser, S.; Soellner, J.; Davis, I.D.; Cebon, J.; Maraskovsky, E. Role of adenosine receptors in regulating chemotaxis and cytokine production of plasmacytoid dendritic cells. *Blood*, **2004,** 103, 1391-1397

[200] Tsutsui, S.; Schnermann, J.; Noorbakhsh, F.; Henry, S.; Yong, V.W.; Winston, B.W.; Warren, K.; Power, C. A1 adenosine receptor upregulation and activation attenuates neuroinflammation and demyelination in a model of multiple sclerosis. *J. Neurosci.*, **2004,** 24, 1521-1529

[201] Chen, G.Q.; Chen, Y.Y.; Wang, X.S.; Wu, S.Z.; Yang, H.M.; Xu, H.Q.; He, J.C.; Wang, X.T.; Chen, J.F.; Zheng, R.Y. Chronic caffeine treatment attenuates experimental autoimmune encephalomyelitis induced by guinea pig spinal cord homogenates in Wistar rats. *Brain Res.*, **2010,** 1309, 116-125

[202] Brothers, H.M.; Marchalant, Y.; Wenk, G.L. Caffeine attenuates lipopolysaccharide-induced neuroinflammation. *Neurosci. Lett.*, **2010,** 480, 97-100

[203] Jhaveri, K.A.; Reichensperger, J.; Toth, L.A.; Sekino, Y.; Ramkumar, V. Reduced basal and lipopolysaccharide-stimulated adenosine A1 receptor expression in the brain of nuclear factor-kappaB p50-/- mice. *Neuroscience*, **2007,** 146, 415-426

[204] Synowitz, M.; Glass, R.; Farber, K.; Markovic, D.; Kronenberg, G.; Herrmann, K.; Schnermann, J.; Nolte, C.; van, R.N.; Kiwit, J.; Kettenmann, H. A1 adenosine receptors in microglia control glioblastoma-host interaction. *Cancer Res.*, **2006,** 66, 8550-8557

[205] Bauer, A.; Langen, K.J.; Bidmon, H.; Holschbach, M.H.; Weber, S.; Olsson, R.A.; Coenen, H.H.; Zilles, K. 18F-CPFPX PET identifies changes in cerebral A1 adenosine receptor density caused by glioma invasion. *J. Nucl. Med.*, **2005,** 46, 450-454

[206] Jansen, K.L.; Faull, R.L.; Dragunow, M.; Synek, B.L. Alzheimer's disease: changes in hippocampal N-methyl-D-aspartate, quisqualate, neurotensin, adenosine, benzodiazepine, serotonin and opioid receptors--an autoradiographic study. *Neuroscience*, **1990,** 39, 613-627

[207] Kalaria, R.N.; Sromek, S.; Wilcox, B.J.; Unnerstall, J.R. Hippocampal adenosine A1 receptors are decreased in Alzheimer's disease. *Neurosci. Lett.*, **1990,** 118, 257-260

[208] Jaarsma, D.; Sebens, J.B.; Korf, J. Reduction of adenosine A1-receptors in the perforant pathway terminal zone in Alzheimer hippocampus. *Neurosci. Lett.*, **1991,** 121, 111-114

[209] Ulas, J.; Brunner, L.C.; Nguyen, L.; Cotman, C.W. Reduced density of adenosine A1 receptors and preserved coupling of adenosine A1 receptors to G proteins in Alzheimer hippocampus: a quantitative autoradiographic study. *Neuroscience*, **1993,** 52, 843-854

[210] Ikeda, M.; Mackay, K.B.; Dewar, D.; McCulloch, J. Differential alterations in adenosine A1 and kappa 1 opioid receptors in the striatum in Alzheimer's disease. *Brain Res.*, **1993,** 616, 211-217

[211] Angulo, E.; Casado, V.; Mallol, J.; Canela, E.I.; Vinals, F.; Ferrer, I.; Lluis, C.; Franco, R. A1 adenosine receptors accumulate in neurodegenerative structures in Alzheimer disease and mediate both amyloid precursor protein processing and tau phosphorylation and translocation. *Brain Pathol.*, **2003,** 13, 440-451

[212] Albasanz, J.L.; Perez, S.; Barrachina, M.; Ferrer, I.; Martin, M. Up-regulation of adenosine receptors in the frontal cortex in Alzheimer's disease. *Brain Pathol.*, **2008,** 18, 211-219

[213] Fukumitsu, N.; Ishii, K.; Kimura, Y.; Oda, K.; Hashimoto, M.; Suzuki, M.; Ishiwata, K. Adenosine A(1) receptors using 8-dicyclopropylmethyl-1-[(11)C]methyl-3-propylxanthine PET in Alzheimer's disease. *Ann. Nucl. Med.*, **2008,** 22, 841-847

[214] Albasanz, J.L.; Rodriguez, A.; Ferrer, I.; Martin, M. Up-regulation of adenosine A1 receptors in frontal cortex from Pick's disease cases. *Eur. J. Neurosci.*, **2007,** 26, 3501-3508

[215] Rodriguez, A.; Martin, M.; Albasanz, J.L.; Barrachina, M.; Espinosa, J.C.; Torres, J.M.; Ferrer, I. Adenosine A1 Receptor Protein Levels and Activity Is Increased in the Cerebral Cortex in Creutzfeldt-Jakob Disease and in Bovine Spongiform Encephalopathy-Infected Bovine-PrP Mice. *J. Neuropathol. Exp. Neurol.*, **2006,** 65, 964-975

[216] Mayne, M.; Shepel, P.N.; Jiang, Y.; Geiger, J.D.; Power, C. Dysregulation of adenosine A1 receptor-mediated cytokine expression in peripheral blood mononuclear cells from multiple sclerosis patients. *Ann. Neurol.*, **1999,** 45, 633-639

[217] Johnston, J.B.; Silva, C.; Gonzalez, G.; Holden, J.; Warren, K.G.; Metz, L.M.; Power, C. Diminished adenosine A1 receptor expression on macrophages in brain and blood of patients with multiple sclerosis. *Ann. Neurol.*, **2001,** 49, 650-658

[218] Liu, H.Q.; Zhang, W.Y.; Luo, X.T.; Ye, Y.; Zhu, X.Z. Paeoniflorin attenuates neuroinflammation and dopaminergic neurodegeneration in the MPTP model of Parkinson's disease by activation of adenosine A1 receptor. *Br. J. Pharmacol.*, **2006,** 148, 314-325

[219] Bekar, L.; Libionka, W.; Tian, G.F.; Xu, Q.; Torres, A.; Wang, X.; Lovatt, D.; Williams, E.; Takano, T.; Schnermann, J.; Bakos, R.; Nedergaard, M. Adenosine is crucial for deep brain stimulation-mediated attenuation of tremor. *Nat. Med.*, **2008,** 14, 75-80

[220] Lara, D.R.; Dall'Igna, O.P.; Ghisolfi, E.S.; Brunstein, M.G. Involvement of adenosine in the neurobiology of schizophrenia and its therapeutic implications. *Prog. Neuropsychopharmacol. Biol. Psychiatry*, **2006,** 30, 617-629

[221] Boison, D.; Singer, P.; Shen, H.Y.; Feldon, J.; Yee, B.K. Adenosine hypothesis of schizophrenia - Opportunities for pharmacotherapy. *Neuropharmacology*, **2011,**

[222] Gotoh, L.; Mitsuyasu, H.; Kobayashi, Y.; Oribe, N.; Takata, A.; Ninomiya, H.; Stanton, V.P., Jr.; Springett, G.M.; Kawasaki, H.; Kanba, S. Association analysis of adenosine A1 receptor gene (ADORA1) polymorphisms with schizophrenia in a Japanese population. *Psychiatr. Genet.*, **2009,** 19, 328-335

[223] Meyer, P.T.; Bier, D.; Holschbach, M.H.; Cremer, M.; Tellmann, L.; Bauer, A. In vivo imaging of rat brain A1 adenosine receptor occupancy by caffeine. *Eur. J. Nucl. Med. Mol. Imaging*, **2003,** 30, 1440

[224] Meyer, P.T.; Elmenhorst, D.; Matusch, A.; Winz, O.; Zilles, K.; Bauer, A. A1 adenosine receptor PET using [18F]CPFPX: displacement studies in humans. *Neuroimage.*, **2006,** 32, 1100-1105

[225] Arch, J.R.; Newsholme, E.A. The control of the metabolism and the hormonal role of adenosine. *Essays Biochem.*, **1978,** 14, 82-123

[226] Newby, A.C.; Holmquist, C.A.; Illingworth, J.; Pearson, J.D. The control of adenosine concentration in polymorphonuclear leucocytes, cultured heart cells and isolated perfused heart from the rat. *Biochem. J.*, **1983,** 214, 317-323

[227] Engler, R. Consequences of activation and adenosine-mediated inhibition of granulocytes during myocardial ischemia. *Fed. Proc.*, **1987,** 46, 2407-2412

[228] Britton, D.R.; Mikusa, J.; Lee, C.H.; Jarvis, M.F.; Williams, M.; Kowaluk, E.A. Site and event specific increase of striatal adenosine release by adenosine kinase inhibition in rats. *Neurosci. Lett.*, **1999,** 266, 93-96

[229] Kowaluk, E.A.; Jarvis, M.F. Therapeutic potential of adenosine kinase inhibitors. *Expert. Opin. Investig. Drugs*, **2000,** 9, 551-564

[230] Kowaluk, E.A.; Bhagwat, S.S.; Jarvis, M.F. Adenosine kinase inhibitors. *Curr. Pharm. Des*, **1998,** 4, 403-416

[231] Sawynok, J.; Sweeney, M.I.; White, T.D. Classification of adenosine receptors mediating antinociception in the rat spinal cord. *Br. J. Pharmacol.*, **1986,** 88, 923-930

[232] Poon, A.; Sawynok, J. Antinociception by adenosine analogs and inhibitors of adenosine metabolism in an inflammatory thermal hyperalgesia model in the rat. *Pain*, **1998,** 74, 235-245

[233] Poon, A.; Sawynok, J. Antinociception by adenosine analogs and an adenosine kinase inhibitor: dependence on formalin concentration. *Eur. J. Pharmacol.*, **1995,** 286, 177-184

[234] McGaraughty, S.; Chu, K.L.; Wismer, C.T.; Mikusa, J.; Zhu, C.Z.; Cowart, M.; Kowaluk, E.A.; Jarvis, M.F. Effects of A-134974, a novel adenosine kinase inhibitor, on carrageenan-induced inflammatory hyperalgesia and locomotor activity in rats: evaluation of the sites of action. *J. Pharmacol. Exp. Ther.*, **2001,** 296, 501-509

[235] Jarvis, M.F.; Yu, H.; Kohlhaas, K.; Alexander, K.; Lee, C.H.; Jiang, M.; Bhagwat, S.S.; Williams, M.; Kowaluk, E.A. ABT-702 (4-amino-5-(3-bromophenyl)-7-(6-morpholinopyridin-3-yl)pyrido[2, 3-d]pyrimidine), a novel orally effective adenosine kinase inhibitor with analgesic and anti-inflammatory properties: I. In vitro characterization and acute antinociceptive effects in the mouse. *J. Pharmacol. Exp. Ther.*, **2000,** 295, 1156-1164

[236] Lee, Y.W.; Yaksh, T.L. Pharmacology of the spinal adenosine receptor which mediates the antiallodynic action of intrathecal adenosine agonists. *J. Pharmacol. Exp. Ther.*, **1996,** 277, 1642-1648

[237] Suzuki, R.; Stanfa, L.C.; Kowaluk, E.A.; Williams, M.; Jarvis, M.F.; Dickenson, A.H. The effect of ABT-702, a novel adenosine kinase inhibitor, on the responses of spinal neurones following carrageenan inflammation and peripheral nerve injury. *Br. J. Pharmacol.*, **2001,** 132, 1615-1623

[238] Kowaluk, E.A.; Mikusa, J.; Wismer, C.T.; Zhu, C.Z.; Schweitzer, E.; Lynch, J.J.; Lee, C.H.; Jiang, M.; Bhagwat, S.S.; Gomtsyan, A.; McKie, J.; Cox, B.F.; Polakowski, J.; Reinhart, G.; Williams, M.; Jarvis, M.F. ABT-702 (4-amino-5-(3-bromophenyl)-7-(6-morpholino-pyridin-3-yl)pyrido[2,3-d]pyrimidine), a novel orally effective adenosine kinase inhibitor with analgesic and anti-inflammatory properties. II. In vivo characterization in the rat. *J. Pharmacol. Exp. Ther.*, **2000,** 295, 1165-1174

[239] Jarvis, M.F.; Yu, H.; McGaraughty, S.; Wismer, C.T.; Mikusa, J.; Zhu, C.; Chu, K.; Kohlhaas, K.; Cowart, M.; Lee, C.H.; Stewart, A.O.; Cox, B.F.; Polakowski, J.; Kowaluk, E.A. Analgesic and anti-inflammatory effects of A-286501, a novel orally active adenosine kinase inhibitor. *Pain*, **2002,** 96, 107-118

[240] Kowaluk, E.A.; Kohlhaas, K.L.; Bannon, A.; Gunther, K.; Lynch, J.J., III; Jarvis, M.F. Characterization of the effects of adenosine kinase inhibitors on acute thermal nociception in mice. *Pharmacol. Biochem. Behav.*, **1999,** 63, 83-91

[241] Lynch, J.J., III; Jarvis, M.F.; Kowaluk, E.A. An adenosine kinase inhibitor attenuates tactile allodynia in a rat model of diabetic neuropathic pain. *Eur. J. Pharmacol.*, **1999,** 364, 141-146

[242] Jarvis, M.F.; Mikusa, J.; Chu, K.L.; Wismer, C.T.; Honore, P.; Kowaluk, E.A.; McGaraughty, S. Comparison of the ability of adenosine kinase inhibitors and adenosine receptor agonists to attenuate thermal hyperalgesia and reduce motor performance in rats. *Pharmacol. Biochem. Behav.*, **2002,** 73, 573-581

[243] Cottam, H.B.; Wasson, D.B.; Shih, H.C.; Raychaudhuri, A.; Di Pasquale, G.; Carson, D.A. New adenosine kinase inhibitors with oral antiinflammatory activity: synthesis and biological evaluation. *J. Med. Chem.*, **1993,** 36, 3424-3430

[244] Firestein, G.S.; Boyle, D.; Bullough, D.A.; Gruber, H.E.; Sajjadi, F.G.; Montag, A.; Sambol, B.; Mullane, K.M. Protective effect of an adenosine kinase inhibitor in septic shock. *J. Immunol.*, **1994,** 152, 5853-5859

[245] Rosengren, S.; Bong, G.W.; Firestein, G.S. Anti-inflammatory effects of an adenosine kinase inhibitor. Decreased neutrophil accumulation and vascular leakage. *J. Immunol.*, **1995,** 154, 5444-5451

[246] Firestein, G.S. Anti-inflammatory effects of adenosine kinase inhibitors in acute and chronic inflammation. *Drug Dev. Res.*, **1996,** 39, 371-376

[247] Poon, A.; Sawynok, J. Antinociceptive and anti-inflammatory properties of an adenosine kinase inhibitor and an adenosine deaminase inhibitor. *Eur. J. Pharmacol.*, **1999,** 384, 123-138

[248] Cronstein, B.N.; Naime, D.; Firestein, G. The antiinflammatory effects of an adenosine kinase inhibitor are mediated by adenosine. *Arthritis Rheum.*, **1995,** 38, 1040-1045

[249] Zhang, G.; Franklin, P.H.; Murray, T.F. Manipulation of endogenous adenosine in the rat prepiriform cortex modulates seizure susceptibility. *J. Pharmacol. Exp. Ther.*, **1993,** 264, 1415-1424

[250] Ugarkar, B.G.; Castellino, A.J.; DaRe, J.M.; Kopcho, J.J.; Wiesner, J.B.; Schanzer, J.M.; Erion, M.D. Adenosine kinase inhibitors. 2. Synthesis, enzyme inhibition, and antiseizure activity of diaryltubercidin analogues. *J. Med. Chem.*, **2000,** 43, 2894-2905

[251] Ugarkar, B.G.; DaRe, J.M.; Kopcho, J.J.; Browne, C.E., III; Schanzer, J.M.; Wiesner, J.B.; Erion, M.D. Adenosine kinase inhibitors. 1. Synthesis, enzyme inhibition, and antiseizure activity of 5-iodotubercidin analogues. *J. Med. Chem.*, **2000,** 43, 2883-2893

[252] McGaraughty, S.; Cowart, M.; Jarvis, M.F.; Berman, R.F. Anticonvulsant and antinociceptive actions of novel adenosine kinase inhibitors. *Curr. Top. Med. Chem.*, **2005,** 5, 43-58

[253] Pagonopoulou, O.; Efthimiadou, A.; Asimakopoulos, B.; Nikolettos, N.K. Modulatory role of adenosine and its receptors in epilepsy: possible therapeutic approaches. *Neurosci. Res.*, **2006,** 56, 14-20

[254] Ishiwata, K.; Furuta, R.; Shimada, J.; Ishii, S.; Endo, K.; Suzuki, F.; Senda, M. Synthesis and preliminary evaluation of [11C]KF15372, a selective adenosine A1 antagonist. *Appl. Radiat. Isot.*, **1995,** 46, 1009-1013

[255] Furuta, R.; Ishiwata, K.; Kiyosawa, M.; Ishii, S.; Saito, N.; Shimada, J.; Endo, K.; Suzuki, F.; Senda, M. Carbon-11-labeled KF15372: a potential central nervous system adenosine A1 receptor ligand. *J. Nucl. Med.*, **1996,** 37, 1203-1207

[256] Wakabayashi, S.; Nariai, T.; Ishiwata, K.; Nagaoka, T.; Hirakawa, K.; Oda, K.; Sakiyama, Y.; Shumiya, S.; Toyama, H.; Suzuki, F.; Senda, M. A PET study of adenosine A1 receptor in anesthetized monkey brain. *Nucl. Med. Biol.*, **2000,** 27, 401-406

[257] Noguchi, J.; Ishiwata, K.; Furuta, R.; Simada, J.; Kiyosawa, M.; Ishii, S.; Endo, K.; Suzuki, F.; Senda, M. Evaluation of carbon-11 labeled KF15372 and its ethyl and methyl derivatives as a potential CNS adenosine A1 receptor ligand. *Nucl. Med. Biol.*, **1997,** 24, 53-59

[258] Ishiwata, K.; Nariai, T.; Kimura, Y.; Oda, K.; Kawamura, K.; Ishii, K.; Senda, M.; Wakabayashi, S.; Shimada, J. Preclinical studies on [11C]MPDX for mapping adenosine A1 receptors by positron emission tomography. *Ann. Nucl. Med.*, **2002,** 16, 377-382

[259] Kiyosawa, M.; Ishiwata, K.; Noguchi, J.; Endo, K.; Wang, W.F.; Suzuki, F.; Senda, M. Neuroreceptor bindings and synaptic activity in visual system of monocularly enucleated rat. *Jpn. J. Ophthalmol.*, **2001,** 45, 264-269

[260] Wang, W.F.; Ishiwata, K.; Kiyosawa, M.; Shimada, J.; Senda, M.; Mochizuki, M. Adenosine A1 and benzodiazepine receptors and glucose metabolism in the visual structures of rats monocularly deprived by enucleation or eyelid suture at a sensitive period. *Jpn. J. Ophthalmol.*, **2003,** 47, 182-190

[261] Qing, G.L.T.; Suzuki, Y.; Kiyosawa, M.; Ishiwata, K.; Mochizuki, M. Functional and neuroreceptor imaging of the brain in bicuculline-induced dystonic rats. *Tohoku J. Exp. Med.*, **2009,** 217, 313-320

[262] Kawamura, K.; Ishiwata, K. Improved synthesis of [11C]SA4503, [11C]MPDX and [11C]TMSX by use of [11C]methyl triflate. *Ann. Nucl. Med.*, **2004,** 18, 165-168

[263] Shimada, Y.; Ishiwata, K.; Kiyosawa, M.; Nariai, T.; Oda, K.; Toyama, H.; Suzuki, F.; Ono, K.; Senda, M. Mapping adenosine A(1) receptors in the cat brain by positron emission tomography with [(11)C]MPDX. *Nucl. Med. Biol.*, **2002,** 29, 29-37

[264] Fukumitsu, N.; Ishii, K.; Kimura, Y.; Oda, K.; Sasaki, T.; Mori, Y.; Ishiwata, K. Imaging of adenosine A1 receptors in the human brain by positron emission tomography with [11C]MPDX. *Ann. Nucl. Med.*, **2003,** 17, 511-515

[265] Fukumitsu, N.; Ishii, K.; Kimura, Y.; Oda, K.; Sasaki, T.; Mori, Y.; Ishiwata, K. Adenosine A1 receptor mapping of the human brain by PET with 8-dicyclopropylmethyl-1-11C-methyl-3-propylxanthine. *J. Nucl. Med.*, **2005,** 46, 32-37

[266] Kimura, Y.; Ishii, K.; Fukumitsu, N.; Oda, K.; Sasaki, T.; Kawamura, K.; Ishiwata, K. Quantitative analysis of adenosine A1 receptors in human brain using positron emission tomography and [1-methyl-11C]8-dicyclopropylmethyl-1-methyl-3-propylxanthine. *Nucl. Med. Biol.*, **2004,** 31, 975-981

[267] Holschbach, M.H.; Olsson, R.A.; Bier, D.; Wutz, W.; Sihver, W.; Schuller, M.; Palm, B.; Coenen, H.H. Synthesis and evaluation of no-carrier-added 8-cyclopentyl-3-(3-[(18)F]fluoropropyl)-1-propylxanthine ([(18)F]CPFPX): a potent and selective A(1)-adenosine receptor antagonist for in vivo imaging. *J. Med. Chem.*, **2002,** 45, 5150-5156

[268] Bauer, A.; Holschbach, M.H.; Cremer, M.; Weber, S.; Boy, C.; Shah, N.J.; Olsson, R.A.; Halling, H.; Coenen, H.H.; Zilles, K. Evaluation of 18F-CPFPX, a novel adenosine A1 receptor ligand: in vitro autoradiography and high-resolution small animal PET. *J. Nucl. Med.*, **2003,** 44, 1682-1689

[269] Bauer, A.; Holschbach, M.H.; Meyer, P.T.; Boy, C.; Herzog, H.; Olsson, R.A.; Coenen, H.H.; Zilles, K. In vivo imaging of adenosine A1 receptors in the human brain with [18F]CPFPX and positron emission tomography. *Neuroimage.*, **2003,** 19, 1760-1769

[270] Meyer, P.T.; Bier, D.; Holschbach, M.H.; Boy, C.; Olsson, R.A.; Coenen, H.H.; Zilles, K.; Bauer, A. Quantification of cerebral A1 adenosine receptors in humans using [18F]CPFPX and PET. *J. Cereb. Blood Flow Metab*, **2004,** 24, 323-333

[271] Meyer, P.T.; Elmenhorst, D.; Bier, D.; Holschbach, M.H.; Matusch, A.; Coenen, H.H.; Zilles, K.; Bauer, A. Quantification of cerebral A1 adenosine receptors in humans using [18F]CPFPX and PET: an equilibrium approach. *Neuroimage.*, **2005,** 24, 1192-1204

[272] Meyer, P.T.; Elmenhorst, D.; Zilles, K.; Bauer, A. Simplified quantification of cerebral A1 adenosine receptors using [18F]CPFPX and PET: analyses based on venous blood sampling. *Synapse*, **2005,** 55, 212-223

[273] Meyer, P.T.; Elmenhorst, D.; Matusch, A.; Winz, O.; Zilles, K.; Bauer, A. 18F-CPFPX PET: on the generation of parametric images and the effect of scan duration. *J. Nucl. Med.*, **2006,** 47, 200-207

[274] Elmenhorst, D.; Meyer, P.T.; Matusch, A.; Winz, O.H.; Zilles, K.; Bauer, A. Test-retest stability of cerebral A1 adenosine receptor quantification using [18F]CPFPX and PET. *Eur. J. Nucl. Med. Mol. Imaging*, **2007,** 34, 1061-1070

[275] Matusch, A.; Meyer, P.T.; Bier, D.; Holschbach, M.H.; Woitalla, D.; Elmenhorst, D.; Winz, O.H.; Zilles, K.; Bauer, A. Metabolism of the A1 adenosine receptor PET ligand [18F]CPFPX by CYP1A2: implications for bolus/infusion PET studies. *Nucl. Med. Biol.*, **2006,** 33, 891-898

[276] Bier, D.; Holschbach, M.H.; Wutz, W.; Olsson, R.A.; Coenen, H.H. Metabolism of the A(1)1 adenosine receptor positron emission tomography ligand [18F]8-cyclopentyl-3-(3-fluoropropyl)-1-propylxanthine ([18F]CPFPX) in rodents and humans. *Drug Metab Dispos.*, **2006,** 34, 570-576

[277] Sihver, W.; Holschbach, M.H.; Bier, D.; Wutz, W.; Schulze, A.; Olsson, R.A.; Coenen, H.H. Evaluation of radioiodinated 8-Cyclopentyl-3-[(E)-3-iodoprop-2-en-1-yl]-1-propylxanthine ([*I]CPIPX) as a new potential A1 adenosine receptor antagonist for SPECT. *Nucl. Med. Biol.*, **2003,** 30, 661-668

[278] Blum, T.; Elmert, J.; Wutz, W.; Bier, D.; Coenen, H.H. First no-carrier added radioselenation of an adenosine A1 receptor ligand. *J. Label. Compd. Radiopharm.*, **2004,** 47, 415-427

[279] Lehel, S.Z.; Horvath, G.; Boros, I.; Mikecz, P.; Marian, T.; Szentmiklosi, A.J.; Tron, L. Synthesis of 5'-N-(2-[18F]fluoroethyl)-carboxamidoadenosine: a promising tracer for investigation of adenosine receptor system by PET technique. *J. Label. Compd. Radiopharm.*, **2000,** 43, 807-815

Chapter II

Small-Animal PET Study of Adenosine A_1 Receptors in Rat Brain: Blocking Receptors and Raising Extracellular Adenosine

Soumen Paul[1], Shivashankar Khanapur[1], Anna A. Rybczynska[1], Chantal Kwizera[1], Jurgen W.A. Sijbesma[1], Kiichi Ishiwata[2], Antoon T.M. Willemsen[1], Philip H. Elsinga[1,3] Rudi A.J.O. Dierckx[1,3] and Aren van Waarde[1]

[1] *Nuclear Medicine and Molecular Imaging, University Medical Center Groningen, University of Groningen, Groningen, The Netherlands*

[2] *Positron Medical Center, Tokyo Metropolitan Institute of Gerontology, Tokyo, Japan*

[3] *Department of Nuclear Medicine, University Hospital Ghent, Ghent, Belgium*

J Nucl Med. 2011; 52:1293–1300

Abstract

Activation of adenosine A_1 receptors (A_1R) in the brain causes sedation, reduces anxiety, inhibits seizures and promotes neuroprotection. Cerebral A_1R can be visualized and apparent receptor densities estimated using 8-dicyclopropyl-methyl-1-[^{11}C] methyl-3-propyl-xanthine (MPDX) and PET. We tested whether MPDX can be employed for quantitative studies of cerebral A_1R in rodents. MPDX was injected (i.v.) into isoflurane-anesthetized male Wistar rats. Uptake of radioactivity in the CNS was continuously monitored, using a microPET Focus 220 camera. A cannula in a femoral artery was used for blood sampling. Three groups of animals were studied (1) controls (i.p. injection of saline); (2) pretreated with the A_1R antagonist DPCPX (1 mg, i.p.); (3) pretreated with a 20% solution of ethanol (4 g/kg body weight) in saline plus the adenosine kinase inhibitor ABT-702 (1 mg, both i.p.). Treatment 2 results in occupancy of cerebral A_1R by non-radioactive DPCPX, whereas treatment 3 is known to result in a large increase of extracellular adenosine. In groups 1 and 3, the brain was clearly visualized. High uptake of the tracer was noted in striatum, hippocampus and cerebellum. In group 2, tracer uptake was strongly suppressed and regional differences were abolished. Treatment 3 resulted in an unexpected 40-45% increase of the cerebral uptake of MPDX as indicated by increases of PET-SUV, distribution volume from Logan plot, binding potential from 2-tissue compartment model fit, and SUV from a biodistribution study performed after the PET scan. The partition coefficient of the tracer (K_1/k_2 from 2-tissue compartment model fit) was not altered under the study conditions. In conclusion: MPDX shows a regional distribution in rat brain consistent with binding to A_1R. Tracer binding is blocked by the selective A_1R antagonist DPCPX. Pretreatment of animals with ethanol and adenosine kinase inhibitor causes a significant increase of MPDX uptake. This increase appears to reflect an increased binding potential of A_1R rather than altered delivery of MPDX to the brain.

Key Words: receptors; adenosine A_1; adenosine kinase inhibitor; brain; positron emission tomography (PET); ethanol

2.1 Introduction

The adenosine receptor (R) family consists of the A_1, A_{2A}, A_{2B} and A_3 subtypes. These are members of the larger P1 family of seven transmembrane purinergic receptors. A_1 and A_3R inhibit whereas A_{2A} and A_{2B} stimulate production of the second messenger, cAMP. A_1R and $A_{2A}R$ are activated by nanomolar concentrations of adenosine whereas A_{2B} and A_3R become activated only when adenosine levels rise into the micromolar range during periods of inflammation, hypoxia or ischemia. [1-3].

A_1Rs are highly expressed and extensively distributed in various regions of the human brain such as the hippocampus, cerebral cortex, thalamic nuclei, and basal ganglia (4, 5). In

the central nervous system, adenosine acts as an endogenous modulator of neurotransmission (6), a neuroprotectant (7), and an anticonvulsant (8). Its neuroprotective action is mediated via A_1R and may be associated with inhibition of the release of excitatory neurotransmitters, hyperpolarization of neurons, and inhibition of Ca^{2+} channels (9). Adenosine acts also as an analgesic, by affecting nociceptive afferent and transmission neurons via A_1R (10). A_1R agonists usually stimulate (11), whereas A_1R antagonists diminish, sleep (12). Thus, such compounds may be therapeutically useful. Yet, A_1R agonists have failed to undergo successful clinical development because of dose-limiting cardiovascular side effects.

Adenosine kinase inhibitors (AKIs) represent an alternative treatment strategy. Adenosine kinase (AK) catalyzes a phosphorylation reaction, converting adenosine to adenosine monophosphate (13, 14). The inhibition of AK decreases the cellular reuptake of adenosine, resulting in increased local adenosine concentrations (14). The feasibility of raising adenosine availability in the central nervous system by inhibiting AK has been demonstrated in hippocampal and spinal cord slices (15) and by in vivo studies on extracellular adenosine in rat striatum, which was increased up to 10-fold (16).The psychoactive drug ethanol also raises extracellular levels of adenosine in the brain (up to 4-fold (17)) by augmenting the rate of adenosine formation (18) and inhibiting adenosine uptake via nucleoside transporters (18–20).The anxiolytic, sedating, and motor-impairing effects of ethanol are related to its interaction with adenosinergic signaling.PET with a radiolabeled A_1R ligand may allow study of the involvement of A_1R in the pathophysiology of disease, the response of the A1R population to therapy, and assessment of the occupancy of A_1R by therapeutic drugs. Several positron emitting A_1R ligands have been prepared for this purpose, but only 2 have been widely used: 8-dicyclopropylmethyl-1-^{11}C-methyl-3-propylxanthine (^{11}C-MPDX) (21) and ^{18}F-8-cyclopentyl-3-(3-fluoropropyl)-1-propyl-xanthine (5). Both ligands bind with high affinity and selectivity to A1R in vivo (Ki and Kd values, 3.0 and 4.4 nM, respectively).

Because small-animal PET studies with [^{11}C]-MPDX had not been performed previously, we tested this ligand for quantitative small-animal PET studies in rodents with the intention of later using this technique for the assessment of changes of A_1R density in rodent models of human disease. In addition, we examined the impact of raised levels of extracellular adenosine on the cerebral binding of ^{11}C-MPDX.

2.2 Materials and Methods

2.2.1 Chemicals

Ethanol and triethylamine were purchased from Merck. The adenosine A_1R antagonist 1, 3-dipropyl-8-cyclopentylxanthine (DPCPX) was a product of Sigma, and the potent adenosine kinase inhibitor 4-amino-5-(3-bromophenyl)-7-(6-morpholino-pyridin-3-yl) pyrido [2, 3-d] pyrimidine dihydrochloride (ABT-702) was obtained from Tocris. Stock

solutions of DPCPX and ABT-702 were prepared in dimethyl sulfoxide. The radioligand [^{11}C]-MPDX was prepared by reaction of ^{11}C-methyl iodide with the appropriate 1-N-desmethyl precursor. Briefly, ^{11}C-methyl iodide was trapped in 0.3 mL of N,Ndimethylformamide containing 1 mg of 1-N-desmethyl precursor and 5 mL of NaOH and was heated at 120ºC for 5 min. After 1.0 mL of 0.1 M HCl had been added, the solution was loaded onto a high-performance liquid chromatography column (Econosphere, C18, 5 mm[Altech]; 10 · 250 mm) and eluted with a mixture of 0.1 M NaH_2PO_4 and ethanol (70/30) at a flow rate of 4 mL/min. The fractions containing [^{11}C]-MPDX were collected. Retention time of [^{11}C]-MPDX was 14 min. The decay-corrected radiochemical yield was 35% ± 5% (based on ^{11}C-methyl iodide), the specific radioactivity was greater than 11 TBq/mmol at the moment of injection, and the radiochemical purity was greater than 98%.

2.2.2 Animal Model

The animal experiments were performed by licensed investigators in compliance with the Law on Animal Experiments of The Netherlands. The protocol was approved by the Committee on Animal Ethics of the University of Groningen. Male Wistar rats were maintained at a 12-h light/12-h dark regime and were fed standard laboratory chow ad libitum (body weights are provided in Table 1).

Table 1. Animal data

Group	Body weight (g)	Injected dose (MBq)	Injected dose (nmol)	ROI size (cm^3)
Control (n = 5)	**299 ± 8**	**24 ± 10**	**2.2 ± 0.9**	**1.02 ± 0.02**
DPCPX (n = 5)	**314 ± 18**	**26 ± 14**	**2.4 ± 1.3**	**1.02 ± 0.04**
EtOH+ABT702 (n=6)	**302 ± 16**	**34 ± 11**	**3.1 ± 1.0**	**1.02 ± 0.03**
Metabolite analysis (n=6)	**314 ± 14**	**20 ± 12**	**1.8 ± 1.1**	**-**

Data are mean ± SD.

2.2.3 Small-Animal PET Scanning

In most experiments, 2 rats were scanned simultaneously, using a Focus 220 microPET camera (Siemens-Concorde). Animals were anesthetized with a mixture of isoflurane/air min (inhalation anesthesia, 5% ratio during induction, later reduced to 2%). A cannula was placed in a femoral artery for blood sampling. Rats were under anesthesia for 30–40 min before tracer injection (time required for cannulation and transmission scan). The tracer ([^{11}C]-MPDX) was injected through the penile vein (injected dose is given in **Table 1**). A list-mode protocol was used (76 min, brain in the field of view). Scanning was started during injection of radioactivity in the lower rat; the upper animal was injected 16 min later. The animal that was injected last was also anesthetized at a later moment. Thus, the duration of anesthesia was similar in all study groups. A series of blood samples (14 samples; volume, 0.10–0.15 mL) was drawn, initially in rapid succession (every 15 s) and later at longer intervals (≤30 min). Plasma was acquired from these samples by short centrifugation (Eppendorf centrifuge, 5 min at 13,000 rpm). Radioactivity in 25 uL of plasma was counted and used as an arterial input function. For examination of the specificity of tracer binding, 5 animals were pretreated by intraperitoneal injection of DPCPX (1 mg, in 0.3 mL of dimethyl sulfoxide, 15–20 min before injection of the tracer). For examination of the impact of raised levels of extracellular adenosine on [^{11}C]-MPDX binding, 5 other rats received ethanol (2 mL of a 20% solution in saline intraperitoneally) and the AKI ABT-702 (1 mg, in 0.3 mL of dimethyl sulfoxide intraperitoneally).Both ethanol and ABT-702 were administered 15–20 min before injection of [^{11}C]-MPDX. Control animals (n = 5) received saline only. The ethanol dose that we administered corresponds to substantial consumption of alcohol in humans (about six 0.33-L bottles of normal beer containing 5% alcohol). List-mode data were reframed into a dynamic sequence of 8 x 30, 3 x 60, 2 x 120, 2 x 180, 3 x 300, 1 x 480, 2 x 600, and 1 x 960 s frames. The data were reconstructed per time frame using an iterative reconstruction algorithm (attenuation-weighted 2-dimensional ordered-subset expectation maximization, provided by Siemens; 4 iterations, 16 subsets; zoom factor, 2). The final datasets consisted of 95 slices, with a slice thickness of 0.8 mm and an inplane image matrix of 128 x 128 pixels of size 1 x 1 mm. Datasets were fully corrected for random coincidences, scatter, and attenuation. A separate transmission scan (duration, 515 s) was acquired for attenuation correction. That scan was made before the emission scan. Images were smoothed with a gaussian filter (1.35 mm in both directions).

2.2.4 Small-Animal PET Data Analysis

Three-dimensional regions of interest (ROIs) were manually drawn around the entire brain. Time–activity curves and volumes (cm^3) for the ROIs were calculated, using standard software (Asi-Pro, version 6.2.5.0; Siemens-Concorde). PET standardized uptake values (SUVs) for brain radioactivity were calculated, using measured body weights and injected

doses and assuming a specific gravity of 1 g/mL for brain tissue and blood plasma. Dynamic PET data were analyzed using plasma radioactivity from arterial blood samples as an input function and a graphical method according to Logan (22). Because [^{11}C]-MPDX proved to be rapidly cleared but slowly metabolized, no metabolite correction of the input function was performed. The error introduced by this procedure (overestimation of the true plasma input) is 10.0% and identical in all study groups; thus, we concluded that metabolite correction could be omitted. Software routines for MatLab 7. (The MathWorks), written by Dr. Antoon T.M. Willemsen (University Medical Center Groningen), were used for curve fitting.The Logan fit was started at 10 min. The cerebral distribution volume (V_T) of the tracer was estimated from the Logan plot.The dynamic PET data were also analyzed using the same input function and software routines, a 2-tissue-compartment model (2TCM), and a fixed blood volume of 3.6%. The partition coefficient (K_1/k_2) and nondisplaceable binding potential (BP_{ND}) (k_3/k_4) of [^{11}C]-MPDX were estimated from the model fit. Similar methods were used previously by Kimura et al. (23) for quantification of A_1R in the human brain. However, A_1Rs are significantly expressed in rat cerebellum, in contrast to human cerebellum, in which A_1R density is negligible. Therefore, the cerebellum cannot be used as a reference region in small-animal PET studies of the rodent brain.

2.2.5 Biodistribution Studies

After the scanning period, the anesthetized animals were sacrificed. Blood was collected, and plasma and a cell fraction were obtained from the blood sample by short centrifugation (5 min at 1,000g). Several brain areas and peripheral tissues (Table 2) were excised. All tissue samples were weighed. The radioactivity in tissue samples was measured using a gamma-counter, applying a decay correction. The results were expressed as dimensionless SUVs. The parameter SUV is defined as tissue activity concentration (MBq/g) x [body weight (g)/injected dose (MBq)].

2.2.6 Metabolite Analysis

A separate group of animals (n = 6) was used for metabolite analysis. In these rats, a small-animal PET scan was obtained and a biodistribution study was performed, but a smaller series of arterial blood samples was drawn (at intervals of 5, 10, 20, 40, and 60 min after tracer injection, volume increasing from 0.3 to 0.7 mL). Plasma was acquired by short centrifugation (Eppendorf centrifuge, 5 min at 13,000 rpm). Protein was removed by mixing plasma with an equivalent volume of 20% trichloroacetic acid in acetonitrile, followed again by short centrifugation. The protein free supernatant was injected into a high-performance liquid chromatography system (stationary phase, uBondapak, 7.8 x 300 mm [Waters]; mobile phase, 3% triethylamine and phosphate, pH 2.0: acetonitrile, 60:40 v/v, with a flow rate of 2

mL/min). The retention time of authentic [^{11}C]-MPDX (and nonradioactive MPDX) was about 11 min. Two radioactive metabolites eluted at shorter retention times (6 and 8 min, respectively). This reversed-phase system is a slightly modified version of a published analytic procedure (24). One-milliliter samples of the eluate were collected at 0.5-min intervals. Radioactivity in these samples was determined.

2.2.7 Statistical Tests

Differences between groups were analyzed using 1-way ANOVA. A probability smaller than 0.05 was considered statistically significant.

2.3 Results

2.3.1 Small-Animal PET Images

Small-animal PET images acquired after injection of [^{11}C]-MPDX are presented in **Figure 1**. In saline-treated control animals, the brain was clearly visualized. High tracer uptake was observed in the hippocampus, cerebellum, and striatum (left panel) in addition to some areas of the cortex (image not shown). After pretreatment of rats with DPCPX, cerebral uptake of the tracer was strongly reduced, and regional differences in tracer uptake were no longer apparent (middle panel). When animals were pretreated with ethanol and the AKI ABT-702, a global increase of tracer uptake was noted, compared with the control group (right panel).

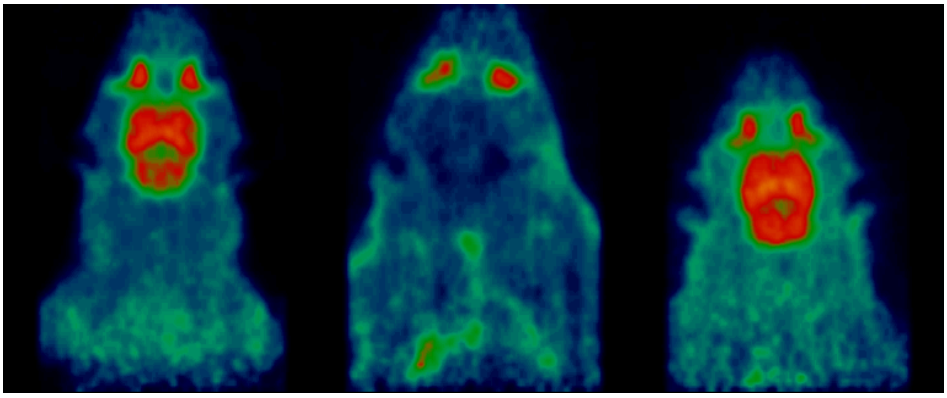

Fig.1 MicroPET images of rat brain acquired after injection of [^{11}C]-MPDX. Left: Untreated control animal, Middle: Animal pretreated with DPCPX, Right: animal pretreated with ethanol and ABT-702.

2.3.2 Kinetics of Radioactivity in Brain and Plasma

Cerebral kinetics of [^{11}C]-MPDX –derived radioactivity (PET SUV in the whole brain as a function of time) are presented in **Fig 2**. In saline-treated control animals, uptake of the tracer rapidly increased to a maximum, which was already reached between 7 and 12 min, and was followed by washout. In animals pretreated with DPCPX, only a rapid washout of tracer was observed, and the cerebral uptake of ^{11}C was strongly reduced. In rats pretreated

with ABT-702 and ethanol, cerebral uptake of radioactivity was significantly increased, compared with the control group. Maximal tracer uptake now occurred after 13–20 min and was followed by washout.

On the basis of SUVs measured with small-animal PET, A_1R densities reported in the literature (e.g., 5,003 fmol of protein per milligram in rat hippocampus (25), injected masses of the tracer (**Table 1**), and assuming that cerebral tissue contains 10% protein, we estimate that less than 5% of the A_1R population in the rat brain was occupied by [^{11}C]-MPDX under the conditions of our study. Kinetics of radioactivity in rat plasma after injection of [^{11}C]-MPDX are presented in **Figure 2.** A rapid, biexponential clearance was observed in all groups. Treatment of animals with DPCPX or a combination of ethanol and AKI (ABT-702) did not significantly affect tracer clearance from the plasma compartment. Areas under the curve (percentage of control) were 100.0 ± 8.4, 95.5 ± 6.6, and 96.0 ± 7.5 for the baseline, ethanol and ABT-702, and DPCPX groups, respectively (mean ± SEM).

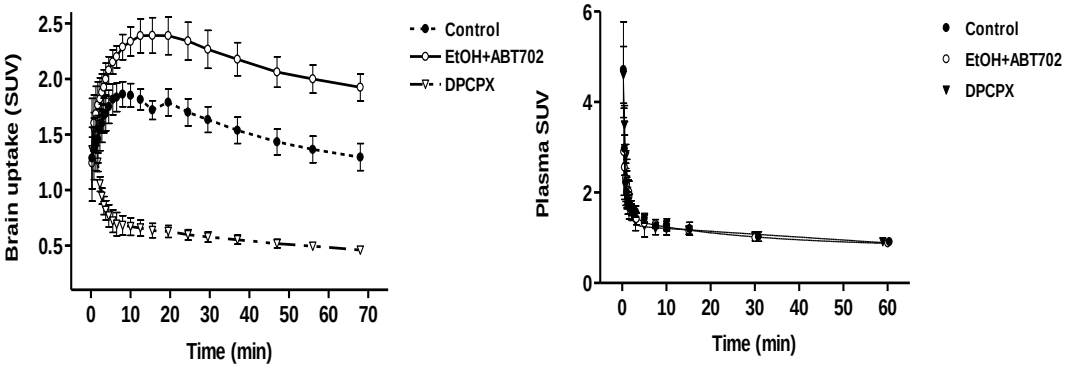

Fig.2. Kinetics of [^{11}C]-MPDX –derived radioactivity in rat brain (left) and plasma (right). Error bars indicate SEM. Plasma data are not corrected for metabolites. ● = control group; o = Ethanol and ABT-702 –treated animals; ▽ = animals pretreated with DPCPX

2.3.3 Metabolite Analysis

The appearance of radiolabeled metabolites in rat plasma after injection of [^{11}C]-MPDX was studied in 2 untreated control animals, 2 rats treated with ethanol and ABT-702, and 2 rats pre-treated with DPCPX. Injected [^{11}C]-MPDX was found to be hardly metabolized. The fraction of parent compound decreased from almost 100% at time zero to 82% – 84% at 60 min (Fig. 3). Pre-treatment did not affect the rate of tracer metabolism **(Fig.3).**

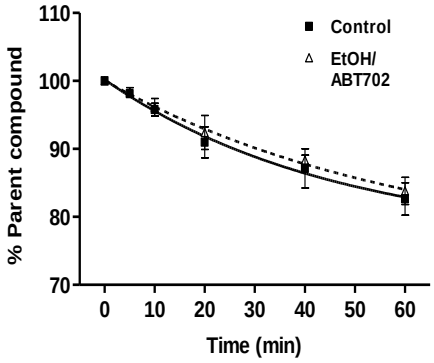

Fig.3. Fraction of plasma radioactivity representing parent [^{11}C]-MPDX. Pooled data are used because group differences were not observed. Error bars indicate SEM.

2.3.4 Biodistribution

Biodistribution data of ^{11}C, acquired 80 min after injection of [^{11}C]-MPDX are presented in **Table 2**. Pre-treatment of animals with DPCPX resulted in a highly significant reduction of tracer uptake in all studied brain areas. Among peripheral organs, a significant reduction of tracer uptake was observed only in the spleen. DPCPX treatment caused a significant increase of the amount of radioactivity in the liver. Renal uptake of the tracer appeared to be increased as well, but the change was relatively small and this trend did not reach statistical significance. Treatment of rats with ethanol and ABT-702 increased uptake of radioactivity in the brain. This increase was statistically significant in the amygdala, cerebellum, entorhinal cortex, hippocampus, medulla, and pons. In other brain areas, an increase was also noted but this trend did not reach statistical significance because of a relatively large individual variance in the study groups. Outside the brain, increases of tracer uptake were noted in lungs, skeletal muscle, pancreas, and red blood cells after treatment of animals with ethanol and ABT-702.

Table 2. Biodistribution data of [^{11}C]-MPDX , 80 min after injection

Tissue	Control animals	DPCPX-pretreated	Difference vs control	EtOH/ABT 702-treated	Difference vs control
Amygdala	0.75 ± 0.09	0.27 ± 0.05	< 0.0001	1.12 ± 0.12	< 0.0005
Bulbus olf	0.64 ± 0.18	0.34 ± 0.07	< 0.01	0.75 ± 0.27	NS
Cerebellum	1.34 ± 0.29	0.46 ± 0.09	0.0001	2.16 ± 0.42	< 0.01
Cingulate	0.88 ± 0.16	0.35 ± 0.08	0.0001	1.13 ± 0.23	0.06
Entorhinal	0.89 ± 0.10	0.37 ± 0.04	< 0.0001	1.27 ± 0.25	< 0.01
Frontal	0.89 ± 0.20	0.30 ± 0.08	0.0002	1.16 ± 0.26	NS
Hippocampus	1.09 ± 0.14	0.31 ± 0.08	< 0.0001	1.47 ± 0.24	0.01
Medulla	0.75 ± 0.18	0.42 ± 0.11	0.01	1.51 ± 0.29	< 0.001
Par/Temp/Occ	0.97 ± 0.20	0.34 ± 0.07	0.0001	1.40 ± 0.48	NS
Pons	0.89 ± 0.21	0.44 ± 0.14	< 0.01	1.45 ± 0.30	< 0.01
Striatum	1.01 ± 0.13	0.31 ± 0.07	< 0.0001	1.18 ± 0.31	NS
Bone	0.24 ± 0.04	0.22 ± 0.09	NS	0.24 ± 0.09	NS
Colon	0.83 ± 0.21	0.61 ± 0.19	NS	0.71 ± 0.06	NS
Duodenum	1.12 ± 0.33	0.95 ± 0.57	NS	1.19 ± 0.17	NS
Fat	1.95 ± 1.15	1.52 ± 0.19	NS	1.06 ± 0.24	NS
Heart	0.69 ± 0.14	0.66 ± 0.08	NS	0.85 ± 0.17	NS
Ileum	1.52 ± 0.52	1.19 ± 0.41	NS	1.38 ± 0.43	NS
Kidney	1.09 ± 0.18	1.26 ± 0.07	0.08	1.50 ± 0.50	NS
Liver	2.94 ± 0.40	4.43 ± 1.03	< 0.02	3.63 ± 0.68	NS
Lung	0.70 ± 0.09	0.73 ± 0.07	NS	0.88 ± 0.07	< 0.01
Muscle	0.40 ± 0.09	0.48 ± 0.07	NS	0.53 ± 0.07	< 0.05
Pancreas	0.98 ± 0.18	1.01 ± 0.23	NS	1.48 ± 0.22	< 0.005
Plasma	0.77 ± 0.06	0.73 ± 0.13	NS	0.71 ± 0.13	NS
Red cells	0.34 ± 0.04	0.38 ± 0.09	NS	0.44 ± 0.07	< 0.02
Spleen	0.95 ± 0.14	0.65 ± 0.06	< 0.005	1.06 ± 0.26	NS
Trachea	0.73 ± 0.15	0.81 ± 0.31	NS	0.85 ± 0.23	NS

SUV values (mean ± S.D.) are listed, NS = not significant

2.3.5 Graphical Analysis of PET Data

V_T of tracer was calculated using a Logan plot (**Fig. 4**), time–activity curves from an ROI drawn around the entire brain, and radioactivity counts from arterial blood samples. V_T of tracer was significantly decreased (by 63%) after pretreatment of animals with DPCPX and significantly increased (by 39%) after pretreatment with ethanol and ABT-702 (**Table 3**).

Table 3. Results from graphical analysis and compartment modeling of PET data (ROI drawn around entire brain)

Parameter	V_T (Logan plot)	K_1/k_2 (2TCM)	BP_{ND} (k_3/k_4) (2TCM)	V_T (2TCM)
Control rats	1.52 ± 0.18	0.62 ± 0.17	1.52 ± 0.10	1.56 ± 0.37
DPCPX pretreated	0.57 ± 0.05 ($p < 0.0001$)	0.58 ± 0.07 (NS)	0.00 ($p < 0.0001$)	0.58 ± 0.07 ($p < 0.0001$)
EtOH/ABT702 pretreated	2.12 ± 0.25 ($p < 0.005$)	0.68 ± 0.17 (NS)	2.34 ± 0.64 ($p < 0.05$)	2.21 ± 0.44 ($p < 0.05$)

Mean ± S.D. P-values relate to the effect of pretreatment compared to untreated controls.

2.3.6 Compartment Modeling of PET Data

A 2TCM was fitted to time–activity curves from an ROI drawn around the entire brain, using radioactivity counts from arterial blood samples as an input function. A 1-tissuecompartment model could not be fitted to the time–activity curves of control and ethanol and ABT-702 –treated animals at all, in contrast to a 2TCM. Thus, the 2TCM was clearly superior. The partition coefficient of [^{11}C]-MPDX (ratio K_1/k_2 from the model fit) was not significantly affected by any of the treatments, in contrast to BP_{ND} (**Table 3**). BP_{ND} was reduced to zero after treatment of animals with DPCPX and significantly increased (by 54%) after treatment with ethanol and ABT-702. V_T calculated from the 2TCM fit corresponded closely to V_T acquired by graphical (Logan) analysis of the PET data, although the intraindividual variability was greater. V_T (from the model fit) was significantly reduced (by 63%) after pretreatment of animals with DPCPX and significantly increased (by 42%) after treatment with ethanol and ABT-702.

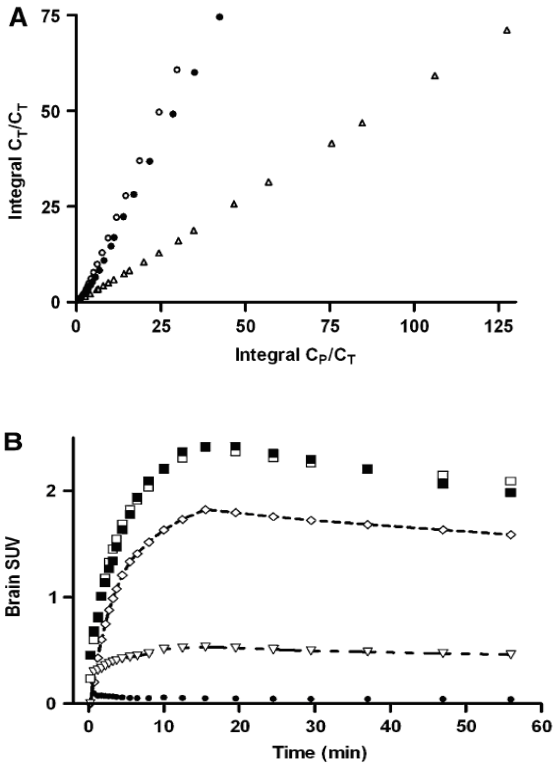

Fig,4. Logan plots (A) of control, ethanol and ABT-702–treated, and DPCPX-treated rats and 2TCM fit (B) for animal pretreated with ethanol and ABT-702. (A) ● = 5 control group; O = ethanol and ABT- 702–treated animals; Δ =animals pretreated with DPCPX. (B) ■ = measured activity in brain; □ = fitted activity in brain, ◊ = specific binding in brain; ▽= nondisplaceable binding in brain and tracer in plasma; ♦ = tracer in plasma.

2.4 Discussion

2.4.1 Specificity of [^{11}C]-MPDX Binding

The regional distribution of radioactivity in the rat brain after injection of [^{11}C]-MPDX (**Fig**. **1**, left) suggests that this tracer is capable of visualizing regional A1R densities. Further evidence for specific in vivo binding of [^{11}C]-MPDX was obtained by pretreating animals with the subtype-selective antagonist DPCPX. In pretreated animals, the brain uptake of radioactivity after injection of [^{11}C]-MPDX was strongly suppressed, and regional differences were no longer evident (**Fig. 1,** middle; **Fig. 2,** top). A biodistribution study,

performed at 80 min after tracer injection, confirmed that uptake of radioactivity was reduced by DPCPX to a low value that was homogeneous throughout the brain (**Table 2**). The greatest declines were observed in the hippocampus (72%), striatum (69%), cerebellum (66%), frontal cortex (66%), parietal cortex (65%), and amygdala (64%). Outside the brain, a reduction of [^{11}C]-MPDX uptake was observed only in the spleen, possibly reflecting specific binding of the tracer to A_1R, because A_1Rs are involved in splenic contraction (26).DPCPX caused a significant increase of the levels of radioactivity in rat liver and tended to increase renal activity levels as well (**Table 2**), indicating that after blocking of the receptor compartment, a greater fraction of the injected dose is taken up by organs involved in tracer excretion.

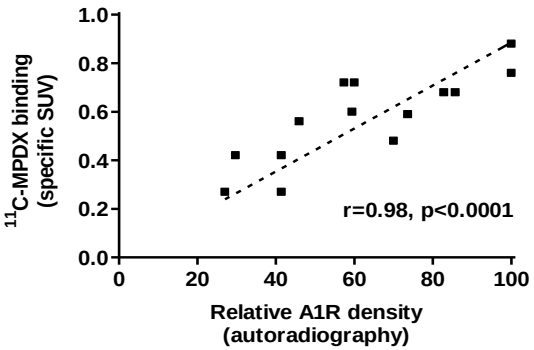

Fig.5. Correlation between specific binding of [^{11}C]-MPDX in rat brain and regional adenosine A_1 receptor density as known from autoradiography

To further test the origin of the PET signal, we plotted the specific binding of [^{11}C]-MPDX in various brain areas (uptake in saline-treated control animals minus uptake in animals pretreated with DPCPX, **Table 2**) against regional A_1R numbers, known from autoradiography (27–29). The regions plotted were the amygdala, cerebellum, cingulate, entorhinal, and frontal cortices; hippocampus; medulla; parietal–temporal–occipital cortex; pons; and striatum. Receptor density in the hippocampus (main target region) was set to 100%, to allow the use of data from several published studies. An excellent correlation was observed between literature values for A_1R density and [^{11}C]-MPDX uptake at 80 min after injection (**Fig. 5**).Data analysis of the cerebral time–activity curves in saline- and DPCPX-treated animals also confirmed specific binding of [^{11}C]-MPDX to cerebral A_1R. Tracer V_T in the entire brain—calculated either by graphical analysis or by kinetic modeling of the PET data—showed a decline (>60%) similar to that of tracer SUV measured after 80 min (**Table 3**). In contrast, BP_{ND} of [^{11}C]-MPDX estimated by fitting a 2TCM was reduced to zero after pretreatment of animals with DPCPX (**Table 3**), suggesting that specific binding of [^{11}C]-MPDX is absent in DPCPX-treated animals.

2.4.2 Effect of Ethanol and Inhibition of Adenosine Kinase

Acute administration of ethanol is known to result in strong increases of extracellular adenosine both in cell culture and in the rat brain in vivo, which can be assessed by microdialysis (17). Two different mechanisms may underlie this effect of ethanol. First, ethanol is metabolized to acetate and acetyl-coA before entering the tricarboxylic acid cycle. Increased flux through acetyl coA-synthetase leads to increased production of adenosine from adenosine monophosphate via 5'-nucleotidase and stimulation of cellular adenosine release (18). Second, ethanol blocks nucleoside transporters in cellular membranes, particularly the type 1 equilibrative nucleoside transporter (19,20,30,31). Increased binding of adenosine to cerebral A_1R is believed to be an important factor underlying the motor incoordination (32–35) and sleep-promoting (36) effects of ethanol

The coadministration of an AKI (e.g., ABT-702) with ethanol leads to even stronger increases of extracellular adenosine, because phosphorylation of adenosine by the enzyme AK is normally the primary route of adenosine metabolism. Inhibition of AK decreases the rate of adenosine inactivation and locally enhances extracellular adenosine concentrations—not at baseline but rather under conditions of increased formation of adenosine. Orally administered AKIs are known to raise regional concentrations of endogenous adenosine in the brain (15, 16), and for this reason, these compounds have therapeutic potential as analgesic, antiinflammatory, and antiepileptic agents (14, 37). Because both ethanol administration and AK inhibition are known to increase the levels of extracellular adenosine, we expected to observe a decreased binding of the PET tracer [^{11}C]-MPDX in the rat brain after acute treatment of rats with ethanol and ABT-702. Competition of adenosine for tracer binding to A_1R is likely to occur, because the affinities of adenosine and [^{11}C]-MPDX for cerebral A_1R are in the same (nanomolar) range (38). However, in ethanol and ABT-702–pretreated animals, we observed a paradoxic increase rather than a decrease of cerebral tracer binding. Statistically significant increases occurred in PET SUV (**Figs. 1 and 2**), SUV from an ex vivo biodistribution study (**Table 2**), and tracer V_T (Table 3).

Kinetic modeling was performed to gain more insight into the mechanisms underlying the paradoxic increase of cerebral radioactivity induced by ethanol and ABT-702. Fitting of a 2TCM to the cerebral time–activity curves of control and treated animals indicated that the partition coefficient of the tracer (K_1/k_2) was not affected by treatment, in contrast to BP_{ND}, which showed a significant increase (**Table 3**). The fit data, and also our data on tracer clearance (**Fig. 2**) and metabolism (**Fig. 3**), suggest that tracer delivery is not changed by treatment. Increases of the apparent A1R densities (on average, 35%; maximally, 55%) in the brain of rats and mice have been reported, both after acute (32,39) and after chronic (39,40) administration of ethanol, using ex vivo binding assays. Such changes could cause increased cerebral binding of [^{11}C]-MPDX after treatment of rodents with ethanol and ABT-702.

However, further studies are necessary to identify the mechanism underlying increased binding of the A_1R ligand under these conditions.

2.5 Conclusion

Our data suggest that regional A_1R densities in rat brain can be assessed using the tracer [^{11}C]-MPDX and small-animal PET. In the brain of untreated control animals, the highest levels of tracer uptake were observed in target regions with a high density of A_1R, such as the hippocampus, striatum, cerebellum, and cerebral cortex (**Fig. 1**). Pretreatment of animals with the specific A_1R antagonist DPCPX resulted in a strong suppression of tracer uptake in the central nervous system and an abolishment of the regional differences (**Fig.1**; **Table 2**). Specific binding of the tracer in various brain regions corresponded closely to regional A_1R densities known from autoradiography (**Fig. 5**). Tracer binding can be quantified both by graphical analysis (Logan plot, calculation of V_T) and by kinetic modeling (BP_{ND} or V_T from 2TCM (**Table 3**). The PET data did not provide evidence for increased competition of endogenous adenosine after acute treatment of animals with ethanol and ABT-702, but a globally increased binding of [^{11}C]-MPDX was noted in the rat brain (**Figs. 1** and **2; Tables 2 and 3**), which may correspond to increases of apparent A_1R density reported in the literature. Further studies are necessary to elucidate the mechanisms underlying the enhanced [^{11}C]-MPDX binding after treatment of animals with ethanol and ABT-702.

.

2.6 References

1. Collis MG, Hourani SM. Adenosine receptor subtypes. Trends Pharmacol Sci 1993; 14(10):360-366.

2. Fredholm BB, Abbracchio MP, Burnstock G, Daly JW, Harden TK, Jacobson KA et al. Nomenclature and classification of purinoceptors. Pharmacol Rev 1994; 46(2):143-156.

3. Haas HL, Selbach O. Functions of neuronal adenosine receptors. Naunyn Schmiedebergs Arch Pharmacol 2000; 362(4-5):375-381.

4. Fastbom J, Pazos A, Probst A, Palacios JM. Adenosine A1 receptors in the human brain: a quantitative autoradiographic study. Neuroscience 1987; 22(3):827-839.

5. Bauer A, Holschbach MH, Meyer PT, Boy C, Herzog H, Olsson RA et al. In vivo imaging of adenosine A1 receptors in the human brain with [18F]CPFPX and positron emission tomography. Neuroimage 2003; 19(4):1760-1769.

6. Williams M. Adenosine - a selective neuromodulator in the mammalian CNS? Trends Neurosci 1984; 7(5):164-168.

7. Fredholm BB. Adenosine and neuroprotection. Int Rev Neurobiol 1997; 40:259-280.

8. Young D, Dragunow M. Status epilepticus may be caused by loss of adenosine anticonvulsant mechanisms. Neuroscience 1994; 58(2):245-261.

9. Dunwiddie TV, Masino SA. The role and regulation of adenosine in the central nervous system. Annu Rev Neurosci 2001; 24:31-55.

10. Sawynok J, Reid A, Poon A. Peripheral antinociceptive effect of an adenosine kinase inhibitor, with augmentation by an adenosine deaminase inhibitor, in the rat formalin test. Pain 1998; 74(1):75-81.

11. Portas CM, Thakkar M, Rainnie DG, Greene RW, McCarley RW. Role of adenosine in behavioral state modulation: a microdialysis study in the freely moving cat. Neuroscience 1997; 79(1):225-235.

12. Lin AS, Uhde TW, Slate SO, McCann UD. Effects of intravenous caffeine administered to healthy males during sleep. Depress Anxiety 1997; 5(1):21-28.

13. Arch JR, Newsholme EA. The control of the metabolism and the hormonal role of adenosine. Essays Biochem 1978; 14:82-123.

14. McGaraughty S, Cowart M, Jarvis MF. Recent developments in the discovery of novel adenosine kinase inhibitors: mechanism of action and therapeutic potential. CNS Drug Rev 2001; 7(4):415-432.

15. Golembiowska K, White TD, Sawynok J. Adenosine kinase inhibitors augment release of adenosine from spinal cord slices. Eur J Pharmacol 1996; 307(2):157-162.

16. Britton DR, Mikusa J, Lee CH, Jarvis MF, Williams M, Kowaluk EA. Site and event specific increase of striatal adenosine release by adenosine kinase inhibition in rats. Neurosci Lett 1999; 266(2):93-96.

17. Sharma R, Engemann SC, Sahota P, Thakkar MM. Effects of ethanol on extracellular levels of adenosine in the basal forebrain: an in vivo microdialysis study in freely behaving rats. Alcohol Clin Exp Res 2010; 34(5):813-818.

18. Nagy LE. Ethanol metabolism and inhibition of nucleoside uptake lead to increased extracellular adenosine in hepatocytes. Am J Physiol 1992; 262(5 Pt 1):C1175-C1180.

19. Nagy LE, Diamond I, Casso DJ, Franklin C, Gordon AS. Ethanol increases extracellular adenosine by inhibiting adenosine uptake via the nucleoside transporter. J Biol Chem 1990; 265(4):1946-1951.

20. Krauss SW, Ghirnikar RB, Diamond I, Gordon AS. Inhibition of adenosine uptake by ethanol is specific for one class of nucleoside transporters. Mol Pharmacol 1993; 44(5):1021-1026.

21. Fukumitsu N, Ishii K, Kimura Y, Oda K, Sasaki T, Mori Y et al. Imaging of adenosine A1 receptors in the human brain by positron emission tomography with [11C]MPDX. Ann Nucl Med 2003; 17(6):511-515.

22. Logan J. Graphical analysis of PET data applied to reversible and irreversible tracers. Nucl Med Biol 2000; 27(7):661-670.

23. Kimura Y, Ishii K, Fukumitsu N, et al. Quantitative analysis of adenosine A1 receptors in human brain using positron emission tomography and [1-methyl-^{11}C] 8-dicyclopropylmethyl-1-methyl-3-propylxanthine. Nucl Med Biol 2004; 31:975–981.

24. Furuta R, Ishiwata K, Kiyosawa M, Ishii S, Saito N, Shimada J et al. Carbon-11-labeled KF15372: a potential central nervous system adenosine A1 receptor ligand. J Nucl Med 1996; 37(7):1203-1207.

25. Elmenhorst D, Basheer R, McCarley RW, Bauer A. Sleep deprivation increases A1 adenosine receptor density in the rat brain. Brain Res. 2009;1258:53–58.

26. Fozard JR, Milavec-Krizman M. Contraction of the rat isolated spleen mediated by adenosine A1 receptor activation. Br J Pharmacol 1993; 109(4):1059-1063.

27. Fastbom J, Pazos A, Palacios JM. The distribution of adenosine A1 receptors and 5'-nucleotidase in the brain of some commonly used experimental animals. Neuroscience 1987; 22(3):813-826.

28. Kanai Y, Araki T, Kato H, Kogure K. Autoradiographic distribution of neurotransmitter and second messenger system receptors in animal brains. Behav Brain Res 1994; 65(1):67-73.

29. Daval JL, Werck MC, Nehlig A, Pereira de Vasconcelos A. Quantitative autoradiographic study of the postnatal development of adenosine A1 receptors and their coupling to G proteins in the rat brain. Neuroscience 1991; 40(3):841-851.

30. Choi DS, Cascini MG, Mailliard W, Young H, Paredes P, McMahon T et al. The type 1 equilibrative nucleoside transporter regulates ethanol intoxication and preference. Nat Neurosci 2004; 7(8):855-861.

31. King AE, Ackley MA, Cass CE, Young JD, Baldwin SA. Nucleoside transporters: from scavengers to novel therapeutic targets. Trends Pharmacol Sci 2006; 27(8):416-425.

32. Clark M, Dar MS. In vitro autoradiographic evidence for adenosine modulation of ethanol-induced motor disturbances in rats. Alcohol Alcohol Suppl 1991; 1:203-206.

33. Phan TA, Gray AM, Nyce JW. Intrastriatal adenosine A1 receptor antisense oligodeoxynucleotide blocks ethanol-induced motor incoordination. Eur J Pharmacol 1997; 323(2-3):R5-R7.

34. Dar MS, Mustafa SJ. Acute ethanol/cannabinoid-induced ataxia and its antagonism by oral/systemic/intracerebellar A1 adenosine receptor antisense in mice. Brain Res 2002; 957(1):53-60.

35. Connole L, Harkin A, Maginn M. Adenosine A1 receptor blockade mimics caffeine's attenuation of ethanol-induced motor incoordination. Basic Clin Pharmacol Toxicol 2004; 95(6):299-304.

36. Thakkar MM, Engemann SC, Sharma R, Sahota P. Role of wake-promoting basal forebrain and adenosinergic mechanisms in sleep-promoting effects of ethanol. Alcohol Clin Exp Res 2010; 34(6):997-1005.

37. Kowaluk EA, Jarvis MF. Therapeutic potential of adenosine kinase inhibitors. Expert Opin Investig Drugs 2000; 9(3):551-564.

38. Noguchi J, Ishiwata K, Furuta R, Simada J, Kiyosawa M, Ishii S et al. Evaluation of carbon-11 labeled KF15372 and its ethyl and methyl derivatives as a potential CNS adenosine A1 receptor ligand. Nucl Med Biol 1997; 24(1):53-59.

39. Jarvis MF, Becker HC. Single and repeated episodes of ethanol withdrawal increase adenosine A1, but not A2A, receptor density in mouse brain. Brain Res 1998; 786(1-2):80-88.

40. Daly JW, Shi D, Wong V, Nikodijevic O. Chronic effects of ethanol on central adenosine function of mice. Brain Res 1994; 650(1):153-15

Chapter III

[^{11}C]-MPDX and PET to study adenosine A_1 receptor occupancy by non-radioactive agonists and antagonists

Soumen Paul[1], Shivashankar Khanapur[1], Jurgen W Sijbesma[1], Kiichi Ishiwata[2], Philip H Elsinga[1], Peter Meerlo[3], Rudi A Dierckx[1], Aren van Waarde[1]

[1] *University of Groningen, University Medical Center Groningen, Nuclear Medicine and Molecular Imaging, Groningen, Netherlands*

[2] *Tokyo Metropolitan Institute of Gerontology, Research Team for Neuroimaging, Tokyo, Japan*

[3] *University of Groningen, Center for Behaviour and Neurosciences, Groningen, Netherlands*

J. Nucl Med.2014; 55(2):315-20

Abstract

Adenosine A_1 receptors (A_1Rs) in human and rodent brain can be visualized with the radioligand [^{11}C]-MPDX and PET. Here we investigated whether A_1R occupancy by non-radioactive agonists and antagonists can be assessed with this technique. **Methods**: MicroPET scans with arterial blood sampling were made in four groups of isoflurane-anesthetized Wistar rats: (1) Controls (n = 7) (2) Pretreated with a centrally active A1R agonist, N^6-cyclopentyladenosine (CPA, 0.25 mg/kg i.p., K_d 0.48 nM, n = 7) (3) Pretreated with a moderate dose of caffeine (antagonist for A_1 and A_{2A} receptors, 4 mg/kg i.p., K_d 11 µM, n = 6) and (4) pretreated with a high dose of caffeine (40 mg/kg i.p., n = 6). **Results:** Administration of CPA resulted in a strong reduction (>50%) of heart rate, and caffeine administration in a small increase (10-15%). A caffeine dose of 4 mg/kg (n=6) resulted in 65.9% A_1R occupancy and a 40 mg/kg dose (n=4) in 98.5% occupancy (calculated from modified Lassen plot). However, administration of CPA resulted in an increase of [^{11}C]-MPDX binding in the brain. **Conclusion:** MicroPET with [^{11}C]-MPDX can be used to assess antagonist but not agonist binding at A1Rs. Changes of tracer uptake after administration of CPA resemble previously reported changes induced by treatment of rats with ethanol and an adenosine kinase inhibitor (ABT702). Thus, administration of an exogenous agonist or raising the levels of the endogenous agonist have similar effects. Agonists and antagonists may bind to different sites on the A_1R protein having allosteric interactions.

Keywords: adenosine A_1 receptor, occupancy, N^6-cyclopentyladenosine, caffeine, brain

3.1 Introduction

Adenosine A_1 receptors (A_1Rs) are G-protein-coupled binding sites for the endogenous neuromodulator adenosine which inhibit formation of the second messenger, cyclic AMP. They are implicated in the regulation of neuronal activity, neuroprotection and neuroinflammation (*1*). Some A_1R agonists may be beneficial in the treatment of atrial arrhythmias, type 2 diabetes and angina (*2*).

Cerebral A_1Rs can be visualized using positron emission tomography (PET) and radiolabeled xanthine antagonists, such as 8-dicyclopropylmethyl-1-^{11}C-methyl-3-propyl-xanthine ([^{11}C]-MPDX) (*3,4*) and 8-cyclopentyl-3-[3-^{18}F-fluoropropyl]-1-propylxanthine (^{18}F-CPFPX) (*5,6*). In a previous study we have reported that [^{11}C]-MPDX can be used to quantify regional A_1R densities in rodent brain with microPET (*7*). PET offers the unique opportunity of measuring the fraction of receptor populations occupied by non-radioactive drugs in the living brain and relating levels of occupancy to the magnitude of the therapeutic effect or to unwanted side effects. Receptor occupancy is estimated by assessing competition of a non-radioactive drug with the radioligand for the same binding sites.

In order to explore the interaction of therapeutic drugs with A_1R, we have treated rats with two different test drugs before a [^{11}C]-MPDX -microPET scan: (i) N^6-cyclopentyladenosine (CPA) and (ii) caffeine. CPA is a potent adenosine receptor agonist (K_d 0.48 nM) with considerable selectivity for the A_1 subtype (*8,9*). Caffeine is a non-subtype-selective adenosine antagonist with moderate affinity (IC_{50} values 11 to 85 µM), which is widely consumed as a recreational drug (*10,11*). Occupancy of cerebral A_1Rs by caffeine or the potent (K_d 0.42 nM) and highly subtype-selective A_1R antagonist DPCPX (*12,13*) has been visualized using the tracers [^{18}F]-CPFPX (*14,15*) or [^{11}C]-MPDX (*7*) and PET. However, PET studies of the occupancy of cerebral A_1R by agonists have never been reported. Our present findings together with previous studies indicate that dose-dependent occupancy of the A_1R population by antagonists can be assessed with PET. However, administration of a high dose of the agonist CPA which strongly decreases heart rate, body temperature and locomotor activity in rodents (*16*) does not result in any measurable decline of binding of the PET tracer [^{11}C]-MPDX in rodent brain.

3.2 Materials and Methods

3.2.1 (Radio) chemicals

CPA and caffeine were purchased from Sigma (St.Louis, MO). The radioligand [^{11}C]-MPDX was prepared as described previously (*7*).

3.2.2 Experimental Animals

All animal experiments were performed by licensed investigators in compliance with the Law on Animal Experiments of The Netherlands. The protocol was approved by the Committee on Animal Ethics of Groningen University. Male outbred Wistar-Unilever (SPF) rats (body weight 304 ± 54 g) were obtained from Charles-River, maintained at a 12-h light/12-h dark regime and fed standard laboratory chow ad libitum. Four groups of animals were studied: 1) Controls (pretreated with saline, i.p., n = 7); 2) Animals pretreated with CPA (0.25 mg/kg, i.p., dissolved in 0.3 mL saline containing < 50 µL dimethyl sulfoxide, n = 7, see (*16*) 3) Animals pretreated with a moderate dose of caffeine (4 mg/kg, i.p., dissolved in saline, n = 6); and 4) Animals pretreated with a high dose of caffeine (40 mg/kg, i.p., dissolved in saline, n = 6). All treatments were given 5 to 10 min before injection of the tracer. Body weights and injected doses are listed in **Table 1**.

Table 1. Animal Data

Group	Body weight (g)	Injected dose (MBq)	Injected dose (nmol)
Control (n=7)	311 ± 56	23.3 ± 4.0	2.1 ± 0.4
CPA (n=7)	312 ± 31	25.7 ± 5.5	2.4 ± 0.5
Caffeine 4 mg/kg (n=6)	317 ± 90	23.4 ± 7.9	2.1 ± 0.7
Caffeine 40 mg/kg (n=6)	275 ± 19	12.1 ± 13.8	1.1 ± 1.3

3.2.3 PET Scanning

Two rats were scanned simultaneously, using a Focus 220 microPET camera (Siemens-Concorde, Knoxville, TN). Animals were anesthetized with a mixture of isoflurane/air (ratio 5% during induction, later reduced to ≤ 2%). Cannulas were placed in a femoral artery and vein for blood sampling and tracer injection, respectively. A transmission scan was made, using an external source of radioactive cobalt, in order to correct subsequently acquired [^{11}C]-MPDX emission images for attenuation and scatter. Rats were under anesthesia for 30–40 min before tracer injection (time required for cannulation and transmission scan). The tracer ([^{11}C]-MPDX, 21.5 ± 9.7 MBq in volume of 1 mL) was injected through the venous cannula, as a slow (1 min) bolus, using a Harvard-style pump. The camera was started as soon as the tracer entered the body of the first rat in the scanner; the second animal of the pair was injected 16 min later. Scanning was then continued for another 60 min. The animal that was injected last was also anesthetized at a later moment. Thus, the duration of anesthesia was similar in all study groups. A list-mode protocol was used (76 min, brain in the field of view). A series of blood samples (18 samples; volume, 0.10–0.15 mL) was drawn, initially in rapid succession (5 s) and later at longer intervals (up to 30 min). Plasma was acquired from these samples by centrifugation (Eppendorf centrifuge, 5 min at 13,000 rpm). Radioactivity in 25 µL of plasma and 25 µL of whole blood was counted and used as an arterial input function. During the entire scanning procedure, heart rate, stroke volume and blood oxygen level of the animals were monitored, using pulse oximeters (Nonin Pulse Sense).

3.2.4 Analysis of PET Data

List-mode data were reframed into a dynamic sequence of 8 × 30, 3 × 60, 2 ×120, 2 × 180, 3 × 300, 1 × 480, 3 × 600, and 1 × 960 s frames. The data were reconstructed per time frame using an iterative reconstruction algorithm (attenuation-weighted 2-dimensional

ordered-subset expectation maximization, provided by Siemens; 4 iterations, 16 subsets; zoom factor 2). The final datasets consisted of 95 slices, with a slice thickness of 0.8 mm and an in-plane image matrix of 128 ×128 pixels of size 1.1 mm. Datasets were fully corrected for random coincidences, scatter, and attenuation. Images were smoothed with a Gaussian filter (1.35 mm in both directions).

Time–activity curves (TACs) and volumes (cm^3) for the regions of interest (ROIs) were calculated using the Siemens Inveon Research Work Place 4.0 (IRW 4.0). ROIs were drawn around the (entire) bulbi olfactorii, frontal cortex, striatum, amygdala, parietal/temporal/occipital cortices, medulla, cerebellum, pons and hippocampus in a template MRI scan that was co-registered with the PET scan of interest by image fusion (*17*). Standardized uptake values measured by PET (PET-SUVs) were calculated, using measured body weights and injected doses [tissue activity concentration (MBq/mL)]/[(injected dose (MBq)/body weight (g)]. The cerebral distribution volume (V_T) of the tracer was estimated either from a Logan plot (linear regression started 10 min after tracer injection) or a 2-tissue-compartment model (2TCM) fit. For Logan graphical analysis, blood volume was fixed to 3.6% (*18*). The partition coefficient (K_1/k_2) and binding potential (k_3/k_4) of [^{11}C]-MPDX were estimated from the model fit.

Since there is no region with negligible A1R expression in the rodent brain, levels of receptor occupancy were calculated by comparing regional V_T levels in control and drug-treated rats, using a modified (i.e., axes-transformed) Lassen plot (*19*).

3.2.5 Biodistribution Studies

After the PET scan, the anesthetized animals were sacrificed. Blood was collected, and plasma was obtained from the blood sample by centrifugation (5 min at 1,000 × *g*). Several areas of the brain were dissected and peripheral organs were excised. These tissue samples were weighed and tissue radioactivity was measured with a gamma counter, applying a decay correction. Tracer uptake was expressed as a dimensionless SUV.

3.2.6 Statistical Tests

Differences between groups were analyzed using 1-way ANOVA. A probability smaller than 0.05 was considered statistically significant.

3.3 Results

3.3.1 Physiological Responses to Drug Treatment

About 5 min after administration of the A_1R agonist CPA, a very strong decline of heart rate was noted (> 50%). This decline persisted for the entire duration of the microPET scan (60 min), although a slight return to baseline occurred near the end of the scan. The decline of heart rate was accompanied by an increase of cardiac stroke volume. Blood oxygenation levels were not significantly altered. Administration of caffeine resulted in small (10 to 15%) increases of heart rate after 5 min which persisted for the entire duration of the scan, and no significant change of blood oxygenation.

3.3.2 Animal PET Images

The PET images that were acquired in this study were very similar to those reported previously (*7*). When animals were pretreated with the A_1R agonist CPA, a global increase of tracer uptake was noted, compared with the control group. After pretreatment of rats with caffeine (particularly at the highest dose), cerebral uptake of the tracer was strongly reduced and regional differences in tracer uptake were no longer apparent.

3.3.3 Kinetics of Radioactivity in Brain and Plasma

Cerebral kinetics of radioactivity were also very similar to those reported previously (*7*). In rats pretreated with CPA, uptake of radioactivity was increased compared to the control group (**Fig. 1**). In animals pretreated with caffeine, a rapid washout of tracer was observed, and the brain uptake of ^{11}C was strongly reduced (**Fig.1**).

Clearance of radioactivity from plasma appeared to be little affected by drug treatment. Although the shape of the plasma curve was different after treatment of animals with CPA, a stronger initial rise of plasma radioactivity being followed by a greater decline (**Fig. 2**), areas under the curve were similar in the four treatment groups. Expressed as a percentage of control, they were 92 ± 9 % (CPA), 112 ± 20% (caffeine 4 mg/kg), 104 ± 19% (caffeine 40 mg/kg) and 100 ± 16% (saline-treated control), respectively. None of these differences were statistically significant.

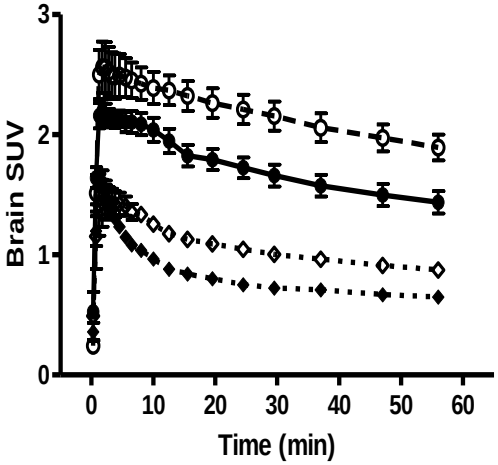

Figure 1: Kinetics of [^{11}C]-MPDX -derived radioactivity in rat brain. Error bars indicate SEM. Closed dots = control animals, open dots = CPA-treated, open squares = caffeine 4 mg/kg, closed squares = caffeine 40 mg/kg. SUV: standardized uptake value

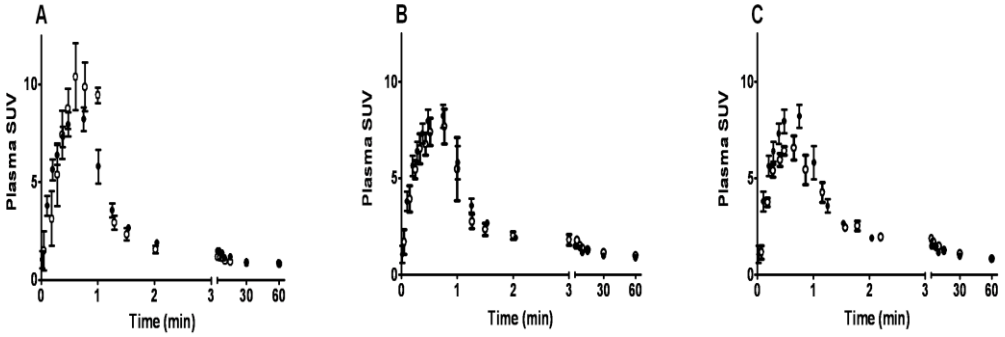

Figure 2 (Lower): Kinetics of [^{11}C]-MPDX -derived radioactivity in rat plasma. Error bars indicate SEM. Closed dots = control animals. Open dots panel A = CPA-treated, open dots panel B = caffeine 4 mg/kg, open dots panel C = caffeine 40 mg/kg. SUV: standardized uptake value

3.3.4 Biodistribution Data

The biodistribution data which were acquired after the PET scan (**Table 2**) corresponded closely to PET-SUV data in the last scan frame. Treatment of rats with CPA did not result in any decrease but rather an increase of cerebral radioactivity. This increase was statistically significant in the amygdala, cerebellum, frontal cortices, hippocampus, medulla, parietal, temporal and occipital cortex, striatum and rest of the brain. In entorhinal cortex and pons, an increase was also noted but this trend did not reach statistical significance because of a relatively large individual variance in the study groups. Outside the brain, tracer uptake was increased only in the liver (**Table 2**).

Pretreatment of animals with caffeine (4 mg/kg) reduced tracer uptake in cingulate, entorhinal, and frontal cortices, hippocampus, medulla and striatum. Among peripheral organs, a significant reduction of tracer uptake was observed only in the spleen. Levels of radioactivity in urine were increased (**Table 2**)

Pretreatment of rats with a high dose of caffeine (40 mg/kg) resulted in a highly significant reduction of tracer uptake in virtually all studied brain areas, with exception of pons and medulla (**Table 2**). Outside the brain, significant reductions of tracer uptake were noticed in spleen and duodenum, whereas uptake in the trachea was increased (**Table 2**).

3.3.5 Graphical Analysis of PET Data

Tracer V_T was calculated using a Logan plot, time–activity curves from an ROI drawn around the entire brain, and radioactivity counts from arterial blood samples. Compared to saline-treated controls, there was a significant increase in V_T after pretreatment of animals with CPA (from 1.60 ± 0.23 to 2.38 ± 0.36, $p = 0.0005$) and a significant decrease after treatment with caffeine (from 1.60 ± 0.23 to 0.86 ± 0.08, $p < 0.0001$, after the 4 mg/kg dose, and to 0.59 ± 0.06, $p < 0.0001$, after the 40 mg/kg dose, (**Fig. 3).**

Table 2. Biodistribution data of [^{11}C]-MPDX, 80 min after injection

Tissue	Control (n = 7)	Treated with CPA (n = 7)	Caffeine 4 mg/kg (n = 6)	Caffeine 40 mg/kg (n = 6)
Amygdala	0.92 ± 0.23	1.29 ± 0.11*	0.69 ± 0.18	0.52 ± 0.08*
Olfactory bulb	0.70 ± 0.24	0.78 ± 0.21	0.58 ± 0.28	0.43 ± 0.13*
Cerebellum	1.41 ± 0.24	2.23 ± 0.50*	1.10 ± 0.32	0.69 ± 0.15*
Cingulate	1.11 ± 0.27	1.05 ± 0.22	0.60 ± 0.16*	0.57 ± 0.18*
Entorhinal	1.23 ± 0.33	1.40 ± 0.20	0.66 ± 0.18*	0.59 ± 0.16*
Frontal	1.04 ± 0.26	1.30 ± 0.16*	0.67 ± 0.17*	0.51 ± 0.09*
Hippocampus	1.18 ± 0.25	1.55 ± 0.15*	0.82 ± 0.30*	0.57 ± 0.12*
Medulla	0.90 ± 0.16	1.23 ± 0.28*	0.70 ± 0.17*	0.71 ± 0.20
Parietal, temporal and occipital cortex	1.19 ± 0.30	1.62 ± 0.39*	0.88 ± 0.24	0.55 ± 0.08*
Pons	0.89 ± 0.27	1.12 ± 0.30	0.72 ± 0.18	0.64 ± 0.24
Striatum	1.13 ± 0.19	1.40 ± 0.20*	0.81 ± 0.23*	0.50 ± 0.07*
Rest of the brain	1.17 ± 0.27	1.53 ± 0.34*	0.89 ± 0.28	0.59 ± 0.10*
Bone	0.29 ± 0.14	0.33 ± 0.11	0.32 ± 0.06	0.35 ± 0.05
Colon	0.80 ± 0.30	0.98 ± 0.44	0.90 ± 0.19	1.01 ± 0.22
Duodenum	1.50 ± 0.29	1.63 ± 0.65	1.74 ± 0.56	1.02 ± 0.28*
Fat	1.78 ±0.43	1.41 ± 0.30	2.37 ± 1.23	1.99 ± 1.02
Heart	0.80 ± 0.14	0.99 ± 0.18	0.91 ± 0.21	0.86 ± 0.15
Ileum	1.24 ± 0.29	1.26 ± 0.38	1.31 ± 0.45	1.12 ± 0.17
Kidney	1.31 ± 0.15	1.49 ± 0.24	1.19 ± 0.25	1.45 ± 0.21
Liver	2.69 ± 0.49	3.25 ± 0.33*	3.09 ± 0.67	2.74 ± 0.48
Lung	0.86 ± 0.10	0.87 ± 0.09	0.85 ± 0.14	0.95 ± 0.19
Muscle	0.45 ± 0.06	0.53 ± 0.11	0.54 ± 0.09	0.50 ± 0.12
Pancreas	1.24 ± 0.27	1.37 ± 0.25	1.37 ± 0.48	1.51 ± 0.46
Plasma	0.90 ± 0.11	0.78 ± 0.10	0.92 ± 0.16	0.87 ± 0.17
Red Cells	0.42 ± 0.06	0.46 ± 0.08	0.41 ± 0.12	0.47 ± 0.09
Spleen	1.22 ± 0.18	1.15 ± 0.20	0.97 ± 0.20*	0.81 ± 0.18*
Trachea	0.64 ± 0.18	0.66 ± 0.13	0.84 ± 0.20	1.15 ± 0.20*
Urine	0.32 ± 0.39	0.03 ± 0.02	1.14 ± 0.73*	0.40 ± 0.88

SUV values are listed as mean ± SD. Significant differences between treatment and control groups are indicated by asterisks.

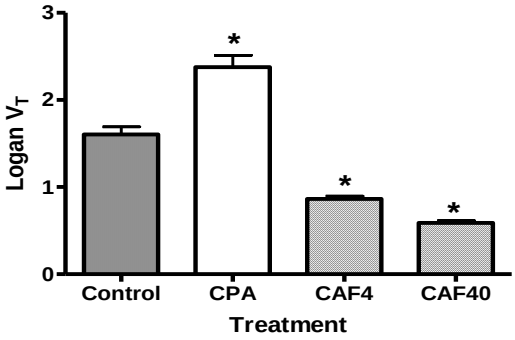

Figure 3. Distribution volume of [^{11}C]-MPDX in whole brain calculated from a Logan plot CPA = value for CPA-treated animals, CAF4 = caffeine 4 mg/kg, CAF40 = caffeine 40 mg/kg.

.

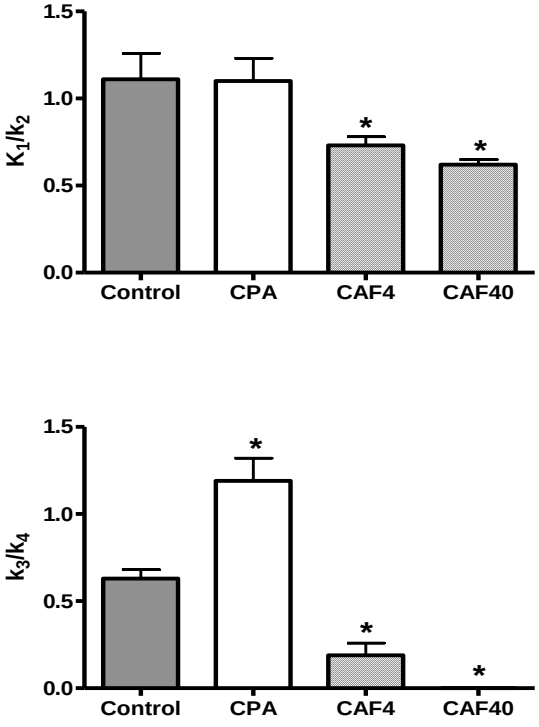

Figure 4. Partition coefficient (K_1/k_2) and binding potential (k_3/k_4) of [^{11}C]-MPDX in whole brain calculated from a 2-tissue compartment model fit.

3.3.6 Compartment Modeling of PET Data

When a 2TCM was fitted to time–activity curves from a ROI drawn around the entire brain, using radioactivity counts from arterial blood samples as input function, the partition coefficient of [^{11}C]-MPDX (ratio K_1/k_2 from the model fit) was found to be not significantly affected by CPA, but significantly decreased after treatment of animals with caffeine (**Fig.4**). Receptor occupancy by caffeine (calculated by the formula $100*(1-BP_{drug\text{-}treated}/BP_{control})$ was 69.8% for the 4 mg/kg dose and 100% for the 40 mg/kg dose. Tracer k_3/k_4 was significantly increased after treatment with CPA and significantly decreased by caffeine **(Fig. 4**). The PET data for the high-dose caffeine group were better fitted by a 1-tissue compartment model (1TCM) than a 2TCM, in contrast to the data from the three other treatment groups. Blood volume could be left floating during the 2TCM or 1TCM fits. The value estimated by the fit program was 3.3 ± 0.4% (mean ± s.e.m., n = 21). However, in some animals the program estimated a blood volume of zero percent. Data of these animals are not included in the mentioned value for blood volume.

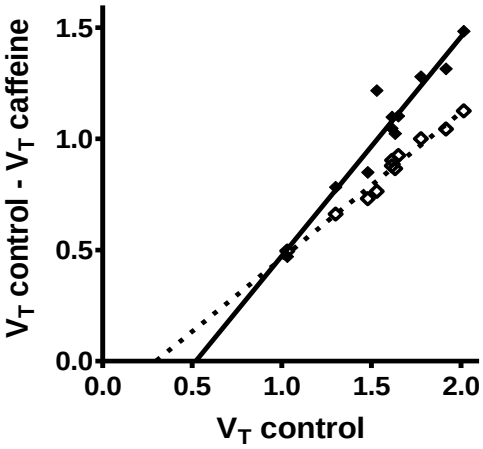

Figure 5. Lassen plots for A_1R occupancy by caffeine (open squares = 4 mg/kg, closed squares = 40 mg/kg). V_T: distribution volume.

3.3.7 Estimation of Receptor Occupancy

Modified Lassen plots were prepared using the regional Logan V_T values of animals in the control, low dose caffeine and high dose caffeine groups (**Fig. 5**). Both plots showed good correlation coefficients with r^2 values of 0.9738 and 0.9086, respectively. Receptor

occupancy by caffeine (estimated from the slope of the plot) was 65.9% for the 4 mg/kg dose and 98.5% for the 40 mg/kg dose. V_T of the nonspecific binding (estimated from the X-intercept of the plot) was about 0.5, i.e. less than 25% of total V_T in the target regions with the highest A_1R expression, hippocampus and cerebellum.

3.4 Discussion

The drug doses which we administered were based on data reported in the literature. CPA, at a dose of 0.25 mg/kg, causes a strong hypothermic response in the rat which persists for at least 2 h. After repeated administration on subsequent days, a downregulation of cerebral A_1R is observed which is particularly significant in the hippocampus and somatosensory cortex, and the A_1R system is functionally desensitized (*16*). Thus, CPA enters the brain and interacts with cerebral A1R. Caffeine, at a dose of 4 mg/kg, has been shown to compete with the ligand ^{18}F-FPCPX for binding to adenosine A1R in rat brain (*14).* Although the agonist mass which we injected was an order of magnitude smaller than the mass of the antagonist (0.25 and 4 mg/kg, respectively), in functional terms the agonist dose was much greater, since the affinity of CPA for A_1R is in the sub-nM range (*8,9*) whereas the affinity of caffeine for A_1R and $A_{2A}R$ is in the 10^{-5} M range (*10,11*). Yet, competition between non-radioactive caffeine and [^{11}C]-MPDX for binding to cerebral A_1R was observed, but competition between non-radioactive CPA and the radioligand was undetectable.

Values of A_1R occupancy by caffeine could be calculated from a modified Lassen plot ((*19*), **Fig.5**). A similar plot made from previously published data (*7*) indicated that administration of 3.2 mg/kg of the selective A_1R antagonist DPCPX was associated with 100% receptor occupancy. However, occupancy of A_1R by CPA could not be detected with [^{11}C]-MPDX , although the CPA dose which we injected caused a very strong decline of heart rate and was close to the upper limit which could be tolerated by our animals. This observation may indicate that purine agonists and xanthine antagonists interact differently with the A_1R pharmacophore. Experiments in which A_1R were chemically modified or altered by site-directed mutagenesis have indeed shown that agonists and antagonists bind to different domains of the A_1R protein (*20,21*).

We observed a paradoxic increase of [^{11}C]-MPDX binding in the rodent brain after administration of CPA (**Figs. 1, 3 and 4; Table 2**). Compartmental analysis of brain TACs using data from arterial plasma samples as input function indicated that K_1/k_2 values were unchanged but binding potential (k_3/k_4) values were elevated after treatment of animals with CPA (Fig. 4). Similar findings were reported previously for [^{11}C]-MPDX data of animals which had been treated with ethanol and the adenosine kinase inhibitor ABT702, in order to raise the endogenous levels of extracellular adenosine (*7*). These kinetic modeling results suggest that tracer delivery or the passage of [^{11}C]-MPDX across the blood-brain barrier are not altered in the presence of CPA (or ethanol and ABT702), but the availability of A_1R or the affinity of A1R for the radioligand is increased.

The most simple explanation for increased cerebral binding of [^{11}C]-MPDX in the presence of CPA or increased levels of extracellular adenosine is the hypothesis that agonists and antagonists bind to different domains on a single A_1R protein or to different protomers in a A_1R homodimer (*22*), agonist binding causing a conformational change of the receptor protein (or receptor complex) which facilitates the subsequent binding of an antagonist. Data from a few reports involving isolated biomembranes or brain slices have suggested that A_1R agonists can indeed increase the binding of A_1R antagonists to A1R (*23*,*24*), and vice versa (*22*).

3.5 Conclusion

Competition of non-radioactive xanthine antagonists (caffeine, DPCPX) with [^{11}C]-MPDX for binding to A_1R in the brain of living rodents was observed with microPET and values for dose-dependent receptor occupancy could be calculated from a modified Lassen plot (**Fig. 5**). However, administration of a high dose of an agonist with purine structure (CPA) did not result in measurable competition with [^{11}C]-MPDX for binding to the target receptor. These data and the data from our previously reported microPET study with ethanol and ABT702 (*7*) suggest that adenosine analogs and xanthines bind to different sites on the A_1R protein which may show allosteric interactions**.**

3.7 References

1. Paul S, Elsinga PH, Ishiwata K, Dierckx RA, van Waarde A. Adenosine A(1) receptors in the central nervous system: their functions in health and disease, and possible elucidation by PET imaging. *Curr Med Chem.* 2011;18:4820-4835.

2. Elzein E, Zablocki J. A1 adenosine receptor agonists and their potential therapeutic applications. *Expert Opin Investig Drugs.* 2008;17:1901-1910.

3. Noguchi J, Ishiwata K, Furuta R, et al. Evaluation of carbon-11 labeled KF15372 and its ethyl and methyl derivatives as a potential CNS adenosine A1 receptor ligand. *Nucl Med Biol.* 1997;24:53-59.

4. Kimura Y, Ishii K, Fukumitsu N, et al. Quantitative analysis of adenosine A1 receptors in human brain using positron emission tomography and [1-methyl-11C]8-dicyclopropylmethyl-1-methyl-3-propylxanthine. *Nucl Med Biol.* 2004; 31:975-981.

5. Holschbach MH, Olsson RA, Bier D, et al. Synthesis and evaluation of no-carrier-added 8-cyclopentyl-3-(3-[(18)F]fluoropropyl)-1-propylxanthine ([(18)F]CPFPX): a potent and selective A(1)-adenosine receptor antagonist for in vivo imaging. *J Med Chem.* 2002;45:5150-5156.

6. Bauer A, Holschbach MH, Meyer PT, et al. In vivo imaging of adenosine A1 receptors in the human brain with [18F] CPFPX and positron emission tomography. *Neuroimage.* 2003; 19:1760-1769.

7. Paul S, Khanapur S, Rybczynska AA, et al. Small-animal PET study of adenosine A1 receptors in rat brain: blocking receptors and raising extracellular adenosine. *J Nucl Med.* 2011;52:1293-1300.

8. Moos WH, Szotek DS, Bruns RF. N6-cycloalkyladenosines. Potent, A1-selective adenosine agonists. *J Med Chem.* 1985; 28:1383-1384.

9. Williams M, Braunwalder A, Erickson TJ. Evaluation of the binding of the A-1 selective adenosine radioligand, cyclopentyladenosine (CPA), to rat brain tissue. *Naunyn Schmiedebergs Arch Pharmacol.* 1986;332:179-183.

10. Snyder SH, Katims JJ, Annau Z, Bruns RF, Daly JW. Adenosine receptors and behavioral actions of methylxanthines. *Proc Natl Acad Sci U S A.* 1981;78:3260-3264.

11. Wu PH, Phillis JW, Nye MJ. Alkylxanthines as adenosine receptor antagonists and membrane phosphodiesterase inhibitors in central nervous tissue: evaluation of structure-activity relationships. *Life Sci.* 1982;31:2857-2867.

12. Bruns RF, Fergus JH, Badger EW, et al. Binding of the A1-selective adenosine antagonist 8-cyclopentyl-1,3-dipropylxanthine to rat brain membranes. *Naunyn Schmiedebergs Arch Pharmacol.* 1987;335:59-63.

13. Haleen SJ, Steffen RP, Hamilton HW. PD 116,948, a highly selective A1 adenosine receptor antagonist. *Life Sci.* 1987;40:555-561.

14. Meyer PT, Bier D, Holschbach MH, et al. In vivo imaging of rat brain A1 adenosine receptor occupancy by caffeine. *Eur J Nucl Med Mol Imaging.* 2003;30:1440.

15. Elmenhorst D, Meyer PT, Matusch A, Winz OH, Bauer A. Caffeine occupancy of human cerebral A1 adenosine receptors: in vivo quantification with 18F-CPFPX and PET. *J Nucl Med.* 2012;53:1723-1729.

16. Roman V, Keijser JN, Luiten PG, Meerlo P. Repetitive stimulation of adenosine A1 receptors in vivo: changes in receptor numbers, G-proteins and A1 receptor agonist-induced hypothermia. *Brain Res.* 2008;1191:69-74.

17. Schweinhardt P, Fransson P, Olson L, Spenger C, Andersson JL. A template for spatial normalisation of MR images of the rat brain. *J Neurosci Methods.* 2003;129:105-113.

18. Julien-Dolbec C, Tropres I, Montigon O, et al. Regional response of cerebral blood volume to graded hypoxic hypoxia in rat brain. *Br J Anaesth.* 2002;89:287-293.

19. Cunningham VJ, Rabiner EA, Slifstein M, Laruelle M, Gunn RN. Measuring drug occupancy in the absence of a reference region: the Lassen plot re-visited. *J Cereb Blood Flow Metab.* 2010;30:46-50.

20. Klotz KN, Lohse MJ, Schwabe U. Chemical modification of A1 adenosine receptors in rat brain membranes. Evidence for histidine in different domains of the ligand binding site. *J Biol Chem.* 1988; 263:17522-17526.

21. Townsend-Nicholson A, Schofield PR. A threonine residue in the seventh transmembrane domain of the human A1 adenosine receptor mediates specific agonist binding. *J Biol Chem.* 1994; 269:2373-2376.

22. Gracia E, Moreno E, Cortes A, et al. Homodimerization of adenosine A(1) receptors in brain cortex explains the biphasic effects of caffeine. *Neuropharmacology.* 2013;71:56-69.

23. Olah M, Stiles GL. Agonists and antagonists recognize different but overlapping populations of A1 adenosine receptors: modulation of receptor number by MgCl2, solubilization, and guanine nucleotides. *J Neurochem.* 1990;55:1432-1438.

24. Schiemann WP, Walther JM, Buxton IL. On the ability of endogenous adenosine to regulate purine nucleoside receptor binding of antagonists in smooth muscle membranes. *J Pharmacol Exp Ther.* 1990;255:886-892.

Chapter IV

Cerebral adenosine A_1 receptors are upregulated in rodent encephalitis

Soumen Paul[1], Shivashankar Khanapur[1], Wytske Boersma[4], Jurgen W Sijbesma[1], Kiichi Ishiwata[2], Philip H Elsinga[1], Peter Meerlo[3], Janine Doorduin[1], Rudi A Dierckx[1], Aren van Waarde[1]

[1] University of Groningen, University Medical Center Groningen, Nuclear Medicine and Molecular Imaging, Hanzeplein 1, 9713GZ Groningen, NETHERLANDS

[2] Tokyo Metropolitan Institute of Gerontology, Research Team for Neuroimaging, 35-2 Sakae-cho, Itabashi-ku, Tokyo, 173-0015, JAPAN

[3] University of Groningen, Center for Behaviour and Neurosciences, Nijenborgh 7, 9747AG Groningen, NETHERLANDS

[4] University of Groningen, University Medical Center Groningen, Department of Medical Oncology, Hanzeplein 1, 9713 GZ Groningen, NETHERLANDS

Accepted to NeuroImage

Abstract

Adenosine A_1 receptors (A_1Rs) are implied in the modulation of neuroinflammation.Activation of cerebral A_1Rs acts as a brake on the microglial response after traumatic brain injury and has neuroprotective properties in animal models of Parkinson's disease and multiple sclerosis. Neuroinflammatory processes in turn may affect the expression of A_1Rs, but the available data is limited and inconsistent. Here, we applied an animal model of encephalitis to assess how neuroinflammation affects the expression of A_1Rs. Two groups of animals were studied: Infected rats (n = 7) were intranasally inoculated with herpes simplex virus-1 (HSV-1, 1 x 10^7 plaque forming units), sham-infected rats (n = 6) received only phosphate-buffered saline. Six or seven days later, microPET scans (60 min with arterial blood sampling) were made using the tracer 8-dicyclopropyl-1-^{11}C-methyl -3-propyl -xanthine ([^{11}C]-MPDX). Tracer clearance from plasma and partition coefficient (K_1/k_2 estimated from a 2-tissue compartment model fit) were not significantly altered after virus infection. PET tracer distribution volume calculated from a Logan plot was significantly increased in the hippocampus (+37%) and medulla (+27%) of virus infected rats. Tracer binding potential estimated from the model fit was significantly increased in cerebellum (+87%) and medulla (+148%) which may indicate increased A_1R expression. This was confirmed by immunohistochemical analysis showing a strong increase of A_1R immunoreactivity in cerebellum of HSV-1-infected rats. Both the quantitative PET data and immunohistochemical analysis indicate that A_1Rs are upregulated in brain areas where active virus is present.

Key words: A_1R, HSV-1, Neuroinflammation, Rats, [^{11}C]-MPDX.

4.1 Introduction

Neuroinflammation is an important aspect of the pathophysiology of neurodegenerative diseases. The nucleoside adenosine may have neuroprotective properties by reducing neuronal excitability [26] and acting as an anti-inflammatory agent [10]. Such effects appear to be mediated by adenosine A_1 receptors (A_1Rs) in the central nervous system. A_1Rs are expressed both on neurons and on glia [16]. Activation of cerebral A_1Rs acts as a brake on the microglial response after traumatic brain injury [17] and has neuroprotective effects in animal models of Parkinson's disease [20] and multiple sclerosis (MS) [9.32]. Neuroinflammation after chronic infusion of lipopolysaccharide (LPS) into the fourth ventricle of young rats, and natural microglia activation in aged rats are both attenuated after treatment of animals with caffeine [6].

Upregulation of A_1Rs in the human brain may also have neuroprotective properties and suppress neuroinflammation. A recent paper reported that a higher cerebrospinal fluid caffeine concentration is associated with a more favorable outcome after severe traumatic brain injury [28]. Moreover, regular caffeine consumption is associated with lower risk for

developing Parkinson's disease [25] or Alzheimer dementia [8]. Changes of A_1R signaling have been reported in patients with MS. Plasma levels of adenosine in such patients are significantly reduced. Stimulation of peripheral blood mononuclear cells (PBMC) with a selective A_1R agonist R-PIA inhibits the mitogen-stimulated production of the inflammatory marker TNF-alpha in healthy volunteers but not in subjects with MS [22].

Taken together, the above-mentioned results indicate that A_1R upregulation and stimulation may affect neurodegenerative and neuroinflammatory processes. In addition, some studies have suggested that neuroinflammation itself may also affect the expression of A_1Rs. For example, A_1R densities in PBMC and in brain tissue from MS-patients are significantly decreased (by 53% and 49%, respectively) compared to age-matched controls [19]. In agreement with this is the finding of reduced densities of A_1Rs in microglia of wild-type mice during experimental autoimmune encephalomyelitis [32]. However, acute inflammation of mouse brain after administration of LPS was shown to increase A_1R expression in cortical areas and this response was dependent on the transcription factor NF-kappaB [18]. If combined, these data suggest that A_1Rs are up-regulated in acute forms of neuroinflammation but down-regulated in chronic forms. Clearly, more data is required.

Here, we performed a microPET study with the potent (K_i 3.0 nM) antagonist 8-dicyclopropyl-1-^{11}C-methyl-3-propylxanthine (^{11}C-MPDX) in a rodent model of encephalitis (nasal infection of Wistar rats with HSV-1). ^{11}C-MPDX has been used previously for PET studies of A_1Rs, both in animals [24, 29, Chapters **2 and 3**] and humans [13-15]. The present study aimed to assess whether binding of ^{11}C-MPDX and immunoreactivity of the A_1R protein are altered in rat brain as a consequence of neuroinflammation.

4.2 Materials and methods

4.2.1 Animals and housing

The animal experiments were performed by licensed investigators in compliance with the Law on Animal Experiments of The Netherlands. The protocol was approved by the Committee on Animal Ethics of the University of Groningen. Male outbred Wistar-Unilever rats were obtained from Charles-River. The rats were housed in Macrolon cages (38 × 26 × 24 cm) maintained at a 12-h light/12-h dark regime and were fed standard laboratory chow ad libitum. Two groups of animals were studied: rats infected with HSV-1 (n = 7) and sham-infected rats (n = 6).

4.2.2 HSV-1 inoculation

The HSV-1 strain was obtained from a human clinical isolate cultured in Vero-cells and assayed for plaque forming units (PFU) per mL. In order to infect rats with HSV-1, the

animals were anesthetized with 5% isoflurane. Subsequently, $1x10^7$ PFU HSV-1 in 100 uL phosphate-buffered saline (PBS) was applied in the nose using a micropipette (50 uL in each nostril). Sham-infected rats received 100 uL PBS without any virus. Clinical symptoms in all rats were observed daily and were recorded by scoring them in an animal welfare diary.

Scores ranged from 0 to 3, with 0 indicating no particular response or symptoms; 1 meaning ruffled fur, dried oral and nasal secretions on the fur, loss of weight; 2 indicating animals showed a hunched posture, increased aggression and paralysis symptoms in the posterior part of the abdomen; and score 3 indicating seizures, severe paralysis, difficulty of breathing, or death. In our study, score 3 was not reached as the ethics committee did not allow a longer interval than 8 days between virus inoculation and PET imaging. On day 6 or 7, the rats were transported to the imaging facility for microPET scanning.

4.2.3 PET scanning

The radioligand [^{11}C]-MPDX was prepared by reaction of ^{11}C-methyl iodide with the appropriate 1-*N*-desmethyl precursor. Briefly, ^{11}C-methyl iodide was trapped in 0.3 mL of *N*, *N*-dimethylformamide containing 1 mg of 1-*N*-desmethyl precursor and 5 uL of NaOH and was heated at 120°C for 5 min. After 1.0 mL of 0.1 M HCl had been added, the solution was loaded onto a high-performance liquid chromatography column (Econosphere, C18, 5 mm [Altech]; 10 x 250 mm) and eluted with a mixture of 0.1 M NaH_2PO4 and ethanol (70/30) at a flow rate of 4 mL/min. The fractions containing [^{11}C]-MPDX were collected. Retention time of [^{11}C]-MPDX was 14 min. The decay-corrected radiochemical yield was 35% ± 5% (based on ^{11}Cmethyl iodide), and the radiochemical purity was greater than 98%. MicroPET (Focus 220 camera, Siemens-Concorde) scans were made on day 6 or 7 after the inoculation with HSV-1. Two rats were scanned simultaneously in each data acquisition protocol. Approximately 30-40 min before tracer injection, animals were anesthetized with a mixture of isoflurane/air (inhalation anesthesia, 5% ratio during induction, later reduced to 2%). During this time, surgery was performed to place a cannula in a femoral artery for blood sampling. Also, a transmission scan was made for attenuation correction (515 s, with Co-57 point source). After completion of the transmission scan, the PET tracer [^{11}C]-MPDX was injected through the penile vein. A dynamic emission scan (76 min) was started during injection of radioactivity in the lower rat; the upper animal was injected 16 min later. A series of blood samples (14 samples; volume, 0.10–0.15 mL) was drawn, initially in rapid succession (every 15 s) and later at longer intervals (up to 30 min). Plasma was acquired from these samples by short centrifugation (Eppendorf centrifuge, 5 min at 13,000 rpm).Radioactivity in 25 uL of plasma was counted and used as an arterial input function. Listmode data were reframed into a dynamic sequence of 8 x 30, 3 x 60, 2 x120, 2 x 180, 3 x 300, 1 x 480, 2 x 600, and 1 x 960 s frames. The data were reconstructed per time frame using an iterative reconstruction algorithm (attenuation-weighted 2-dimensional ordered-subset expectation maximization, provided by Siemens; 4 iterations, 16 subsets; zoom factor 2). The final datasets consisted of 95 slices, with a slice thickness of 0.8 mm and an in-plane image

matrix of 128 * 128 pixels of size 1 * 1 mm. Datasets were fully corrected for random coincidences, scatter, and attenuation. Images were smoothed with a Gaussian filter (1.35 mm in both directions).

4.2.4 PET image data analysis

Time–activity curves, volumes (mL) for the ROIs, partition co-efficient (K_1/k_2) and binding potential (BP_{ND}) by two-tissue reversible compartment model (2TCM) were calculated using the Siemens Inveon Research work place 4.0 (IRW 4.0). ROIs were drawn around the bulbus olfactorius, frontal cortex, striatum, amygdala, parietal/temporal/occipital cortex, medulla, cerebellum, pons and hippocampus in a template MRI scan that was co-registered with the PET scan of interest by image fusion. The cerebral distribution volume (V_T) of the tracer was estimated from a Logan plot [21].

4.2.5 Biodistribution studies

After the PET scan and 80 min after tracer injection, the anesthetized animals were sacrificed. Blood was collected, and plasma was obtained from the blood sample by short centrifugation (5 min at 1,000 x *g*). Several areas of the brain were dissected and peripheral organs were excised (see **Table 2**). The brain areas and peripheral organs were weighed and the radioactivity in these tissue samples was measured with a gamma counter, applying a decay correction. Tracer uptake was expressed as a dimensionless biodistribution SUV [tissue activity concentration (MBq/g)]/ [(injected dose (MBq)/body weight (g)].

4.2.6 A_1R immunohistochemistry

In a parallel experiment, male Wistar-Unilever rats were sham-infected or infected with HSV-1 as described above. On day 6 or 7, animals were terminated by deep anesthesia with a mixture of isoflurane/air (ratio 5%) and perfused intracardially with 150 ml of 0.9% saline followed by 250-300 mL of freshly prepared 4% paraformaldehyde in 0.1 M phosphate buffer (PBS), pH 7.4. The brain was removed and post-fixed in paraformaldehyde for 24 h.The next day, the organ was embedded in paraffin. Coronal brain sections of 4 um were cut, using a microtome. Sections were collected on slides, dried in a hot air oven at 55°C overnight and then the tissue sections were ready for staining.

In order to remove paraffin, the tissue sections were washed in xylene, 100, 96 and 70% of ethanol and demi-water. For the antigen retrieval step, sodium citrate buffer (10mM sodium citrate) was added and the sections on the slides were boiled for 15-20 min in a microwave oven, followed by cooling down for 20-25 min and washing with PBS. The blocking step was carried out by adding 0.3% H_2O_2 in PBS to the slides, keeping them in this solution for 30 min followed by extensive washing with PBS and treatment with avidine and

biotine complex reagents for 30 min (Vectastain Elite ABC kit, Vector Laboratories), followed by 10% goat serum. The sections were incubated with primary antibody (Abcam rabbit polyclonal anti-A_1 adenosine receptor diluted 1:100 in 1% bovine albumin solution in PBS) for 24 h at 4°C.Sections were then washed thoroughly with PBS and incubated in secondary antibody (Swine anti rabbit biotylated diluted in 1:300 in 1 % bovine albumin solution with PBS) for 30 min. After major rinsing of the sections in PBS, the tertiary antibody (streptavidine HRP diluted in 1:300 in 1 % bovine albumin solution with PBS) was added to the sections and incubation was continued for 30 min. As a negative control, sections were only incubated with secondary and tertiary (not the primary) antibody. The staining was visualized with 3,3'-diaminobenzidine (DAB) which was applied for 10 min. The sections were counterstained with haematoxylin for 1 min, and the stained sections were dehydrated with a graded series of ethanol and tap water (70, 96 and 99% ethanol). The final dehydration step was followed by drying, and mounting with Eulcitt (hardening medium) below a coverslip. Stained slides were examined using a microscope (Zeiss Axioskop 2, Carl Zeiss, Germany).

4.2.7 Statistical tests

Differences between groups were analyzed using 1-way ANOVA. A probability smaller than 0.05 was considered statistically significant.

4.3 Results

4.3.1 Animal model

Disease symptoms were only observed after a delay of several days following HSV-1 infection. Initial symptoms occurred usually at day 5 (irritated nose and eyes). More severe symptoms were seen on the scanning day (day 6 or 7); these included piloerection, a hunched posture and a sluggish response to stimuli. On the day of the PET scan, HSV-1-infected rats showed a significantly reduced body weight compared to sham-infected controls (267 ± 32 vs 314 ± 30 g, $p<0.02$), reflecting a reduction of food intake. None of the animals reached the stage of advanced disease, since severe symptoms (seizures, complete paralysis, impaired breathing, and premature death) did never occur. Five animals reached score 1 and only two animals reached score 2. Thus, all animals were scanned in a relatively early phase of encephalitis. All infected animals became sick but sham-infection did not result in any symptoms.

4.3.2 Small-Animal PET

[^{11}C]-MPDX images of a HSV-1- and sham-infected animal are presented in **Fig. 1.** In both groups of animals the brain was clearly visualized. Tracer uptake was particularly high in hippocampus, cerebellum, striatum and some areas of the cortex, as observed previously in healthy rats (**Chapter 2**).

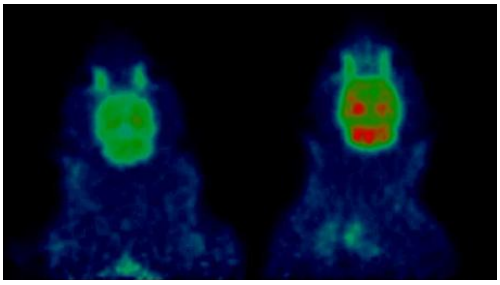

Figure 1. Small-animal PET images of rat brain acquired after injection of [^{11}C]-MPDX Sham-infected animal (left), HSV-infected animal (right).

4.3.3 Time - activity curves in brain

Time-activity curves for hippocampus, cerebellum and medulla are presented in **Fig. 2.** These brain areas are known to have a rather high A_1R expression (hippocampus, cerebellum) (**Chapter 2)** and/or to be vulnerable to the viral infection [1,3,12,23]. Both in sham-infected and virus-infected animals, tissue uptake of radioactivity rapidly increased to a maximum which was followed by washout. However, uptake in the virus-infected animals was significantly greater than in sham-infected rats at intervals between 3 and 50 min. At intervals greater than 50 min, the difference in tracer uptake between healthy and diseased animals had virtually disappeared.

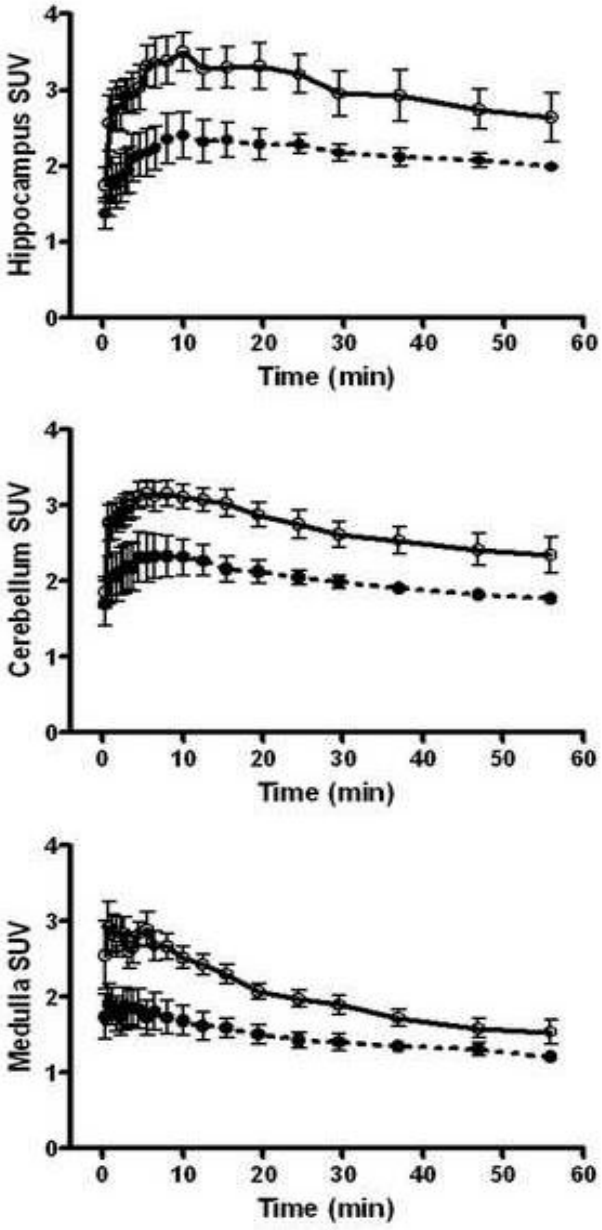

Figure 2: Time-activity curves of [^{11}C]-MPDX in three regions of rat brain. Standardized uptake values (PET-SUVs) are plotted as mean ± SEM. Solid symbols indicate data from sham infected animals, open symbols data from HSV-1 -infected rats.

4.3.4 Time - activity curves in plasma

A biexponential clearance of radioactivity from blood plasma was observed after injection of [^{11}C]-MPDX in both groups (**Fig. 3**). Infection of animals with HSV-1 did not significantly affect tracer clearance. Expressed as percentages of control, areas under the curve were 100 ± 4.2% for sham-infected animals and 97.8 ± 2.6% for virus-infected rats (mean ± SEM).

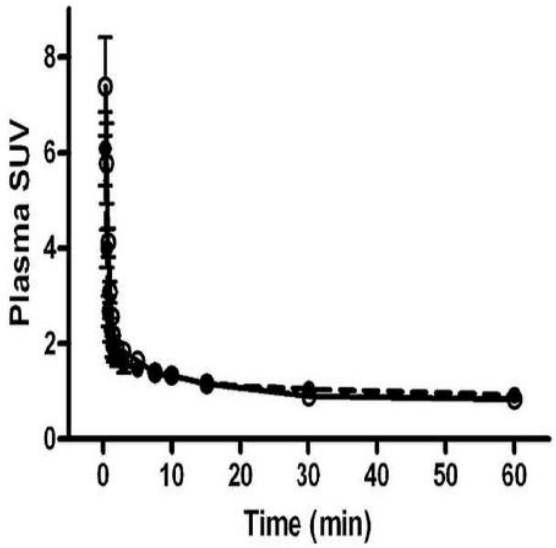

Figure 3: Time-activity curves of [^{11}C] MPDX in rat plasma. Standardized uptake values (SUVs) are plotted as mean ± SEM. Solid symbols indicate data from HSV-1 infected animals, open symbols data from sham-infected rats.

4.3.5 Graphical analysis of PET data

Logan plots of the uptake of [^{11}C]-MPDX in individual brain regions were similar to those presented previously for [^{11}C]-MPDX uptake in the entire brain (**Chapter 2**). Logan V_T of the tracer in the hippocampus and medulla of virus-infected rats was significantly increased (+37 and +40%, respectively) compared to the sham-infected controls (Table 1). In cerebellum, a trend towards increased V_T was also noted but this trend did not reach statistical significance.

Table 1. Logan graphical analysis and 2 Tissue Compartment Model Fit of PET Data

Parameter	V_T (Logan)	K_1/k_2 (2TCM)	BP_{ND} (k_3/k_4, 2TCM)
Sham animals (n=6)			
Hippocampus	1.99 ± 0.54	0.41 ± 0.07	4.21 ± 0.66
Cerebellum	1.80 ± 0.48	0.48 ± 0.08	3.09 ± 0.71
Medulla	1.31 ± 0.34	0.59 ± 0.20	1.61 ± 0.67
Infected rats (n=7)			
Hippocampus	2.72 ± 0.55*	0.39 ± 0.24 (NS)	7.46 ± 4.13 (NS)
Cerebellum	2.44 ± 0.58 (NS)	0.38 ± 0.15 (NS)	5.79 ± 2.70*
Medulla	1.84 ± 0.41*	0.41 ± 0.17 (NS)	4.00 ± 1.68*

Data are listed as mean ± SD. NS = difference between groups not-significant.

4.3.6 Compartment modeling

A two-tissue compartment model with reversible tracer binding (2TCM) fitted well to time – activity curves from different ROIs in the brain, using radioactivity counts from arterial blood samples as an input function. Similar fits (for healthy rats) have been presented previously (**Chapter 2**). The partition coefficient of [^{11}C]-MPDX (ratio K_1/k_2 from the model fit) was not significantly affected by viral infection. However, BP_{ND} was significantly increased in cerebellum (+87%) and medulla (+148%) of virus-infected rats. BP_{ND} in hippocampus tended to be increased as well but this trend did not reach statistical significance due to a large variability in the infected group (**Table 1**). Animals with disease score 1 showed higher values for BP_{ND} than animals with disease score 2 (**Fig.4**).

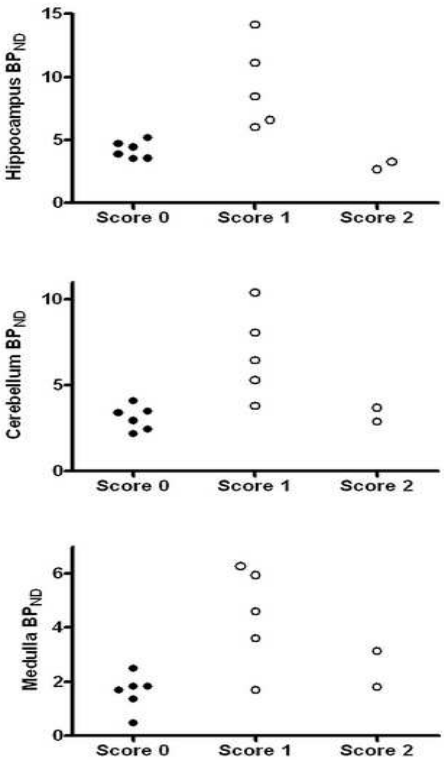

Figure 4. Calculated binding potential (BP_{ND}) values of [^{11}C]-MPDX in cerebellum, medulla and hippocampus of HSV-1- and sham-infected rats. Animals with a low disease score (score 1) have higher BP_{ND} than animals which are really sick (score 2).

4.3.7 Biodistribution data

Biodistribution data acquired 80 min after injection of [^{11}C]-MPDX is presented in **Table 2.** In pons and brainstem of HSV-1-infected animals, significantly higher SUVs of [^{11}C]-MPDX was found compared to sham-infected rats. In peripheral organs, no significant changes in tracer uptake after viral infection were noted, with exception of a decreased uptake in duodenum.

Table 2. Animal weight, injected dose and bistribution data of [^{11}C]-MPDX

	Sham-infected	HSV-1-infected
Number of animals	6	7
Body weight (g)	314 ± 30	267 ± 32*
Tracer dose (MBq)	15.1 ± 4.6	11.3 ± 7.9
Amygdala	1.31 ± 0.41	1.31 ± 0.22
Bulbus olfactorius	0.66 ± 0.13	0.69 ± 0.14
Cerebellum	2.21 ± 0.28	2.24 ± 0.37
Cingulate cortex	1.18 ± 0.29	1.27 ± 0.33
Entorhinal cortex	1.31 ± 0.14	1.45 ± 0.31
Frontal cortex	1.34 ± 0.30	1.42 ± 0.46
Hippocampus	1.69 ± 0.40	1.83 ± 0.44
Medulla	1.10 ± 0.19	1.16 ± 0.43
Parietal etc cortex	1.55 ± 0.18	1.49 ± 0.20
Pons/brainstem	1.18 ± 0.28	1.55 ± 0.25*
Striatum	1.51 ± 0.30	1.39 ± 0.27
Rest of brain	1.56 ± 0.19	1.76 ± 0.36
Bone	0.30 ± 0.09	0.41 ± 0.11
Colon	0.99 ± 0.14	0.92 ± 0.09
Duodenum	1.73 ± 0.42	1.23 ± 0.42*
Fat	2.07 ± 1.14	3.55 ± 2.26
Heart	0.94 ± 0.13	0.91 ± 0.15
Ileum	1.28 ± 0.28	1.46 ± 0.44
Kidney	1.41 ± 0.19	1.53 ± 0.41
Liver	3.13 ± 0.35	3.59 ± 1.02
Lung	0.91 ± 0.17	0.96 ± 0.27
Muscle	0.53 ± 0.10	0.53 ± 0.19
Pancreas	1.22 ± 0.20	1.89 ± 1.12
Plasma	0.91 ± 0.07	0.97 ± 0.19
Red blood cells	0.43 ± 0.09	0.51 ± 0.22
Spleen	1.41 ± 0.20	1.38 ± 0.26
Trachea	0.65 ± 0.14	0.73 ± 0.23
Urine	1.47 ± 1.50	0.63 ± 0.83

Mean tissue radioactivity 80 min after tracer injection listed as SUV ± SD. Significant differences with sham group indicated by asterisks.

4.3.8 Immunohistochemistry

In the cerebellum of HSV-1-infected rats, we observed specific and strong A_1R immunohistochemistry staining at different sites. Cerebellum from sham infected animals showed light A_1R staining compared to cerebellum from HSV-1 infected animals (**Fig. 5**). IHC slides of HSV-1-infected rats showed intense staining in the dendritic tree and cell bodies of Purkinje cells. Cerebellar granule cells also exhibited strong staining. Astrocytes in the white matter showed weaker staining than Purkinje or granule cells although their staining was also increased compared to that observed in sham-infected rats.

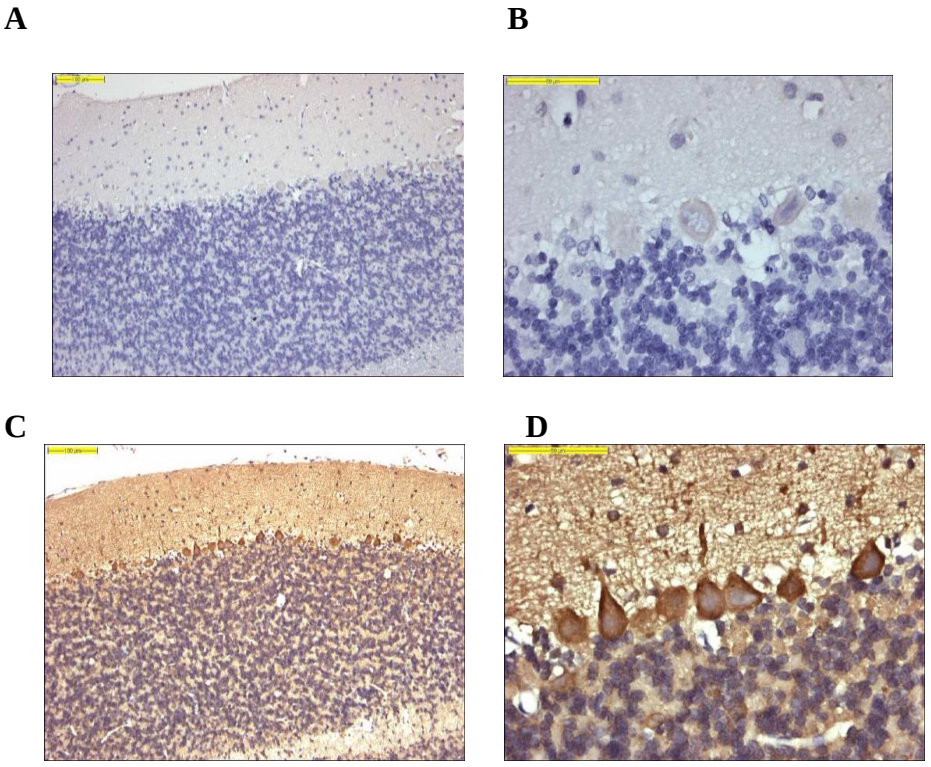

Figure 5. Immunohistochemistry images of the cerebellum of sham-infected (panels A, B) and HSV-1-infected (panels C, D) rats. Panels A and C present an overview whereas panels B and D show details.

4.5 Discussion

4.5.1 MicroPET data

Time-activity curves showed a significant increase of radioactivity uptake (PET-SUV) in several brain regions (hippocampus, cerebellum and medulla) of HSV-infected rats as compared to sham-infected controls (**Fig. 1**). Different mechanisms could be underlying this increased uptake, viz. changes of cerebral blood flow, greater blood-brain barrier permeability, upregulation of A_1Rs or increased affinity of A_1Rs for the radioligand. In order to clarify the mechanisms underlying increased tracer uptake, the PET data were analyzed by pharmacokinetic modeling. Partition coefficient of the tracer (K_1/k_2 from a 2TCM fit) was not significantly altered, but tracer distribution volume (V_T estimated by

graphical Logan analysis) tended to be increased in several brain areas, statistical significance being reached in hippocampus and medulla (**Table 1**). Striking increases of tracer binding potential (BP_{ND}, k_3/k_4 from a 2TCM fit) were observed in cerebellum and medulla (**Table 1**). These modeling data suggest that the observed increases of tracer uptake are related to increases of the expression and/or the affinity of A_1Rs for the radioligand rather than changes of flow or blood-brain barrier permeability. Clearance curves of [^{11}C]-MPDX in plasma (Fig. 2) indicated that tracer delivery to the brain was not significantly different in HSV-1- and sham-infected rats.

The HSV-1 encephalitis model which we employed has been examined previously with PET imaging. ^{18}F-FHPG scans of the whole brain have indicated that replicating virus is present 7 days after infection [7]. ^{18}F-FEAnGA scans detected increased expression of ß-glucuronidase in frontopolar and frontal cortex, bulbus olfactorius, cerebral cortex, cerebellum and brainstem [2]. Scans with translocator protein (TSPO) ligands indicated the presence of activated microglia in brainstem and cerebellum [11].

Immunohistochemical techniques have also been used to characterize the HSV-1 encephalitis model. The virus is known to move from the nasal mucosa to the brainstem via the trigeminal nerve and from the brainstem to the spinal cord via fiber connections. Six to seven days after the infection, viral antigen is detected in several brain areas (brain stem, amygdala, hippocampus, cerebellum, piriform and entorhinal cortex) and spinal cord but not in peripheral organs (lung, liver, spleen, kidney, adrenals). The virus is present both in neurons and glia [1, 3, 12, and 23]. The temporal and spatial pattern of inducible NO synthase expression, a marker of the neuroinflammatory response, coincide with those of viral propagation [12]. Loss of granule cells from the dentate gyrus in the hippocampus is noted in HSV-1 infected rats and may be responsible for memory deficits in humans following encephalitis [1].

Increases of tracer BP_{ND} in cerebellum and medulla which we noted in the present study may thus reflect upregulation of A_1Rs in brain areas where active virus is present

4.5.2 Biodistribution data

The biodistribution study revealed a significant increase of tracer uptake only in pons and brainstem of the virus infected animals (31%, **Table 2).** No differences in other brain areas were noted, probably due to the fact that the biodistribution study was performed after the PET scan. A long interval had elapsed between tracer injection and tissue excision (80 min); thus, the differences between the two groups had virtually disappeared (see **Fig. 1**). Moreover, variability in the biodistribution data was rather large since this interval corresponds to 4 half-lives of ^{11}C. Increased tracer uptake in pons and brainstem may be related to viral invasion in trigeminal ganglia and principal sensory nucleus located in the brain stem [30].

4.5.3 Immunohistochemistry data

Immunohistochemical analysis showed weak to normal staining of A_1R in the cerebellum of sham-infected rats but intense staining in HSV-1-infected animals (Fig. 3). These data suggest that A_1R are upregulated after viral infection. This upregulation may be neuroprotective and it seems to occur predominantly in neurons, particularly Purkinje cells. Increased expression and stimulation of A_1R reduces neuronal excitability and may thus protect neurons from excessive stimulation. Neuroinflammation can be accompanied by release of the excitatory neurotransmitter glutamate [4,31] that may eventually cause neuronal death. On the other hand, increased expression and stimulation of A_1R in cerebellar granule cells inhibits the release of glutamate and may thus contribute to neuroprotection [5,27]. Finally, activation of A_1R on astrocytes and microglia may act as a brake on the inflammatory response [17]. Because of the combined action of these three mechanisms, activation of cerebral A_1R is neuroprotective in animal models of Parkinson's disease [20], traumatic brain injury [17] and multiple sclerosis (MS) [9,32].

4.6 Conclusion

The present study demonstrated an upregulation of adenosine A_1 receptor (A_1R) in HSV-1 induced rodent encephalitis that could be quantified with the A_1R antagonist [^{11}C]-MPDX and PET imaging. Data from our animals support the idea that upregulation of A_1R occurs during the early (acute) phase of encephalitis and has a beneficial effect. The five animals with relatively low disease score (score 1) showed the highest values for tracer BP_{ND} in cerebellum, medulla and hippocampus, whereas the two rats with a higher disease score (score 2) showed a less striking increase of BP_{ND} **(Fig.4).** Thus, A_1R upregulation and encephalitis symptoms may be inversely correlated. Additional studies are necessary to further characterize the role of A_1R signaling in rodent neuroinflammation.

4.7 Acknowledgements

We would like to thank Dr.Wilfred F.A. den Dunnen for helping in the immunohistochemical analysis and M.A.Khayum for assistance during the scan. This research was supported by grants from the Jan Kornelis De Cock- Stichting.

5. References

1) Ando Y, Kitayama H, Kawaguchi Y,Koyanagi Y (2008) Primary target cells of herpes simplex virus type 1 in the hippocampus. Microbes Infect 10:1514-1523.

2) Antunes IF, Doorduin J, Haisma HJ, Elsinga PH, van Waarde A, Willemsen AT, Dierckx RA,de Vries EF (2012) ^{18}F-FEAnGA for PET of beta-glucuronidase activity in neuroinflammation. J Nucl Med 53:451-458.

3) Beers DR, Henkel JS, Schaefer DC, Rose JW,Stroop WG (1993) Neuropathology of herpes simplex virus encephalitis in a rat seizure model. J Neuropathol Exp Neurol 52:241-252.

4) Bezzi P, Domercq M, Brambilla L, Galli R, Schols D, De Clercq E, Vescovi A, Bagetta G, Kollias G, Meldolesi J,Volterra A (2001) CXCR4-activated astrocyte glutamate release via TNFalpha: amplification by microglia triggers neurotoxicity. Nat Neurosci 4:702-710.

5) Boeck CR, Kroth EH, Bronzatto MJ,Vendite D (2005) Adenosine receptors co-operate with NMDA preconditioning to protect cerebellar granule cells against glutamate neurotoxicity. Neuropharmacology 49:17-24.

6) Brothers HM, Marchalant Y,Wenk GL (2010) Caffeine attenuates lipopoly-saccharide-induced neuroinflammation. Neurosci Lett 480:97-100.

7) Buursma AR, de Vries EF, Garssen J, Kegler D, van Waarde A, Schirm J, Hospers GA, Mulder NH, Vaalburg W,Klein HC (2005) [^{18}F]FHPG positron emission tomography for detection of herpes simplex virus (HSV) in experimental HSV encephalitis. J Virol 79:7721-7727.

8) Cao C, Loewenstein DA, Lin X, Zhang C, Wang L, Duara R, Wu Y, Giannini A, Bai G, Cai J, Greig M, Schofield E, Ashok R, Small B, Potter H, Arendash GW (2012) High blood caffeine levels in MCI linked to lack of progression to dementia. J Alzheimers Dis. 30:559-572.

9) Chen GQ, Chen YY, Wang XS, Wu SZ, Yang HM, Xu HQ, He JC, Wang XT, Chen JF,Zheng RY (2010) Chronic caffeine treatment attenuates experimental autoimmune encephalomyelitis induced by guinea pig spinal cord homogenates in Wistar rats. Brain Res 1309:116-125

10) Cronstein BN (1994) Adenosine, an endogenous anti-inflammatory agent. J Appl Physiol 76:5-13.

11) Doorduin J, Klein HC, Dierckx RA, James M, Kassiou M,de Vries EF (2009) [^{11}C]-DPA-713 and [^{18}F]-DPA-714 as new PET tracers for TSPO: a comparison with [^{11}C]-(R)-PK11195 in a rat model of herpes encephalitis. Mol Imaging Biol 11:386-398.

12) Fujii S, Akaike T,Maeda H (1999) Role of nitric oxide in pathogenesis of herpes simplex virus encephalitis in rats. Virology 256:203-212.

13) Fukumitsu N, Ishii K, Kimura Y, Oda K, Hashimoto M, Suzuki M,Ishiwata K (2008) Adenosine A(1) receptors using 8-dicyclopropylmethyl-1-[^{11}C] methyl-3-propylxanthine PET in Alzheimer's disease. Ann Nucl Med 22:841-847.

14) Fukumitsu N, Ishii K, Kimura Y, Oda K, Sasaki T, Mori Y,Ishiwata K (2005)Adenosine A1 receptor mapping of the human brain by PET with 8-dicyclopropylmethyl-1-^{11}C-methyl-3-propylxanthine. J Nucl Med 46:32-37.

15) Fukumitsu N, Ishii K, Kimura Y, Oda K, Sasaki T, Mori Y,Ishiwata K (2003) Imaging of adenosine A1 receptors in the human brain by positron emission tomography with [^{11}C]MPDX. Ann Nucl Med 17:511-515.

16) Gebicke-Haerter PJ, Christoffel F, Timmer J, Northoff H, Berger M,Van Calker D (1996) Both adenosine A1- and A2-receptors are required to stimulate microglial proliferation.Neurochem Int 29:37-42.

17) Haselkorn ML, Shellington DK, Jackson EK, Vagni VA, Janesko-Feldman K, Dubey RK, Gillespie DG, Cheng D, Bell MJ, Jenkins LW, Homanics GE, Schnermann J, Kochanek PM (2010) Adenosine A1 receptor activation as a brake on the microglial response after experimental traumatic brain injury in mice. J Neurotrauma 27:901-910.

18) Jhaveri KA, Reichensperger J, Toth LA, Sekino Y,Ramkumar V (2007) Reduced basal and lipopolysaccharide-stimulated adenosine A1 receptor expression in the brain of nuclear factor-kappaB p50-/- mice. Neuroscience 146:415-426.

19) Johnston JB, Silva C, Gonzalez G, Holden J, Warren KG, Metz LM,Power C (2001) Diminished adenosine A1 receptor expression on macrophages in brain and blood of patients with multiple sclerosis. Ann Neurol 49:650-658.

20) Liu HQ, Zhang WY, Luo XT, Ye Y,Zhu XZ (2006) Paeoniflorin attenuates Neuroinflammation and dopaminergic neurodegeneration in the MPTP model of Parkinson's disease by activation of adenosine A1 receptor. Br J Pharmacol 148:314-325.

21) Logan J (2000) Graphical analysis of PET data applied to reversible and irreversible tracers.Nucl Med Biol 27:661-670.

22) Mayne M, Shepel PN, Jiang Y, Geiger JD,Power C (1999) Dysregulation of adenosine A1 receptor-mediated cytokine expression in peripheral blood mononuclear cells from multiple sclerosis patients. Ann Neurol 45:633-639.

23) Merkel KH,Maibach EA (1984) Experimental herpes simplex encephalitis in rats after intranasal inoculation. An immunohistologic study. Histochem J 16:467-469.

24) Nariai T, Shimada Y, Ishiwata K, Nagaoka T, Shimada J, Kuroiwa T, Ono K, Ohno K, Hirakawa K,Senda M (2003) PET imaging of adenosine A1 receptors with $^{[11C]\text{-MPDX}}$ as an indicator of severe cerebral ischemic insult. J Nucl Med 44:1839-1844.

25) Palacios N, Gao X, McCullough ML, Schwarzschild MA, Shah R, Gapstur S, Ascherio A (2012) Caffeine and risk of Parkinson's disease in a large cohort of men and women. Mov Disord. 27:1276-1282.

26) Paul S, Elsinga PH, Ishiwata K, Dierckx RA, van Waarde A (2011a) Adenosine A1 receptors in the central nervous system: Their functions in health and disease, and possible elucidation by PET imaging. Curr Med Chem 18:4820-4835.

27) Poli A, Lucchi R, Vibio M,Barnabei O (1991) Adenosine and glutamate modulate each other's release from rat hippocampal synaptosomes. J Neurochem 57:298-306.

28) Sachse KT, Jackson EK, Wisniewski SR, Gillespie DG, Puccio AM, Clark RS, Dixon CE,Kochanek PM (2008) Increases in cerebrospinal fluid caffeine concentration are associated with favorable outcome after severe traumatic brain injury in humans. J Cereb Blood Flow Metab 28:395-401.

29) Shimada Y, Ishiwata K, Kiyosawa M, Nariai T, Oda K, Toyama H, Suzuki F, Ono K,Senda M (2002) Mapping adenosine A1 receptors in the cat brain by positron emission tomography with [11C]MPDX. Nucl Med Biol 29:29-37.

30) Stroop WG, Rock DL,Fraser NW (1984) Localization of herpes simplex virus in the trigeminal and olfactory systems of the mouse central nervous system during acute and latent infections by in situ hybridization. Lab Invest 51:27-38.

31) Takaki J, Fujimori K, Miura M, Suzuki T, Sekino Y,Sato K (2012) L-glutamate released from activated microglia downregulates astrocytic L-glutamate transporter expression in neuroinflammation: the 'collusion' hypothesis for increased extracellular L-glutamate concentration in neuroinflammation. J Neuroinflammation 9:275-2094-9-275.

32) Tsutsui S, Schnermann J, Noorbakhsh F, Henry S, Yong VW, Winston BW, Warren K,Power C (2004) A1 adenosine receptor upregulation and activation attenuatesneuroinflammation and demyelination in a model of multiple sclerosis. J Neurosci 24:1521-1529.

Chapter V

Micro PET to study adenosine A_1 and A_{2A} receptor agonist induced changes of blood brain barrier permeability

Soumen Paul[1], Shivashankar Khanapur[1], Jurgen W Sijbesma[1], Siddesh Hartimath[1],Vladimir Shalgunov[1],Philip H Elsinga[1], Rudi A Dierckx[1], Aren van Waarde[1]

[1] *University of Groningen, University Medical Center Groningen, Nuclear Medicine and Molecular Imaging, Groningen, Netherlands*

Abstract

Adenosine and adenosine analogs modulate BBB permeability in mice and rats through stimulation of A_1 and A_{2A} receptors. We performed a PET study to determine whether changes of BBB permeability after administration of A_1 or A_{2A}R agonists can be assessed by examining changes of the in vivo kinetics of hydrophilic radioligands. **Methods:** MicroPET scans combined with arterial blood sampling were made in three groups of isoflurane-anesthetized Wistar rats: (1) controls; (2) pretreated with A1R agonist CPA, dose 0.26mg/kg; (3) pretreated with A2A agonist Lexiscan, dose 0.05mg/kg. We used two hydrophilic radioligands i) the CXCR4 antagonist [^{11}C]CH_3-AMD3465 (clogP=-0.89) and ii) the dopamine agonist [^{18}F]-AMC 15(clogP=1.54). **Results:** Administration of CPA (0.26 mg/kg) resulted in a strong (> 50%) and administration of Lexiscan in a moderate (< 10 %) reduction of heart rate. We failed to observe BBB opening, as judged by tracer distribution volumes (V_T) calculated from a Logan plot. Pretreatment of animals with CPA did not increase V_T of [^{11}C]CH_3-AMD3465 (0.085 ± 0.052 vs. 0.135 ± 0.052 in controls). Also, no increment in V_T of [^{18}F]-AMC15 was noted after pretreatment of animals with CPA or Lexiscan (0.034 or 0.017 vs 0.035 in controls). Striatal binding of [^{18}F]-AMC15 was never observed. **Conclusion**: BBB opening could not be demonstrated by PET. Both radioligands failed to enter the rodent brain after pretreatment with an A_1 or A_{2A} agonist.

Keywords: A_1R, BBB, agonist, MicroPET, [^{11}C]CH_3-AMD3465, [^{18}F]-AMC 15

5.1 Introduction

The blood-brain barrier (BBB) is composed of endothelial cells [2] which line the microvasculature of the brain and are connected by tight junctions. These cells are functionally placed between brain and periphery. The BBB is divided into three sections: 1) the actual BBB, 2) blood-cerebrospinal fluid barrier, and 3) arachnoid barrier [1]. All three sections are involved in protection of the central nervous system by limiting the entry of toxic substances into the brain. Lipophilic molecules may pass the barrier in different ways. Small molecules can enter via i) ion channels ii) dissolving in the hydrophobic cell membrane followed by barrier passage by passive diffusion, and iii) facilitated transport. Such transporters may be either carrier-mediated or receptor-mediated [3]. Other transporters, like P-glycoprotein (P-gp), multidrug resistance-associated protein (MRP) and breast cancer resistance protein (BCRP), are actually limiting substance entry into the brain by actively pumping molecules back to the blood after they have entered the brain by passive diffusion. The efficiency of the BBB is proven by the fact that more than 98% of all molecules with molecular weight greater than 500 Da do not enter the brain. With increasing prevalence of brain disorders there is an increasing demand for CNS drugs, but

many potential candidates fail to cross the barrier Thus, there is a need to modulate BBB permeability and facilitate the entry of therapeutic drugs into the CNS.
Adenosine receptors are G-protein coupled and play several roles in mammalian physiology, including modulation of immune responses. Adenosine receptors can be divided in the A_1R, $A_{2A}R$, $A_{2b}R$ and A_3R subtypes. Adenosine analogs can modulate BBB permeability in mice and rats through stimulation of A_1R and $A_{2A}R$ receptors [4]. Activation of A_1R and $A_{2A}R$ on brain endothelial cells causes cytoskeletal remodeling and changes in endothelial cells size and shape. Such stimulation appears to result in temporary opening of the tight junctions between the endothelial cells, allowing short-term entry of large molecules, like dextran or antibodies, into the brain [4].

Thus far, no PET studies have been performed to assess changes of BBB permeability after administration of A_1R or $A_{2A}R$ agonists. A PET assay for measurement of tight junction opening could employ a hydrophilic compound labeled with a positron emitter. Under normal conditions, such a compound will not enter the brain, but remains in the vascular compartment. After administration of a permeability-modulating drug (like the A_1R agonist cyclopentyladenosine or the A_{2A} agonist Lexiscan), the tracer may enter the brain resulting in a detectable PET signal. Uptake of radiolabeled compounds in the rodent brain can be quantified by calculating standardized uptake value (SUV), distribution volume (V_T), or non-displaceable binding potential (BP_{ND}) of the radiotracer (see chapter 2 of this thesis).

5.2 Materials and Methods:

5.2.1 (Radio) pharmaceuticals

CPA and Lexiscan were purchased from Sigma (St.Louis, MO) and IDB Holland, respectively. The radioligand [^{11}C]CH_3-AMD3465 was prepared in the following way. [^{11}C]Methane was produced via the $^{14}N(p,\alpha)$ ^{11}C nuclear reaction by irradiating an N_2+5 % H_2 target gas with 17 MeV protons using a Scanditronix MC17 cyclotron. Typical beam currents were 5 to 8μA. [^{11}C] CH_3I was prepared from [^{11}C] methane via procedures that were previously described in the literature [5]. [^{11}C]Methyl triflate was formed by reacting [^{11}C] methyl iodide with silver triflate bound on α-alumina using an on-line gas/solid exchange reaction at 240°C. [^{11}C]Methyl triflate was transferred by a stream of helium (25ml/min) to a v-shaped reaction vial containing 0.4 mg of tri fluoroacetyl-AMD3465 in 300 μl acetone, cooled in an ice bath. After trapping of [^{11}C] methyl triflate, the reaction mixture was heated at 80^0C for 5 min. Subsequently, 300μl of methanol and 100μl of NaOH (1M) were added and the reaction mixture was heated at 80^0C for another 5 min. The reaction mixture was diluted with 0.6ml (16μl H_3PO_4) HPLC

eluent, and purified by HPLC using a Zorbax SB C18 (250x 7.8 mm) column with sodium phosphate buffer (pH 2.0)/EtOH (95/ 5 v/v %) as the eluent, at a flow rate of 4 ml/min. The radioactive product with a retention time of 12 ± 1 min was collected, neutralized with 1M NaOH (~400 µl) and passed over a Millex 0.22-µm GV filter (Millipore, Ireland) to yield a sterile solution of N-[^{11}C]methyl-AMD3465 ready for injection. The decay-corrected radiochemical yield of the tracer was 60 ± 2 % (n=20) and the total synthesis time was less than 50 min including the HPLC purification. An aliquot of this solution was analyzed by HPLC using a Jupiter C18 column (300 x 7.8 mm, Phenomenex) and water (pH 2.0)/ acetonitrile (90:10 v/v) as the eluent at a flow of 1 mL/min (retention time: 8 ± 1 min). The radiochemical purity was > 99 % and the specific radioactivity 30 ± 5 GBq/umol.

[^{18}F]-AMC 15 was prepared by reaction of 2-[^{18}F] fluoroethyl tosylate with the precursor(*R*) 1-(4-Hydroxyphenyl)-4-(4-(7-(methoxymethoxy) chroman-2-yl)-3-azabutyl)–piperazine. 2-[^{18}F] fluoroethyl tosylate was purified by HPLC (Alltima C18 5u 250x10 mm column eluted with acetonitrile/10 mM sodium acetate buffer pH 4.0 (60/40 v/v) at 5 ml/min (tR = 6.8 min, k'= 3.8)). At the end of the deprotection step, the reaction mixture was diluted with 10 ml water, titrated with 1 M NaOH to pH of 4 to 7 and then put through an Oasis HLB SPE cartridge. Adsorbed activity was eluted from the cartridge with 1 ml acetonitrile/DMF (1/1 v/v). The eluate was further diluted with water to a total volume of 1.5 to 2 ml and injected onto an Alltima C18 5u 250x10 mm HPLC column for purification of [^{18}F] AMC 15**.**

[^{18}F]AMC 15 was purified using an Alltima C18 5u 250x10 mm column eluted with a gradient of acetonitrile in 10 mM sodium acetate buffer: isocratic 45% acetonitrile during the first 2 min, then a linear decrease from 45 % at 2 min to 30% acetonitrile at 15 min (retention time of [^{18}F] AMC15 is 10.6 min, k' = 5.9). HPLC conditions for the identity confirmation and RCP assessment were: Platinum EPS 5u 250x4.6 column eluted with acetonitrile/10 mM phosphate buffer pH 7 (65/35 v/v) at 2 ml/min (t_R = 11.0 min, k' = 7.3). Quality control TLC conditions were: dichloromethane: methanol: ammonia 100:5:1 (R_f = 0.25) and ethyl acetate: methanol: ammonia: triethylamine 100:5:5:1 (R_f = 0.3). Before putting radioactive samples onto the TLC plates, drops of AMC 15 oxalate standard solution containing 2 µg of compound were put onto the start positions of each lane to exclude on-plate decomposition of no-carrier-added [^{18}F]-compound.

5.2.2 Experimental Animals

All animal experiments were performed by licensed investigators in compliance with the Law on Animal Experiments of The Netherlands. The protocol was approved by the Committee on Animal Ethics of University of Groningen. Male outbred Wistar-Unilever (SPF) rats (body weight 304 ± 54 g) were obtained from Charles-River, maintained at a

12-h light/12-h dark regime and fed standard laboratory chow ad libitum. Three groups of animals were studied for [^{11}C]CH_3-AMD3465: 1) Controls (pretreated with saline, i.p., n =3); 2) Animals pretreated with CPA (0.25 mg/kg, i.p., dissolved in 0.3 mL saline containing < 50 µL dimethyl sulfoxide, n = 2, see [6]; 3) Animals pretreated with Lexiscan (0.05 mg/kg, i.v., dissolved in saline, n = 1). Three groups of animals were studied for [^{18}F]-AMC 15: 1) Controls (pretreated with saline, i.p., n = 1; 2) Animals pretreated with CPA (0.25 mg/kg, i.p., dissolved in 0.3 mL saline containing < 50 µL dimethyl sulfoxide, n = 1 see [6] 3) Animals pretreated with Lexiscan (0.05 mg/kg, i.v., dissolved in saline, n = 1); The very small number of animals in each group is due to the fact that this study is a pilot which was still ongoing by the time the PhD thesis was written

5.2.3 PET scanning

Two rats were scanned simultaneously, using a Focus 220 microPET camera (Siemens-Concorde, Knoxville, TN). Animals were anesthetized with a mixture of isoflurane/air (ratio 5% during induction, later reduced to ≤ 2%). Cannulas were placed in a femoral artery and vein for blood sampling and tracer injection, respectively. A transmission scan was made, using an external source of radioactive cobalt, in order to correct the subsequently acquired [^{11}C]CH_3-AMD3465 and [^{18}F]-AMC 15 emission images for attenuation and scatter. Rats were under anesthesia for 30–40 min before tracer injection (time required for cannulation and transmission scan). The tracer ([^{11}C]CH_3-AMD3465 and [^{18}F]-AMC 15 in volume of 1 mL) were injected through the venous cannula, as a slow (1 min) bolus, using a Harvard-style pump. The camera was started as soon as the tracer entered the body of the first rat in the scanner; the second animal of the pair was injected 16 min later. Scanning was then continued for another 60 min. The animal that was injected last was also anesthetized at a later moment. Thus, the duration of anesthesia was similar in all study groups. A list-mode protocol was used (76 min, brain in the field of view). A series of blood samples (18 samples; volume, 0.10–0.15 mL) was drawn, initially in rapid succession (5 s) and later at longer intervals (up to 30 min). Plasma was acquired from these samples by centrifugation (Eppendorf centrifuge, 5 min at 13,000 rpm). Radioactivity in 25 µL of plasma and 25 µL of whole blood was counted and used as an arterial input function. During the entire scanning procedure, heart rate, stroke volume and blood oxygen level of the animals were monitored, using pulse oximeters (Nonin Pulse Sense).

5.2.4 Analysis of PET Data

List-mode data were reframed into a dynamic sequence of 8 × 30, 3 × 60, 2 ×120, 2 × 180, 3 × 300, 1 × 480, 3 × 600, and 1 × 960 s frames. The data were reconstructed per time frame using an iterative reconstruction algorithm (attenuation-weighted 2-dimensional ordered-subset expectation maximization, provided by Siemens; 4 iterations, 16 subsets; zoom factor 2). The final datasets consisted of 95 slices, with a slice thickness of 0.8 mm and an in-plane image matrix of 128 ×128 pixels of size 1.1 mm. Datasets were fully corrected for random coincidences, scatter, and attenuation. Images were smoothed with a Gaussian filter (1.35 mm in both directions).

Volumes (cm^3) for the regions of interest (ROIs) were calculated using the Siemens Inveon Research Work Place 4.0 (IRW 4.0). ROIs were drawn around the (entire) bulbi olfactorii, frontal cortex, striatum, amygdala, parietal/temporal/occipital cortices, medulla, cerebellum, pons and hippocampus in a template MRI scan that was co-registered with the PET scan of interest by image fusion (*17*). Standardized uptake values measured by PET (PET-SUVs) were calculated, using measured body weights and injected doses [tissue activity concentration (MBq/mL)]/[(injected dose (MBq)/body weight (g)]. The cerebral distribution volume (V_T) of the tracer was estimated either from a Logan plot or a 2-tissue-compartment model (2TCM) fit. The partition coefficient (K_1/k_2) and binding potential (K_3/k_4) of [^{11}C]CH_3-AMD3465 and [^{18}F]-AMC 15 were estimated from the model fit.

5.3 Results

5.3.1 Small-Animal PET Images

Small animal PET images were acquired after injection of [^{11}C]CH_3-AMD3465 and [^{18}F]-AMC15 . Neither in control animals, nor in animals pretreated with CPA or Lexiscan any brain uptake of the tracers was observed. The brain appeared like a black hole in all PET images.

5.3.2 Graphical Analysis of PET Data

Tracer V_T was calculated using a Logan plot, time–activity curves from an ROI drawn around the entire brain, and radioactivity counts from arterial blood samples. There was no increase in V_T of [^{11}C]CH_3-AMD3465 after pretreatment of animals with CPA compared to controls (0.085 ± 0.052 vs 0.135 ± 0.052, respectively). Also no increment in V_T of [^{18}F]-AMC15 was observed after pretreatment of animals with CPA or Lexiscan compared to controls (0.034 vs 0.017 or 0.035, respectively).

5.3.3 Compartment Modeling of PET Data

When a 2TCM was fitted to time–activity curves from a ROI drawn around the entire brain, using radioactivity counts from arterial blood samples as input function, the partition coefficients of [^{11}C]CH_3-AMD3465 and [^{18}F]-AMC15 (ratio K_1/k_2 from the model fit) were found not to be affected by CPA or Lexiscan (**Table 4 and 5**) . The ratio of k_3/k_4, a measure of tracer binding potential, for [^{11}C]CH_3-AMD3465 remained unaltered after pretreatment with the A_1R or A_{2A}R agonist (**Table 4**). k_3/k_4 of [^{18}F]-AMC 15 appeared to show some increase after pretreatment with the A_1 agonist but was unaltered after treatment with the A_{2A} agonist compared to control (**Table 5**).

.

5.3.4 Biodistribution Data

Biodistribution data of [^{11}C]CH_3-AMD3465 and [^{18}F]-AMC15, acquired 80 min after injection of [^{11}C]CH_3-AMD 3465 and [^{18}F]-AMC15, are presented in **Table 1 and 2**. Pretreatment of animals with CPA and Lexiscan, did not result in significant increases of [^{11}C]CH_3-AMD3465 and [^{18}F]-AMC 15 uptake in brain areas and peripheral organs

5.3.5 Physiological response

After i.p. administration of the A_1 agonist CPA a very strong decline of heart rate was observed within 5 min (from 340 to about 100) and after i.v injection of A_{2A} agonist Lexiscan, we also noticed decline of heart rate (from 340 to 320).

Table 1: Biodistribution Data of [^{11}C]CH_3-AMD3465, 80 minutes after Injection

Tissue	Control animals (n = 3)	Treated with 0.26mg/kgCPA (n = 1)	Lexiscan 0.05mg/kg (n = 1)
Brain 1	0.208 ± 0.047	0.179	0.075
Brain 2	0.532 ± 0.136	0.126	0.107
Bone	0.518 ± 0.099	0.304	0.297
Colon	0.574 ± 0.195	0.937	0.549
Duodenum	1.304 ± 0.150	0.226	0.693
Fat	0.488 ± 0.122	1.420	0.261
Heart	0.820 ± 0.204	0.140	0.418
Ileum	1.436 ± 0.133	28.232	0.358
Kidney	11.180 ± 5.351	9.976	9.928
Liver	10.990 ± 3.665	1.203	8.210
Lung	0.437 ± 0.274	0.110	0.769
Muscle	0.463 ± 0.077	0.716	0.205
Pancreas	0.7320 ± 0.120	1.814	0.307
Plasma	1.121 ± 0.563	0.863	0.257
Red cells	0.768 ± 0.235	1.823	0.506
Spleen	1.560 ± 0.433	1.449	0.757
Urine	4.779 ± 1.820	0.131	25.024

Control: Mean ± SD

Table 2: Biodistribution Data of [^{18}F]-AMC 15, 80 Minutes after Injection

Tissue	Control animals (n = 1)	Treated with 0.26mg/kgCPA (n = 1)	Lexiscan 0.05mg/kg (n = 1)
Brain 1	0.082	0.065	0.035
Brain 2	0.059	0.069	0.026
Brain 3	0.075	0.057	0.035
Bone	0.151	0.664	0.205
Colon	0.822	0.401	0.327
Duodenum	1.702	12.670	9.241
Fat	0.251	0.196	0.113
Heart	0.113	0.565	0.240
Ileum	0.263	0.567	1.114
Kidney	0.367	2.928	1.168
Liver	1.119	1.651	2.052
Lung	1.229	5.572	2.842
Muscle	0.076	0.291	0.164
Pancreas	0.617	3.489	0.999
Plasma	0.097	0.223	0.200
Red cells	0.037	0.104	0.081
Spleen	1.427	2.157	1.564
Urine	0.936	0.006	0.001

Table 3: Biodistribution Data of different regions of brain, [^{11}C]CH_3-AMD3465, 80 Minutes after Injection

Tissue	Control animals (n = 1)	Treated with CPA (n = 1)
Amygdala	0.094	0.095
Olfactory bulb	0.211	0.167
Cerebellum	0.170	0.246
Cingulate	0.717	0.235
Entorhinal	0.244	0.132
Frontal	0.178	0.097
Hippocampus	0.083	0.152
Medulla	0.360	0.149
Parietal, temporal and occipital cortices	0.151	0.051
Pons	0.234	0.095
Striatum	0.134	0.065
Rest of the brain	0.172	0.095

5.4 Discussion

This ongoing project aimed to answer the question whether transient opening of the blood-brain barrier after treatment of animals with adenosine receptor agonists can be detected with hydrophilic radiotracers and PET. Such tracers do not pass the normal barrier, but may pass after BBB opening.

For initial attempts we used [^{11}C]CH_3-AMD3465 (CXCR4 antagonist) and [^{18}F]-AMC15 ligand (dopamine D2 agonist). The clogP of [^{11}C]CH_3-AMD3465 is -0.89 and [^{18}F]-AMC15 is 1.54. But the preliminary PET data and microPET images showed no differences in brain uptake between animals treated with adenosine receptor agonists and untreated controls. A biodistribution study, performed 80 min after tracer injection, also did not indicate any increases of radioactivity in the brain of pretreated animals. A 2TCM was fitted to time–activity curves from a ROI drawn around the entire brain, using radioactivity counts from arterial blood samples as input function. This kinetic modeling approach indicated that neither the partition coefficient (K_1/k_2) nor the binding potential (k_3/k_4) of [^{11}C]CH_3-AMD3465 were affected by the treatment but k_3/k_4 of [^{18}F]-AMC 15 seemed increased after pretreatment with the A_1 agonist CPA, whereas K_1/K_2 remained unchanged. Since this increase is based on the analysis of data of just a single animal and did not result in visibility of the striata in microPET images, the modeling result may not be significant. Extremely low values for tracer partition coefficient suggested that the tracer did never pass the blood-brain barrier (**Table 5**).

According to Carman et al. [4], transient BBB opening should occur after treatment of animals with an A_1R or $A_{2A}R$ agonist and should persist for several hours. In our experiments, the agonists were administered properly as proven by strong physiological responses of the rats (decline of heart rate, increase of stroke volume). However, we could not detect any BBB opening with PET. We failed to observe hydrophilic tracer uptake in rat brain after pretreatment with A_1 and A_{2A} agonists. This negative finding could be related to different underlying mechanisms:

1. Hydrophilic tracers may be rapidly cleared from the circulation (i.e., within 5 or 10 min after injection) whereas opening of the barrier may occur only later, after a prolonged interval (e.g., more than 20 min after agonist administration). Thus the barrier would open at a moment when the bulk of the injected tracer has already been cleared from the circulation.

2. Because of certain physiological conditions of the animals during the scanning procedure (anesthesia, acidosis, hypercapnia or hypothermia) the BBB may not have opened after pretreatment with an A_1R or $A_{2A}R$ agonist. In the published study describing barrier opening [4], animals were only anesthetized at the end of the experiment for the purpose of euthanasia.

In a follow-up study, we plan to test our experimental procedure with a widely used and generally accepted assay for BBB permeability, the Evans Blue assay. This assay can answer the question whether the BBB was in fact opened, or did not open at all. It is important to know whether the failure of the PET assay was due to inappropriate tracer kinetics (mechanism 1) or failure of the experimental animals to respond to the adenosinergic stimulus (mechanism 2).

Table 4: Results from Graphical Analysis and Compartment Modeling of PET Data (ROI Drawn Around Entire Brain) of [^{11}C]CH_3-AMD3465

Group	$\boldsymbol{V_T}$ (Logan)	$\mathbf{K_1/k_2}$ (2TCM)	$\boldsymbol{BP_{ND}}$ (k_3/k_4) (2TCM)
Control (n=3)	0.352±0.052	0.046±0.011	2.822±1.055
CPA (n=2)	0.116±0.012	0.033±0.003	2.187±0.619
Lexiscan (n=1)	0.105	0.047	1.936

Table 5: **Results from Graphical Analysis and Compartment Modeling of PET Data (ROI Drawn Around Entire Brain) of [^{18}F]-AMC 15**

Group	$\boldsymbol{V_T}$ (Logan)	$\mathbf{K_1/k_2}$ (2TCM)	$\boldsymbol{BP_{ND}}$ (k_3/k_4) (2TCM)
Control (n=1)	0.0349	0.0001	7.4381
CPA (n=1)	0.0344	0.0001	12.635
Lexiscan (n=1)	0.0166	0.0056	7.1144

5.5 Conclusion

In a preliminary microPET study with the hydrophilic ligands [^{11}C]CH_3-AMD3465 or [^{18}F]-AMC15 we could not demonstrate BBB opening after adenosine receptor stimulation. Both tracers did not enter the brain after pretreatment of rats with A_1 or A_{2A} agonists. Further studies are necessary to determine whether this negative finding is due to inappropriate kinetics of the tracers or failure of anesthetized animals to respond to adenosine receptor stimulation.

5.6 References

1) Abbott NJ (2013). Blood-brain barrier structure and function and the challenges for CNS drug delivery. J Inherit Metab Dis 36:437-449.

2) Abbott NJ, Dolman DE, Drndarski S, Fredriksson SM (2012). An improved in vitro blood-brain barrier model: rat brain endothelial cells co-cultured with astrocytes. Methods Mol Biol 814:415-430.

3) Wong AD, Ye M, Levy AF, Rothstein JD, Bergles DE,Searson PC (2013). The blood-brain barrier: an engineering perspective. Front Neuroeng 6:7.

4) Carman AJ, Mills JH, Krenz A, Kim DG,Bynoe MS (2011). Adenosine receptor signaling modulates permeability of the blood-brain barrier. J Neurosci 31:13272-13280.

5) Larsen P, Ulin J, Dahlstr¢m K, Jensen M (1997). Synthesis of [^{11}C]iodomethane by iodination of [^{11}C]methane. Appl.Rad.Isotop. 48:153-157

6) Roman V, Keijser JN, Luiten PG, Meerlo P (2008). Repetitive stimulation of adenosine A1 receptors in vivo: changes in receptor numbers, G-proteins and A1 receptor agonist -induced hypothermia. *Brain Res* 1191:69-74.

7) Cosolo WC, Martinello P, Louis WJ, Christophidis N (1989) Blood-brain barrier disruption using mannitol: Time course and electron microscopy studies. Am.J.Physiol. 256:R443-R447

Chapter VI

Summary

Adenosine is a neuromodulator with several functions in the central nervous system (CNS), such as inhibition of neuronal activity in many signaling pathways. The adenosine receptor (AR) family consists of the A_1, A_{2A}, A_{2B} and A_3 subtypes (A_1R. A_{2A}R, A_{2B}R and A_3R, respectively). A_1R and A_3R inhibit whereas A_{2A}R and A_{2B}R stimulate production of the second messenger, cAMP. Adenosine A_1 receptors (A_1R) stimulation may result in neuroprotection and suppression of neuroinflammation.

Positron Emission Tomography (PET) is a powerful *in vivo* imaging tool which can be applied to investigate the physiologic and pathologic roles of A_1R in the human and rodent brain. Several ligands for PET imaging of A_1R have been prepared. The best-characterized tracers are [^{11}C] MPDX and [^{18}F] CPFPX. Both can be applied for PET studies of cerebral A_1R in humans.

This thesis is focused on validation of the radiolabeled xanthine [^{11}C]-MPDX (8-dicyclopropylmethyl-1-[^{11}C]-methyl-3-propyl-xanthine) for preclinical studies of A_1R in rodent brain – including use of the tracer to determine the regional pattern of A_1R expression, changes of expression as a consequence of disease and the dose-dependent occupancy of cerebral A_1R by non-radioactive agonists and antagonists.

Chapter 1 provides an introduction to adenosine A_1R imaging and discusses roles of A_1R in health and disease. In **Chapter 2,** we applied [^{11}C]-MPDX for visualization of A_1R in rat brain. High uptake of radioactivity was noted in striatum, hippocampus, and cerebellum. Specific binding of the tracer in individual brain regions corresponded closely to regional A_1R densities known from autoradiography (see Figure 5 in Chapter 2). Pretreatment of animals with the selective A_1R antagonist DPCPX resulted in a strong suppression of tracer binding and regional differences of uptake were abolished. Raising levels of the endogenous agonist, adenosine, by treating rats with a 20% solution of ethanol in saline (2 mL) plus the adenosine kinase inhibitor 4-amino-5-(3-bromophenyl)-7-(6-morpholino-pyridin3-yl) pyrido [2,3-d] pyrimidine dihydrochloride (ABT-702) did not result in measurable competition of adenosine with [^{11}C]-MPDX for binding to A_1R, but rather in an unexpected global increase of the cerebral uptake of radioactivity (by 40% to 45%). Kinetic modeling suggested that this increase is not related to altered blood flow or altered blood-brain barrier passage of the radioligand, but rather to increased binding at the receptor level.

In **Chapter 3** we examined whether A_1R occupancy by therapeutic drugs (non-radioactive agonists and antagonists) can be assessed with [^{11}C]-MPDX and PET. As an A_1R agonist we used N^6-cyclopentyladenosine (CPA, 0.25mg/kg, i.p) and as an A_1R antagonist caffeine (4 and 40 mg/kg, i.p.). Administration of CPA resulted in a strong reduction (>50%) of heart rate, and caffeine administration in a small increase (10-15%). The low dose of caffeine resulted in 65.9% A_1R occupancy and the high dose in 98.5% occupancy, as calculated by a modified Lassen plot. Administration of CPA did not result in measurable competition of the agonist with [^{11}C]MPDX for binding to A_1R in the brain, but rather in a paradoxic increase of tracer uptake similar to the increase we noticed after raising the level of endogenous adenosine (Chapter 2). Kinetic modeling of tracer binding suggested that adenosine analogs may increase the fraction of A_1R that can bind the radioligand. Thus, [^{11}C]MPDX is a suitable tracer for determining occupancy of A_1R by non-radioactive xanthine antagonists but not purine agonists.

In **Chapter 4** we assessed changes of A_1R expression in a rat model of encephalitis. Wistar rats were intranasally infected with herpes simplex virus-1 and scanned after an interval of six or seven days when they began to show the symptoms of cerebral inflammation. Regional distribution volumes of [^{11}C]MPDX (V_T) calculated from a Logan plot indicated significant increases of tracer uptake in hippocampus and medulla of virus-infected rats. A 2-tissue compartmental model fit of the microPET data indicated significant increases of tracer binding potential in hippocampus, cerebellum and medulla which may indicate increased A_1R expression. The partition coefficient of [^{11}C]-MPDX (ratio K_1/k_2 from the model fit) was not significantly altered after virus infection. Immunohistochemical staining showed a strong increase of A_1R immunoreactivity in cerebellum of HSV-1-infected rats. These data indicate an upregulation of adenosine A_1 receptors (A_1R) in the early phase of rodent encephalitis that can be detected with the A_1R antagonist [^{11}C]-MPDX and PET imaging. This upregulation may limit the release of excitatory neurotransmitters such as glutamate, and reduce neuronal excitability, resulting in protection of neurons from excessive stimulation.

In **Chapter 5** we investigated whether transient opening of the blood-brain barrier after treatment of animals with (non-radioactive) adenosine A_1 and A_{2A} receptor agonists can be detected with hydrophilic radiotracers and PET. Such tracers do not pass the intact barrier, but may pass after BBB opening. For our initial pilot, we used [^{11}C]CH_3-AMD3465 (CXCR4 antagonist) and [^{18}F]AMC 15 (Dopamine D_2 receptor agonist). Cerebral uptake (SUV) and distribution volume (V_T) of both tracers was not increased after pretreatment of animals with CPA or Lexiscan. Further studies are necessary to determine whether this negative finding is due to inappropriate kinetics of the used tracers or to lack of blood-brain barrier opening in anesthetized rats.

The thesis ends with a **Summary** (in English) and a discussion of **Future Perspectives**

Chapter VII

Conclusion and Future Perspective

Conclusion

1. [^{11}C]MPDX and PET can be used to assess regional adenosine A_1R expression in the rodent brain (**Chapter 2**). Regional distribution volume (V_T) from a Logan plot or k_3/k_4-ratio from a two-tissue compartment model may be used to quantify [^{11}C] MPDX binding to A_1R.

2. Occupancy of A_1R by non-radioactive xanthines (antagonists) can be assessed with [^{11}C] MPDX and PET (**Chapters 2 and 3**).

3. However, occupancy of A_1R by non-radioactive agonists (adenosine, CPA, i.e. purines) can not be assessed with this technique. This may be due to the fact that adenosine analogs and xanthine antagonists bind to different domains of the A_1R which show allosteric interactions, or adenosine analogs increase the fraction of A_1R that can bind the radioligand (**Chapters 2 and 3**).

4. Herpes-simplex virus-induced encephalitis is associated with an upregulation of A_1R in several brain areas (cerebellum, hippocampus, pons/midbrain, and medulla). This upregulation appears to occur particularly in the early - or acute - phase of viral inflammation. A_1R upregulation may protect neurons against excessive stimulation by excitatory neurotransmitters such as glutamate (**chapter 4**).

5. Blood-brain barrier opening could not be demonstrated using two hydrophilic tracers (the CXCR4 receptor antagonist [^{11}C]CH_3-AMD3465 or dopamine D_2 receptor agonist [^{18}F]-AMC 15) and small animal PET. We did not observe any tracer uptake in rat brain after the animals were pretreated with an A_1 or A_{2A}R agonist (**Chapter 5**)

Future Perspectives

Data presented in this thesis show that the PET tracer [^{11}C] MPDX can be used to visualize regional A_1R expression in the rodent brain (**chapter 1**) and to assess changes of A_1R binding as a consequence of disease **(chapter 4**). Occupancy of cerebral A_1R by non-radioactive xanthine antagonists (but not purine agonists) is measurable with [^{11}C] MPDX and PET (chapters **1, 3**). In future studies, the PET tracer may be applied to answer several interesting research questions

Impact of anesthetics

Based on findings reported in the literature, we expect that anesthesia has an impact on the measured (apparent) A_1R densities in rodent brain. At anesthetic dose, halothane inhibits the binding of an A_1R agonist by 20-30% (1). On the other hand, A_1R may be involved in some actions of anesthetics and in known interactions between anesthetics and recreational drugs such as ethanol. Adenosine is formed during the metabolism of ethanol, which results in stimulation of A_1R (2-4) and potentiation of isoflurane anesthesia (2). Halothane anesthesia is potentiated after treatment of animals with the A_1R agonist L-phenylisopropyladenosine (L-PIA); such treatment reduces the minimum anesthetic concentration (MAC) of halothane by 49% (5). The expression of the enzyme ecto 5'-nucleotidase (CD73) which is responsible for the formation of extracellular adenosine by converting extracellular AMP to adenosine is increased by isoflurane (6). Neuroprotective effects of isoflurane (e.g. after cerebral injury) (7) and cardioprotective effects of fentanyl (8) and desflurane (9) during myocardial ischemia may be related to A_1R stimulation, since some of these beneficial effects could be prevented by co-administration of an A_1R antagonist (8).

In future experiments, animals could be anesthetized with different anesthetics during the PET scan, or the biodistribution of [^{11}C] MPDX in awake and anesthetized animals could be compared, in order to study the impact of anesthesia on apparent A_1R expression. We expect changes of [^{11}C] MPDX binding as a consequence of anesthesia. To gain more insight in the mechanisms underlying the impact of anaesthetics, therapeutics or recreational drugs on the in vivo binding of [^{11}C] MPDX, microPET scans could be combined with measurements of extracellular adenosine by microdialysis (10).

Neuroinflammation

Additional studies are necessary to further characterize the role of A_1R signaling in rodent neuroinflammation. We have examined only a single inflammation model (virus-induced), involving a rather acute form of inflammation. Also, we could scan only a limited number of animals. Our data suggest that A_1R upregulation may be transient and limited to the early phase of encephalitis, but we have not actually proven this (see **chapter 4).** In future experiments, the impact of acute and chronic inflammation on adenosine A_1R expression could be compared. We expect an upregulation of A_1R in the acute phase and a downregulation in the chronic phase of neuroinflammation, as acute inflammation induced by injection of lipopolysaccharide (11) was associated with an upregulation of A_1R in mouse brain (12) whereas chronic experimental allergic encephalomyelitis (EAE) was associated with a downregulation of A_1R (13).

Traumatic brain injury

Adenosine and A_1R are involved in the suppression of neuronal hyperactivity and limitation of the inflammatory response after traumatic brain injury. When normal and A_1R knockout mice were subjected to controlled cortical impact, seizure scores were much higher in the knockouts and only knockout animals developed lethal status epilepticus [14]. Similarly, unilateral hippocampal kainate injection caused nonconvulsive status epilepticus in wild-type mice but severe convulsions and subsequent death in A_1R knockouts [15]. Status epilepticus is associated with widespread release of adenosine throughout the brain and suppression of the excitability of neurons remote from the epileptic focus *via* stimulation of A_1R. In A_1R knockout mice, this protective mechanism is lacking, so that severe convulsions and lethal status epilepticus can develop [15]. A_1R knockout mice display a 20-50% enhanced microglial response after mild traumatic brain injury compared to their wild-type littermates. Stimulation of A_1R in immortalized mouse microglia (BV-2) cells results in inhibition of microglial proliferation [16]. Thus, longitudinal microPET studies with [^{11}C] MPDX in a rat model of traumatic brain injury could be an interesting research project. A_1R expression may be different shortly and several weeks after controlled cortical impact. In a rat model of acute general seizure (i.p. injection of a convulsive dose of bicuculline), a widespread increase of A_1R expression was noted [17] but in animal models of chronic epilepsy prominent losses of A_1R were seen [18-20].

Chronic sleep deprivation

Many endogenous factors are involved in maintenance of sleep-wake cycle, one of these is adenosine which reduces wakefulness by activation of A_1R in pre- and postsynaptic regions, resulting in inhibition of the release of excitatory neurotransmitters and dampening of the response of neurons to these signals (21). A_1Rs are known to be involved in homeostatic sleep regulation. An increment in cerebral A_1R expression was noted both in animals (22-25) and humans (26) after acute sleep deprivation. Short periods of total sleep deprivation (3 or 6 h) result in increases of A_1R mRNA but no detectable increases of A_1R expression in rat brain [22]. However, longer periods of total sleep deprivation in rodents (12 or 24 h) are accompanied by a significant upregulation of A_1R (up to 14%) in several brain areas [23, 24]. Saturation binding assays have indicated that A_1R densities in cortical and subcortical regions of rat brain are increased not only after total sleep deprivation, but also after 48 and 96 h of partial, rapid eye movement (REM) sleep deprivation, whereas affinity (K_d) values for agonist ([^{3}H]PIA) binding are not significantly altered (25). Most reported studies about involvement of A1R in sleep have examined the impact of acute, total sleep deprivation. In future, longitudinal PET studies the impact of various intervals (2 days, 5 days, 30 days) of severe sleep deprivation (20 hrs/day) could be directly compared. Such studies might answer the question whether acute and chronic sleep deprivations have different effects, and if the upregulation of A_1R is transient or permanent.

Animal models of anxiety

Adenosine and A_1R may be involved in the control of anxiety. Mice lacking A_1R show increased anxiety-like behavior compared to normal mice (27). Moreover, selective A_1R agonists (like 2-chloro-N (6)-cyclopentyladenosine, CCPA) have anxiolytic effects both in mice (28) and rats (29). Anxiety-like behavior in mice during acute ethanol withdrawal is weakened after acute administration of CCPA (30). Chronic treatment of mice with the A_1R antagonist DPCPX results in upregulation of A1R and reduced exploratory behavior, which is suggestive of reduced anxiety (31). No PET study has ever been performed to assess regional differences of cerebral A_1R expression in anxiety-prone and normal rodents, or changes of cerebral A_1R expression after stress-induced anxiety. In the latter case, a modest upregulation of A_1R may be expected, since a 15% increase of A_1R density in hypothalamic membranes was observed after chronic stress-induced anxiety in rats (32).

Human studies

Besides the preclinical studies in rodents proposed above, PET studies in humans are possible and could be focused on the role of A_1R in the following disorders of the brain.

1. **Multiple sclerosis (MS).**

A_1R densities and the coupling of A_1R to cytokine signaling systems appear to be altered in MS. A_1R numbers in peripheral blood mononuclear cells (PBMC) and in brain tissue from MS-patients are significantly decreased (by 53% and 49%, respectively) compared to age-matched controls (33). Plasma levels of TNF-alpha in such patients are significantly higher and levels of adenosine are significantly lower than in control subjects. Stimulation of PBMC with a selective A_1R agonist (R-PIA) inhibits the mitogen-stimulated production of TNF-alpha in healthy subject but not in MS patients, whereas the opposite is observed for the mitogen-stimulated production of interleukin-6 (34) PET studies with A_1R ligands in MS patients and age-matched controls have not yet been performed. Based on post mortem findings in brain samples, a downregulation of cerebral A_1R can be expected (33)

2. **Schizophrenia**

A partial loss of A_1R during birth and a corresponding reduction of the control of dopamine activity in later life has been proposed to play a role in the inhibitory deficit in schizophrenia (35, 36). In a Japanese population, schizophrenia was found to be associated with a single nucleotide polymorphism of the A_1R gene (rs3766553) (37). PET studies of cerebral A_1R in schizophrenic patients may reveal regional losses of A_1R.

References

1) Martin DC, Dennison RL, Introna RP, Aronstam RS (1991) Influence of halothane on the interactions of serotonin1A and adenosine A1 receptors with G proteins in rat brain membranes. Biochem Pharmacol 42:1313-1316.

2) Campisi P, Carmichael FJ, Crawford M, Orrego H,Khanna JM (1997) Role of adenosine in the ethanol-induced potentiation of the effects of general anesthetics in rats. Eur J Pharmacol 325:165-172.

3) Carmichael FJ, Orrego H, Israel Y (1993) Acetate-induced adenosine mediated effects of ethanol. Alcohol Alcohol Suppl 2:411-418.

4) Ruby CL, Adams CA, Knight EJ, Nam HW,Choi DS (2010) An essential role for adenosine signaling in alcohol abuse. Curr Drug Abuse Rev 3:163-174.

5) Birch BD, Louie GL, Vickery RG, Gaba DM,Maze M (1988) L-phenylisopropyadenosine (L-PIA) diminishes halothane anesthetic requirements and decreases noradrenergic neurotransmission in rats. Life Sci 42:1355-1360.

6) Kim M, Ham A, Kim JY, Brown KM, D'Agati VD,Lee HT (2013) The volatile anesthetic isoflurane induces ecto-5'-nucleotidase (CD73) to protect against renal ischemia and reperfusion injury. Kidney Int 84:90-103.

7) Liu Y, Xiong L, Chen S,Wang Q (2006) Isoflurane tolerance against focal cerebral ischemia is attenuated by adenosine A1 receptor antagonists. Can J Anaesth 53:194-201.

8) Kato R, Ross S,Foex P (2000) Fentanyl protects the heart against ischaemic injury via opioid receptors, adenosine A1 receptors and KATP channel linked mechanisms in rats. Br J Anaesth 84:204-214.

9) Hanouz JL, Yvon A, Massetti M, Lepage O, Babatasi G, Khayat A, Bricard H,Gerard JL (2002) Mechanisms of desflurane-induced preconditioning in isolated human right atria in vitro. Anesthesiology 97:33-41.

10) Sharma R, Engemann SC, Sahota P,Thakkar MM (2010) Effects of ethanol on extracellular levels of adenosine in the basal forebrain: an in vivo microdialysis study in freely behaving rats. Alcohol Clin Exp Res 34:813-818.

11) Dobos N, de Vries EF, Kema IP, Patas K, Prins M, Nijholt IM, Dierckx RA, Korf J, den Boer JA, Luiten PG,Eisel UL (2012) The role of indoleamine 2,3-dioxygenase in a mouse model of neuroinflammation-induced depression. J Alzheimers Dis 28:905-915.

12) Jhaveri KA, Reichensperger J, Toth LA, Sekino Y,Ramkumar V (2007) Reduced basal and lipopolysaccharide-stimulated adenosine A1 receptor expression in the brain of nuclear factor-kappaB p50-/- mice. Neuroscience 146:415-426.

13) Tsutsui S, Schnermann J, Noorbakhsh F, Henry S, Yong VW, Winston BW, Warren K,Power C (2004) A1 adenosine receptor upregulation and activation attenuates neuroinflammation and demyelination in a model of multiple sclerosis. J Neurosci 24:1521-1529.

14) Kochanek PM, Vagni VA, Janesko KL, Washington CB, Crumrine PK, Garman RH, Jenkins LW, Clark RS, Homanics GE, Dixon CE, Schnermann J,Jackson EK (2006) Adenosine A1 receptor knockout mice develop lethal status epilepticus after experimental traumatic brain injury. J Cereb Blood Flow Metab 26:565-575.

15) Fedele DE, Li T, Lan JQ, Fredholm BB,Boison D (2006) Adenosine A1 receptors are crucial in keeping an epileptic focus localized. Exp Neurol 200:184-190.

16) Haselkorn ML, Shellington DK, Jackson EK, Vagni VA, Janesko-Feldman K, Dubey RK, Gillespie DG, Cheng D, Bell MJ, Jenkins LW, Homanics GE, Schnermann J,Kochanek PM (2010) Adenosine A1 receptor activation as a brake on the microglial response after experimental traumatic brain injury in mice. J Neurotrauma 27:901-910.

17) Daval J, Werck M (1991) Autoradiographic changes in brain adenosine A1 receptors and their coupling to G proteins following seizures in the developing rat. Brain Res Dev Brain Res 59:237-247.

18) Ochiishi T, Takita M, Ikemoto M, Nakata H,Suzuki SS (1999) Immunohistochemical analysis on the role of adenosine A1 receptors in epilepsy. Neuroreport 10:3535-3541.

19) Ekonomou A, Sperk G, Kostopoulos G,Angelatou F (2000) Reduction of A1 adenosine receptors in rat hippocampus after kainic acid-induced limbic seizures. Neurosci Lett 284:49-52.

20) Rebola N, Coelho JE, Costenla AR, Lopes LV, Parada A, Oliveira CR, Soares-da-Silva P, de Mendonca A,Cunha RA (2003) Decrease of adenosine A1 receptor density and of adenosine neuromodulation in the hippocampus of kindled rats. Eur J Neurosci 18:820-828.

21) Landolt HP, Retey JV,Adam M (2012) Reduced neurobehavioral impairment from sleep deprivation in older adults: contribution of adenosinergic mechanisms. Front Neurol 3:62.

22) Basheer R, Halldner L, Alanko L, McCarley RW, Fredholm BB,Porkka-Heiskanen T (2001) Opposite changes in adenosine A1 and A2A receptor mRNA in the rat following sleep deprivation. Neuroreport 12:1577-1580.

23) Basheer R, Bauer A, Elmenhorst D, Ramesh V,McCarley RW (2007) Sleep deprivation upregulates A1 adenosine receptors in the rat basal forebrain. Neuroreport 18:1895-1899.

24) Elmenhorst D, Basheer R, McCarley RW,Bauer A (2009) Sleep deprivation increases A(1) adenosine receptor density in the rat brain. Brain Res 1258:53-58.

25) Yanik G,Radulovacki M (1987) REM sleep deprivation up-regulates adenosine A1 receptors. Brain Res 402:362-364.

26) Elmenhorst, D.; Meyer, P.T.; Winz, O.H.; Matusch, A.; Ermert, J.; Coenen, H.H.; Basheer, R.; Haas, H.L.; Zilles, K.; Bauer, A (2007) Sleep deprivation increases A1 adenosine receptor binding in the human brain: a positron emission tomography study. J Neurosci 27:2410-2415.

27) Johansson B, Halldner L, Dunwiddie TV, Masino SA, Poelchen W, Gimenez-Llort L, Escorihuela RM, Fernandez-Teruel A, Wiesenfeld-Hallin Z, Xu XJ, Hardemark A, Betsholtz C, Herlenius E,Fredholm BB (2001) Hyperalgesia, anxiety, and decreased hypoxic neuroprotection in mice lacking the adenosine A1 receptor. Proc Natl Acad Sci U S A 98:9407-9412.

28) Florio C, Prezioso A, Papaioannou A,Vertua R (1998) Adenosine A1 receptors modulate anxiety in CD1 mice. Psychopharmacology (Berl) 136:311-319.

29) Bruno AN, Fontella FU, Bonan CD, Barreto-Chaves ML, Dalmaz C,Sarkis JJ (2006) Activation of adenosine A(1) receptors alters behavioral and biochemical parameters in hyperthyroid rats. Behav Brain Res 167:287-294.

30) Prediger RD, da Silva GE, Batista LC, Bittencourt AL,Takahashi RN (2006) Activation of adenosine A1 receptors reduces anxiety-like behavior during acute ethanol withdrawal (hangover) in mice. Neuropsychopharmacology 31:2210-2220.

31) Vollert C, Forkuo GS, Bond RA,Eriksen JL (2013) Chronic treatment with DCPCX, an adenosine A(1) antagonist, worsens long-term memory. Neurosci Lett 548:296-300.

32) Anderson SM, Leu JR,Kant GJ (1987) Effects of stress on [3H]cyclohexyladenosine binding to rat brain membranes. Pharmacol Biochem Behav 26:829-833.

33) Johnston JB, Silva C, Gonzalez G, Holden J, Warren KG, Metz LM, Power C (2001) Diminished adenosine A1 receptor expression on macrophages in brain and blood of patients with multiple sclerosis. Ann Neurol 49:650-658

34) Mayne M, Shepel PN, Jiang Y, Geiger JD, Power C (1999) Dysregulation of adenosine A1 receptor-mediated cytokine expression in peripheral blood mononuclear cells from multiple sclerosis patients. Ann Neurol 45: 633-639

35) Lara DR, Dall'Igna OP, Ghisolfi ES,Brunstein MG (2006) Involvement of adenosine in the neurobiology of schizophrenia and its therapeutic implications. Prog Neuropsychopharmacol Biol Psychiatry 30:617-629.

36) Boison D, Singer P, Shen HY, Feldon J,Yee BK (2012) Adenosine hypothesis of schizophrenia--opportunities for pharmacotherapy. Neuropharmacology 62:1527-1543.

37) Gotoh L, Mitsuyasu H, Kobayashi Y, Oribe N, Takata A, Ninomiya H, Stanton VP,Jr, Springett GM, Kawasaki H,Kanba S (2009) Association analysis of adenosine A1 receptor gene (ADORA1) polymorphisms with schizophrenia in a Japanese population. Psychiatr Genet 19:328-335.

Chapter VIII

Samenvatting

SAMENVATTING

Adenosine is een neuromodulator met uiteenlopende functies in het centraal zenuwstelsel, zoals inhibitie van neuronale activiteit in vele signaalroutes. De adenosine receptor (AR) familie bestaat uit de subtypes A_1, A_{2A}, A_{2B} en A_3 (afgekort als A_1R, $A_{2A}R$, $A_{2B}R$ en A_3R). A_1R en A_3R remmen de vorming van de "second messenger" cyclisch AMP, terwijl $A_{2A}R$ en $A_{2B}R$ deze vorming stimuleren. Activatie van adenosine A_1 receptoren (A_1R) kan leiden tot bescherming van neuronen en tot onderdrukking van neuroinflammatie.

Positron Emissie Tomografie (PET) is een krachtige techniek voor *in vivo* imaging die kan worden toegepast om de (patho)fysiologische betekenis van A_1R in het brein van knaagdieren en mensen beter te gaan begrijpen. Er zijn meerdere liganden voor PET imaging van A_1R beschikbaar. [^{11}C]MPDX en [^{18}F]CPFPX zijn daarvan het best gekarakteriseerd. Beide liganden kunnen worden toegepast voor PET studies van A_1R in het menselijk brein.

Dit proefschrift is gericht op validatie van het radioactief gemerkte xanthine [^{11}C]-MPDX (8-dicyclopropylmethyl-1-[^{11}C]-methyl-3-propyl-xanthine) voor preklinische studies van A_1R in het knaagdierbrein. Dit houdt in: gebruik van de tracer om het regionale patroon van A_1R expressie en veranderingen van deze expressie ten gevolge van ziekte vast te stellen, plus de dosis-afhankelijke bezetting van A_1R door niet-radioactieve agonisten en antagonisten.

Hoofdstuk 1 verschaft een inleiding tot imaging van A_1R en bespreekt de rol van A_1R in het gezonde en zieke brein. In **hoofdstuk 2** hebben wij [^{11}C]MPDX toegepast om A_1R in het rattenbrein te visualiseren. Een hoge opname van radioactiviteit werd waargenomen in striatum, hippocampus en cerebellum. De specifieke binding van de tracer in individuele hersengebieden kwam overeen met regionale dichtheden van de A_1R zoals die bekend zijn uit autoradiografie (zie Figuur 5 in hoofdstuk 2). Voorbehandeling van proefdieren met de selectieve A_1R antagonist DPCX resulteerde in een sterke onderdrukking van de tracerbinding en regionale verschillen in opname waren niet langer aanwezig. Indien de niveaus van de endogene agonist adenosine werden verhoogd, door ratten voor te behandelen met een oplossing van 20% ethanol in fysiologisch zout (2 ml) plus de adenosine kinase remmer 4-amino-5-(3-bromophenyl)-7-(6-morpholino-pyridin3-yl) pyrido [2,3-d] pyrimidine dihydrochloride (ABT-702) leidde dit niet tot meetbare competitie van adenosine met [^{11}C]MPDX voor binding aan A_1R, maar tot een onverwachte globale verhoging (40 tot 45%) van de opname van radioactiviteit in het brein. Door tracer-kinetisch modelleren werd de indruk gewekt dat deze toename niet was te wijten aan veranderde doorbloeding of een veranderde permeabiliteit van de bloed-hersenbarrière, maar aan een toename van de tracer binding op het niveau van de receptor.

In **hoofdstuk 3** onderzochten we of de bezetting van A_1R door geneesmiddelen (niet-radioactieve agonisten en antagonisten) met behulp van [^{11}C]MPDX en PET kan worden vastgesteld. Als A_1R agonist gebruikten we N^6-cyclopentyladenosine (CPA, 0.25 mg/kg, i.p.) en als A_1R antagonist caffeïne (4 en 40 mg/kg, i.p.). Toediening van CPA resulteerde in een sterke afname (> 50%) van de hartslag, en toediening van caffeïne in een kleine toename (10 tot 15%). De laagste dosis caffeïne resulteerde in 65.9% bezetting van de A_1R populatie en de hoogste dosis in 98.5%, berekend via een Cunningham-Lassen plot. Toediening van CPA leidde niet tot meetbare competitie van de agonist met [^{11}C]MPDX voor binding aan A_1R in het brein, maar in een paradoxale toename van de traceropname die vergelijkbaar was met de toename die we eerder hadden waargenomen na verhoging van het niveau van endogeen adenosine (Hoofdstuk 2). Door kinetisch modelleren van de tracer binding werd de indruk gewekt dat adenosine analoga de fractie van de A_1R populatie die het radioligand kan binden kunnen verhogen. [^{11}C]MPDX is dus een geschikte tracer om de bezetting van A_1R door niet-radioactieve antagonisten vast te stellen, maar de bezetting van de receptorpopulatie door agonisten kan niet worden vastgesteld.

In **hoofdstuk 4** schonken we aandacht aan veranderingen van de expressie van A_1R in een diermodel van encephalitis. Wistar ratten werden via de neus geïnfecteerd met herpes simplex virus-1 en gescand na een interval van zes of zeven dagen, wanneer ze de symptomen van hersenontsteking begonnen te vertonen. Het regionale distributievolume van [^{11}C]MPDX in hippocampus en medulla van geïnfecteerde ratten bleek significant te zijn verhoogd (V_T berekend uit een Logan plot). De bindingspotentiaal van het radioligand (k_3/k_4 berekend op grond van de fit van een model met 2 weefselcompartimenten) bleek in hippocampus, cerebellum en medulla significant te zijn toegenomen, wat op verhoogde expressie van A1R zou kunnen wijzen. De partitiecoëfficiënt (K_1/k_2) van [^{11}C]MPDX was echter niet significant gewijzigd na virusinfectie. Immunohistochemische kleuring liet een sterke toename van de immunoreactiviteit van A_1R zien in het cerebellum van HSV-1 geïnfecteerde ratten. Deze data wijzen op een up-regulatie van A_1R in de vroege fase van encephalitis die kan worden gedetecteerd met de A_1R antagonist [^{11}C]MPDX en PET. Zo'n up-regulatie zou de release van exciterende neurotransmitters als glutamaat kunnen beperken, en de prikkelbaarheid van neuronen in het brein kunnen verminderen, waardoor de betrokken neuronen tegen de negatieve gevolgen van overstimulatie worden beschermd.

In **hoofdstuk 5** onderzochten we of transiënte opening van de bloed-hersen barrière na behandeling van proefdieren met (niet-radioactieve) adenosine A_1 en A_{2A} receptor agonisten met behulp van hydrofiele radiofarmaca en PET kan worden waargenomen. Zulke tracers kunnen de intacte bloed-hersen barrière niet passeren, maar kunnen die wel passeren wanneer de barrière is geopend. Voor deze pilotstudie maakten we gebruik van [^{11}C]CH_3-AMD3465 (een $CXCR_4$ antagonist) en [^{18}F]AMC15 (een dopamine D_2 receptor agonist). De hersenopname (SUV) en het distributievolume (V_T) van beide tracers waren niet verhoogd na voorbehandeling van proefdieren met CPA of Lexiscan. Verder onderzoek

is noodzakelijk om vast te stellen of deze negatieve bevinding te wijten is aan een ongeschikte kinetiek van de gebruikte radiofarmaca of aan het niet-opengaan van de bloed-hersen barrière in verdoofde ratten.

Het proefschrift eindigt met een Engels- en Nederlandstalige **samenvatting** en een bespreking van enkele **toekomstperspectieven**.

Acknowledgement

I am solely thankful to the almighty eyes which are behind the blue sky that always blessed and guided me for completion of this dissertation work. At the earliest, I consider this as an opportunity to express my deep sense of heartfelt gratitude and sincere thanks to my esteemed supervisor Dr.Aren van Waarde for his valuable suggestions, the necessary help and facilities for my work and also for his constant support, motivation, guidance and co-operation during my thesis work.

I am gratefully indebted to my primary promotor Prof.dr. Rudi Dierckx who provided me the opportunity to do my Ph.D research in his group. I am deeply indebted to Dr. Erik FJ de Vries who also selected me as PhD candidate in the NGMB group.

It is a great pleasure to express my special thanks to Prof.dr.Philip Elsinga for his support which made the study a success.

I would like to thank the members of the reading committee, Prof.dr.C.Halldin, Prof.dr.P.G.M.Luiten and Prof.dr.H.P.H. Kremer for spending time in reading and approving my thesis.

My genuine thanks to Prof.Dr.Kiichi Ishiwata, Dr.Peter Meerlo, Wytske Boersma, Dr.Janine Doorduin, Chantal Kwizera for their valuable contributions in my research work.

I am sincerely thankful to Jurgen Sijbesma for his special help during "small animal imaging experiments, particularly instruction and assistance with canulations".and thanks to everyone from the Central Animal Facility, special thanks to Annemieke Smit, Michel Weij and Miriam van der Meulen .

I extend my sincere thanks to our department manager Annegrit Wijker for extending my Ph.D contract and also to Riekje Banus, Maaike Bansema and all other staff members of the GUIDE office.

I also convey my thanks to my dear colleagues and friends: Shivashankar, Khayum, Siddesh, Gaurav Brother, Vineet, Willem Jan, Chao, Vladimir, Andrea, Nisha, Anniek, Ines, Mershima, Alexander, Anna, Klaas Willem, Joost, Rolf, Bram and all other NGMB students and staff members.

This work would never have been successful without the moral support from Mr. Tapan Kumar Bhowmik, Mrs. Manika Kar, Mr.Hasan Mahmud Rana, Mr. Md.Atiqul Islam, Mrs.Mithila Ferdous Rinky, Mrs.Rukhsana Rushmi, Mr. Vinoth Kumar, Ee Soo Lee, Sonor, Mr.Hans van Seventer, and Mrs.JoAn van Seventer-Keltie.

Last but not least, I would like to thank all my Indian friends, Dutch friends, my wife and family.

S.Paul
February, 2014

Full papers in international journals

1. **Paul S,** Khanapur S, Rybczynska AA, Kwizera C, Sijbesma JW, Ishiwata K, Willemsen AT, Elsinga PH, Dierckx RA, van Waarde A. Small-animal PET study of adenosine A (1) receptors in rat brain: blocking receptors and raising extracellular adenosine. **J Nucl Med**. 2011; 52(8):1293-300.

2. **Paul S**, Elsinga PH, Ishiwata K, Dierckx RA, van Waarde A (2011).Adenosine A1 receptors in the central nervous system: Their functions and disease,and possible elucidation by PET Imaging. **Curr Med Chem**. 2011; 18(31):4820-35.

3. **Paul S**, Khanapur S, Elsinga PH, Ishiwata K, Sijbesma JW, Meerlo P, Dierckx RA, van Waarde A. [^{11}C]MPDX and PET to study adenosine A1 receptor occupancy by non-radioactive agonists and antagonists. **J Nucl Med.2014**; 55(2):315-20

4. **Paul S**, Khanapur S, Elsinga PH, Ishiwata K, Sijbesma JW, Boersma W, Meerlo P, Dierckx RA, van Waarde A. Cerebral adenosine A1 receptor are upregulated in rodent encephalitis. Accepted for publication in **NeuroImage.**

5. Khanapur S, **Paul S**, Shah A,Koole MJB,Zijlma R,Dierckx, R.A,Luurtsema G, Garg P, van Waarde A, Elsinga PH. Development of [^{18}F]-Labeled SCH442416 analogs for imaging adenosine A2A receptors with PET. Submitted to **J Med Chem**.

Conferences paper

1) Vancouver, Canada, 2013/6 :**Paul S**,Khanapur S, Khayum MA,Sijbesma JW, Ishiwata K, Elsinga PH,Meerlo P,Dierckx RA van Waarde A, "MicroPET studies of antagonist/agonist competition with ligand binding to adenosine A1 receptors in rat brain". Abstract Society of Nuclear Medicine. J Nucl Med. 2013; 54 (Supplement 2):247

2) Vancouver, Canada, 2013/6 : **Paul S**, Khanapur S,Khayum MA, Sijbesma JW, Ishiwata K, Elsinga PH, Doorduin J,Meerlo P, Dierckx RA, van Waarde A, "Changes of binding of cerebral adenosine A1 receptor antagonist 11C-MPDX in rodent encephalitis." Abstract.Society of Nuclear Medicine. J Nucl Med. 2013; 54 (Supplement 2):244

3) Milan, Italy, 2012/10 : **Paul S**, Khanapur S,Khayum MA,Sijbesma J.W, Doorduin J,Ishiwata, Meerlo P,Elsinga PH, Dierckx RA,van Waarde A, "Encephalitis changes binding of the adenosine A1 receptor antagonist 11C-MPDX in rat Pons." Abstract European Association of Nuclear Medicine. EJNMMI.2012; 39 (S303-S303).

4) Bangalore, India, 2011/12: **Paul S**,Elsinga PH,Dierckx RA, van Waarde A, "Visualization of adenosine A1 receptors in rat brain, using 11C-MPDX and micro PET." Poster Indian Pharmaceutical Congress.

5) Dublin, Ireland, 2011/9 : **Paul S**, Khayum MA,Khanapur S, Sijbesma JW, Ishiwata K, Elsinga PH,Dierckx RA, van Waarde A, "Validation of 11C-MPDX for imaging of cerebral adenosine A1 receptors in rodents." Poster World Molecular Imaging Congress.

6) Lyon, France, 2013/10: Khanapur S, **Paul S**, Shah A, Luurtsema G, Zijlma R, Dierckx RA, Garg P, Van Waarde A, Elsinga PH, "Development and Preclinical Evaluation of a Novel F-18 Labeled SCH442416 Analog for Imaging Adenosine A2A Receptors."Abstract European Association of Nuclear Medicine. EJNMMI.2013; 40 (S199-S199).

7) Vienna, Austria, 2010/10: van Waarde A,Rybczynska AA,**Paul S**, Khanapur S, Sijbesma JWA, Ishiwata K, Elsinga PH, Dierckx RA, "Visualization of adenosine A1 receptors in rat brain, using 11C-MPDX and microPET: effect of raised levels of extracellular adenosine." Abstract European Association of Nuclear Medicine. EJNMMI.2010; 37 (Supplement 2) S209:S210.